Modeling Infrastructure Interdependency with Extended Petri-Net and Markov Chain Analysis for Emergency Management

SHARMIN SULTANA

A Thesis

in

The Department

of

Building, Civil and Environmental Engineering

Presented in Partial Fulfillment of the Requirements
for the Degree of Master of Applied Science (Civil Engineering) at
Concordia University
Montreal, Quebec, Canada.

July, 2007

Your file Votre référence
ISBN: 978-0-494-34782-9
Our file Notre référence
ISBN: 978-0-494-34782-9

ABSTRACT

Modeling Infrastructure Interdependency with Extended Petri-Net and Markov Chain Analysis for Emergency Management

Sharmin Sultana

This research introduces a novel and dynamic mathematical modeling methodology of infrastructure interdependency which has been examined through two case studies. The urban infrastructure interdependency was illustrated with a case example of California electricity outage in 2001. The developed Petri-Net model captured the interdependencies among the infrastructures in the network of a power plant, oil refinery, natural gas plant, fuel transporting pipes and tanks, water supplying pipes, and telecom. Extended Petri-Net and Markov Chain have been applied to the part of the network to assess the safety of the infrastructures. The developed modeling tools have been used to demonstrate the floodplain infrastructure interdependency with a case study of Canyon Ferry reservoir area having the infrastructures network of a water storage multi-purpose concrete gravity dam, penstock, power plant, transformer substation, intake pipes and pumping station, irrigation systems, municipal water supplying systems, and telecom. Additionally, gravity dam vulnerability assessment with empirical and analytical fragility curves and flood frequency analysis have been integrated with the extended Petri-Net analysis. The obtained results are reasonable showing that the more interdependent infrastructures present in the network, the more vulnerable they are. Also, higher degree of interdependency results in intense coupling leading towards higher vulnerability. Overall, this research contributes to the emergency management planning for safety assessment of the critical infrastructures.

Acknowledgement

I gratefully acknowledge the continuous support and guidance of my thesis supervisor, Dr. Chen. It has been a great pleasure to conduct this research and I am thankful to him for assigning me in such a challenging project.

This research was supported by the Joint Infrastructure Interdependencies Research Program (JIIRP) from the Natural Science and Engineering Research Council Canada (NSERC) and the Public Safety and Emergency Preparedness Canada (PSEPC). I wish to express my appreciation to these granting agencies.

I am also very grateful to all of my family members in Bangladesh for their invaluable supports, inspirations and affections all the way through, which kept me going in an enthusiastic manner. Finally, I would like to thank my husband for his help, love, patience, and valuable suggestions.

Table of Contents

List of Figures

List of Tables

List of Symbols

A_c = area of dam cross section (m^2);

B = absorbing probability matrix;

b_1 = top width of dam (m);

b_2 = width of the intersection line of block 1 and block 2 of dam (m);

b_3 = base width of dam (m);

b_{b1}, b_{b2} = width of the acting area of vertical hydrostatic pressure at upstream and downstream sides of dam, respectively (m);

C = incidence matrix;

C_s = coefficient of skew;

F_f = friction force along the contact plane (kN/m);

FS_o = factor of safety for overturning against the toe of dam;

FS_s = factor of safety against sliding along the contact plane of the dam and foundation;

H_{b1}, H_{b2} = height of block 1 and block 2, respectively (m);

H_d = height of dam (m);

H_h = Horizontal projection of hydrostatic pressure (kN/m);

H_v = vertical projection of hydrostatic pressure (kN/m);

H_{w1}, H_{w2} = upstream and downstream water levels, respectively (m);

I = identity matrix;

IFS_o = inverse of FS_o;

IFS_s = inverse of FS_s;

K = frequency factor (function of return period and assumed frequency distribution);

M_o = overturning moment (kN-m/m);

M_R = righting moment (kN-m/m);

N = fundamental matrix;

p = steady state vector of Markov Chain;

Q = transient matrix;

q = transition probability;

R_v = vertical projection of reaction force, at the base of dam (kN/m);

T_r = transition matrix;

T = return period (year);

t = matrix of number of steps in transient states before being absorbed in absorbing states;

u = uplift pressure (kN/m);

W_c = weight of gravity dam (kN/m);

x_{b1}, x_{b2}, x_c, x_u = distance of the center of gravity of block 1, block 2, dam concrete weight, acting of uplift pressure, respectively, from the toe of the dam (m);

x_T = random hydrologic series data with a return period T;

y = place invariants;

y_T = value of variate x for a given return period T;

γ_c = unit weight of dam (kN/m^3);

γ_w = unit weight of water (kN/m^3);

σ_x = standard deviation of samples;

μ = coefficient of friction along contact planes.

Chapter 1: Introduction

Infrastructure is the underlying foundation or basic framework of a community. It includes all the basic facilities, services, and installations needed for the functioning of the community or society; also for strengthening the military forces operations. According to 'President's Commission on Critical Infrastructure Protection, (PCCIP 1997)', 'infrastructure is a network of independent, mostly privately owned, man-made systems and processes that function collaboratively and synergistically to produce and distribute a continuous flow of essential goods and services'. Rinaldi et al. (2001) described infrastructure interdependency as a linkage or connection between two infrastructures, through which the state of one infrastructure influences or correlates to that of the other; interdependencies were termed as the 'system of systems' or, several sets of interactions among the infrastructures. 'Public Safety and Emergency Preparedness Canada, (PSEPC)' referred the critical infrastructures as the physical and interconnected information technology networks, utilities, and services which if disrupted or destroyed would have a serious impact on the health, safety, security or economic well-being of Canadians or the effective functioning of governments (PSEPC 2005).

Modern community consists of a complicated system of interconnected infrastructures where they are highly interdependent; disruption of one infrastructure induces disruption in one or more interconnected infrastructures. Robert (2004) stated that lifeline infrastructure networks are highly interrelated, which favors the propagation of vulnerabilities from one network to another through cascading effects. In a system, multiple infrastructures are connected at multiple points through a wide variety of mechanisms. There must be some interactions among the infrastructures in a system.

Understanding or analysis of one infrastructure independently is not possible without relating it with the other surrounding infrastructures. Consequently, study of the interdependencies among critical infrastructures has become important to address the cascading effects of a failed infrastructure on the entire network so as to help emergency management team in decision making (Mendonca and Wallace 2006).

Infrastructure interdependency issues are directly related to the environmental or economical risks or losses. Vulnerability assessment using fragility curves is widely practiced for risk analysis of infrastructure systems. Chock (2005) examined the fragilities and associated risks of a wide variety of buildings using a GIS supported hurricane damage database. Developing fragility curves, among other measures, were considered for infrastructure risk assessment by Hall et al. (2003).

Recently, network-based models had been employed to study the behavior of interconnected engineering infrastructure systems. For example, Petri-Net is a system analysis method put forward by Carl Adam Petri during the early 1960s (Petri 1962), which can be used to determine the interdependencies among system components. Hura (1987) pointed out possible applications of Petri-Net and considered this analysis technique for modeling the performance of software systems. Gursesli and Desrochers (2003) used the graph based Petri-Net for identifying qualitative vulnerabilities of the infrastructures by evaluating their interdependencies.

Several types of mathematical models were explored for quantitative analysis of infrastructure interdependency. A mathematical framework of the interconnected infrastructures network was developed by Nozick et al. (2005) using the Semi-Markov model to estimate the infrastructure performance. Ezell et al. (2000) developed an event tree analysis based risk model to assess risks associated with interconnectedness and interdependencies of water infrastructure systems. Haimes and Jiang (2001) developed a Leontief input-output theory based model to demonstrate the degree of intra and inter-connectedness of critical infrastructures.

The types of infrastructure interdependency and their failure modes have been defined by Rinaldi et al. (2001). There are four types of interdependencies: physical, cyber, geographic, and logical interdependency. Physical interdependency occurs between two mutually dependent infrastructures where the state or function of each is dependent on that of the other. As the computerization and automation based information technology is spreading widely over the last few decades, cyber interdependency is emerging where one infrastructure state depends on the information transmitted through the other information infrastructure. When a local environmental change affects the other infrastructures close to it, geographic interdependency occurs mainly due to the spatial proximity of the infrastructures. In the logical interdependency, change in one infrastructure causes change in others without any direct physical, cyber or geographic connection; rather, human intervention and decisions play the predominant role.

Infrastructure interdependency is closely linked to the infrastructure failure. Depending on the connections and interactions among the infrastructures, failure types can be categorized as, cascading, escalating, and common cause failure (Rinaldi et al. 2001). Cascading failure occurs when disruption in one infrastructure causes the failure of a second one, which subsequently causes disruption in the third one. Escalating failure occurs when an existing infrastructure disruption exacerbates an independent disruption of a second infrastructure, generally in the form of increasing the severity or the time for recovery of the second failure. The common cause failure induces disruptions in two or more infrastructure networks simultaneously as they occupy the same geographical space or because the root problem is widespread.

1.1 Current problems

In Canada, many roads-bridges, water distribution and sewer networks, public buildings, dams, dykes are now more than 50 years old, even some pipe networks are about 100 years old; moreover, the percentage of GDP spent has declined for the last few decades which made the renovation of these critical infrastructures mandatory to various degrees (OCIPEP 2003). PSEPC (2005) has identified Canadian critical infrastructures at the national level in ten key sectors: energy and utilities, communications and information technology, finance, health, food, water, transportation, safety, government, and manufacturing.

Most of the research works considered the infrastructure system as an isolated feature for vulnerability assessment; whereas, infrastructure vulnerability is also the function of the behavior of other infrastructures interconnected with it. There is a lack of comprehensive study to address this issue.

1.2 Objectives of the study

This study is intended to investigate the limitations of the previous studies on infrastructure interdependency analysis and aims to identify the overall vulnerabilities of critical infrastructures, thus to help the decision support system for taking proper initiatives e.g. renovation of the structures to ensure the safety of the society. Briefly, the objectives are:

- Developing a new dynamic methodology for modeling infrastructure interdependency and safety assessment.
- Applying the developed model into real case examples in the North America.
- Examining the overall performance of interconnected infrastructures through integrated analysis for emergency management.

1.3 Thesis organization

This dissertation is organized with the following six chapters:

- Chapter one: General introduction to the infrastructure interdependency issue, types of interdependencies and failure modes, infrastructure interdependency related problems, objective of the study.
- Chapter two: Detailed literature survey of the previous research works on the infrastructure vulnerability and interdependency.
- Chapter three: Theoretical background of the modeling tools and development of the integrated methodologies.
- Chapter four: Application of the network model in a case study of California electricity outage in 2001, results and discussion.
- Chapter five: Case study of the integrated vulnerability assessment and network analysis applied in Canyon Ferry Dam area, results and discussion.
- Chapter six: Research summary, contributions, and future recommendations.

Chapter 2: Literature Review

Infrastructure interdependency is comparatively a new area of study. There has been extensive works on the risk assessment of single independent infrastructure. Although, such analysis has importance in risk assessment, but interdependencies among interlinked infrastructures should be considered for overall vulnerability assessment. But studies on the issue are very few in number. In this chapter, previous research works of infrastructure risk assessment with different approaches will be investigated extensively. These approaches of vulnerability assessment can be categorized as the fragility curves analysis, network approach, Leontief input-output model, probabilistic techniques, agent based modeling, etc. These are discussed below.

2.1 Fragility curves and risk analysis

The definition of basic damage states, corresponding fragility curves and conditional probabilities for estimating damage matrices had been discussed in detail by Filliben et al. (2002). Simpson et al. (2005) proposed an interdisciplinary modeling framework based on the development of fragility curves of each single critical infrastructure in a community for multi hazards to maximize the allocation of the limited preparedness resources; it was discussed that fragility curves based vulnerability is the function of the age, redundancy, construction types of the infrastructures. Until today, fragility curves have been mostly developed for the urban infrastructures such as bridges, steel structures, buildings, storage tanks, etc. mainly for earthquake disaster. Shinozuka et al. (1994) modeled structural water system damage estimation for a seismic hazard using the Monte Carlo simulation technique; Chang et al. (2000) added the economic loss estimation with this approach. Hwang et al. (2000) presented a method for evaluating seismic damages to the bridges and highway systems in earthquake prone area like Memphis and Shelby County, Tennessee, by developing fragility curves for different classes of bridges. Kim and Shinozuka (2004) enhanced the developed fragility curves of the bridges in that area to study the nonlinear dynamic responses of the bridges before and after the retrofitting the curves by means of steel jacketing of bridge columns. Yamaguchi and Yamazaki (2001) developed fragility curves for low-rise residential buildings using the recorded motions and the building damage data from the intensive field survey to estimate the distribution of ground motion in Kobe, Japan. Fragility curves and damage probability matrices were proposed for developing earthquake intensity-damage relations and the method was applied for reinforce-concrete frame-wall structures e.g. multi-storied buildings, by Jovanoska (2000). Erberik and Elnashai (2004) developed fragility curves of flat-slab structures under earthquake hazards. Fragility curves were developed for roof sheathing in light frame constructions in high wind regions by Lee and Rosowsky (2005); the methodology could be used to develop design guidelines for wood frame structures in high wind regions. O'Rourke et al. (2000) developed seismic fragility curves for on-grade steel tanks with the performance data of over 400 tanks for different earthquake events.

Fragility curves development is a strong tool for vulnerability assessment, but availability of required huge historical database is often a critical issue. Also, if the uncertain parameters are not incorporated properly, it will lead towards a wrong assessment. But if the fragility curves are developed soundly, it is a very straightforward and robust tool for vulnerability assessment of the critical infrastructures.

2.2 Network approach and modeling tools

Critical infrastructure systems can be represented as nodes in a network where they are connected through a set of links depicting the logical relationship among them; damage or malfunction in one node affects the functioning of the connected succeeding node (Moselhi et al. 2005). A framework was proposed to implement this concept of network based analysis of interdependencies among the urban critical infrastructures, e.g. physical and information networks, utilities, and services, etc. The steps of the framework can be summarized as identifying the critical components in the network of the interdependent critical infrastructures, modeling the cascading effects of a disaster on critical infrastructures, and, developing a decision support system (DSS) to allocate funds for rehabilitation of infrastructures on a priority basis. The proposed network analysis method is a strong tool to quantify the interdependencies of critical infrastructure, but implementation of this method requires detailed knowledge of programming and advanced mathematics.

In traditional practices, network based modeling tools are applied in software modeling. Recently, efforts have been made to use this modeling concept in different areas. Graph theory is very famous concept for network modeling of the real life case problems, especially for infrastructure of a community (Watts and Strogatz 1998, Leonardo et al. 2004). Another graph theory based network modeling tool is Petri-Net which is very robust for modeling and analyzing the network characteristics. It was originally introduced by Carl Adam Petri in early 1960s (Petri 1962). Afterwards, more improvement had been incorporated by other researchers in this field (Peterson 1981, Manson 1988, Murata 1989, Bobbio 1990).

2.2.1 Basic Petri Net tool

Basic Petri-Net can be applied to determine the interdependencies among the infrastructures in a network; Gursesli and Desrochers (2003) used the graph based Petri-Net for identifying the interdependencies among critical urban infrastructures defined by Rinaldi et al. (2001). The network consisting of the critical infrastructure such as electric power, oil, transportation, natural gas, telecommunications, and water sectors, was analyzed to examine the interdependencies among these infrastructures due to the failure of the main supporting infrastructure, power plant. The model execution starts with the occurrence of a hazard and the execution stops when all the interconnected infrastructures are disrupted. It was shown that the developed Petri-Net is capable of representing the in-service or failed conditions of the infrastructures before and after the power disruption. Thus, Petri-Net is a very strong modeling tool to capture the interrelationships among the infrastructures. However, the model didn't consider the recovery strategies in the network. Petri-Net is also applied in other fields. Regarding biological application, Koch et al. (2005) modeled the sucrose breakdown pathway using the Petri-Net, representative results were obtained.

2.2.2 Extended Petri Net analysis

In addition to the basic Petri-Net, a few extensions have been made to capture the time duration associated with an event. When the time is deterministic, it is called deterministic Petri-Net. If the transition of the net contains stochastic time distribution, it is called Stochastic Petri-Net (SPN). The original Petri-Net extension theory was first introduced by Ramchandani (1974) to show the techniques of executing a stochastic

Petri-Net. Later, Zuberek (1980, 1985, 1987, 1988, 1991) carried out that study successively to make the methodology clearer for practically applying the theory in real life problems. Cirado and Lindemann (1993) presented a time and space efficient algorithm for computing steady state solutions of deterministic and stochastic Petri-Net (DSPN) with both stochastic and structural analysis. Petri-Net based coordination mechanisms were performed for multi workflow (Raposo et al. 2000); an extensible model was proposed which consists of a set of temporal and resource management relations to specify task interdependencies, Petri-Net was then applied to model the coordination mechanisms. A simple Generalized Stochastic Petri Net (GSPN) model having immediate and timed events was introduced for identifying common mode faults for modeling the cascading failures of critical infrastructures (Krings and Oman 2003).

2.3 Safety assessment of infrastructures with probabilistic techniques

The probabilistic methods e.g. Markov Chain analysis, event tree/fault tree analysis are very useful tools for determining infrastructure interdependency. These techniques were mentioned and discussed by several researchers. Nozick et al. (2005) developed a unifying mathematical framework of the interconnected infrastructure networks and described the algorithms using the Markov-Semi Markov model to estimate the performance hence to optimize the investment; the methodology was applied to a case study of delivering gas and electricity services, and gas network SCADA (Supervisory Control and Data Acquisition) infrastructure. Markov Chain analysis was also applied for determining the interactions among the lifeline systems e.g. electric power supply, gas supply, water supply, transportation, communication under seismic conditions by Bao-hua et al. (2004). Interactions among the infrastructures were documented theoretically first; then interactions were analyzed by systems fragility data, and WebGIS technology. Hwang and Chou (1998) evaluated the seismic performance of an electric substation supplying electricity to several hospitals in downtown Memphis with the technique of event tree/fault tree analysis. Ezell et al. (2000) developed a probabilistic 'Infrastructure Risk Analysis Model (IRAM)' for addressing a water infrastructure system's interconnectedness and interdependencies. This model disintegrates the system along the dimensions of component, identifies and rates the threats and vulnerabilities, shapes the model scenarios and constructs a probabilistic model with event tree analysis (ETA) to assess the risks of the detected sources, calculates the expected and extreme losses, infrastructure surety, and finally, establishes a management system where alternatives are generated and tradeoff analysis is done.

2.4 Leontief Input-Output model

The famous Nobel Prize winning Leontief input-output model (Leontief 1966) was originally developed for the decision making purposes in economics by Leontief. Later, other researchers adjusted this modeling concept to apply in their own research fields, especially in risk assessment. Based on the Leontief model, Haimes et al. (2005) developed the 'Inoperability Input-Output Model (IIM)' to describe the degree of interconnectedness among critical infrastructures and the cascading failures through the interconnected systems. The output is the inoperability that may occur by one or multiple failures due to their inherent complexity or external perturbations e.g., natural hazards, accidents, etc. When an impact occurs, before reaching at equilibrium, the interconnected infrastructures interact among themselves. The physical based IIM states,

$$x_i^P = \sum_j a_{ij}^P x_j^P + c_i^P \Leftrightarrow x^P = A^P x^P + c^P \qquad (2.1)$$

where, the vector c^P stands for the *input* representing perturbations in the form of natural events e.g. flood-earthquake-tornado, accidents, or willful attacks to the interconnected infrastructures; x^P denotes the *output* representing the resulting vector of inoperability of the different infrastructures, due to their interconnections; the superscript *P* is included to the original Leontief model formula to distinguish IIM from the original model; matrix *A* can be defined as the infrastructure-to-infrastructure technical coefficient showing the input hazards from infrastructure *i* to *j*, expressed as a proportion of the total inoperability inputs to infrastructure *j*.

2.5 Agent based modeling

Few researchers have proposed agent-based modeling for simulating infrastructures interdependency. Tolone et al. (2004) reported the use of 'Intelligent Software Agents' for integration, modeling and simulation. The software agent was defined as autonomous program acting by sensing its environmental characteristics without the intervention of human. The authors structured the model to allow end users to execute simulations seamlessly within the context of a GIS environment where the users will initiate simulations by selecting and disabling infrastructure features and will be able to visualize the impacts of these actions through the GIS visualization support. The developed agents could collectively sense changes within infrastructures and reason about the changes. Panzieri et al. (2005) proposed an agent based modeling approach for handling heterogeneous infrastructures into a single framework by describing the behavior of agents with a sufficiently high level of abstraction to allow the use of the quantities e.g. operation level, requirements, faults representing the state of each agent. Interaction among the agents is determined by induced and propagated faults, requirements and operative level of the agents.

2.6 Other studies

Several researchers addressed infrastructure interdependencies through the documentation of economic losses and other types of losses due to the occurrence of a hazard. Schiff (2004) developed and discussed a detailed guideline for the improvement of the performance of lifelines e.g. electric power, communication system during and after the earthquake hazard. Single interdependency between two infrastructures was also done by few researchers. Interdependency between natural gas and electricity infrastructures was analyzed by Shahidehpour and Wiedman (2005) where the influencing factors were reported as the physical characteristics and capabilities of infrastructures, operational procedures, types of generating plants, supply level, transmission and delivery systems and market prices. Lambert and Sarda (2003) carried out a risk based disaster planning for infrastructures and societal networks. Direct interactions were identified across the superposition of networks, indirect interactions were generated through rippling of scenarios across network components, and high order interactions were identified for multiple network components.

2.7 Summary

The infrastructure interdependency had rarely been addressed directly, rather, independent analysis of infrastructures have been done for risk assessment. In this literature review, the studies related to this issue directly or indirectly, have been discussed. Vulnerability assessment of individual infrastructure with fragility curves developments for different kinds of infrastructures e.g. bridge, water infrastructure, steel structure, concrete structure, etc have been reviewed. Network approach and available network models such as Petri-Net, extended Petri-Net tool, their application in different fields are discussed. Works on the performance evaluation with probabilistic techniques of event tree analysis, Markov-Semi Markov Chain analysis are pointed out in this review. Nobel winning Leontief economic input-output model and its conversion into 'Inoperability Input-Output Model' for infrastructure interdependency simulation are illustrated. Available research work on agent based modeling are mentioned. There have been also a number of documentations on the economic and other types of losses of the infrastructures due to the exposure to the hazards.

2.8 Scopes of the current study

In this chapter, the models and methods related to infrastructure interdependency had been studied extensively to investigate their strengths and weaknesses. The literature review shows that there is a lack of a comprehensive study which can address the infrastructure interdependency dynamically. For example, basic Petri-Net model had been applied for capturing interdependency qualitatively which doesn't include any quantitative analysis. Leontief model is applied mainly to identify economic vulnerability; structural vulnerability measurement by this method is very few.

Mostly, vulnerability assessment for a single infrastructure is carried out for independent risk assessment, but there is a demand for the interdependent vulnerability assessment of a network of infrastructure systems. Therefore, this study is aimed to address the infrastructure interdependency with a new integrated modeling methodology. It is intended to introduce the methodology for the first time where the qualitative as well as the quantitative interdependencies will be captured. The approach of determining the structural vulnerability which is the function of the vulnerabilities of other interconnected infrastructures will be shown with case examples. Thus, it is hoped that this study will contribute significantly to address the current infrastructure safety problems.

Chapter 3: Development of the Modeling Framework

This research proposes a new methodology for addressing infrastructure interdependency and overall safety assessment. Two different types of 'infrastructure interdependency' will be demonstrated with case studies. One infrastructure network consists of the modern urban infrastructures upon which today's civil communities are highly dependent; disruptions of these infrastructures cause severe impacts on the community. The second kind represents the network of flood plain infrastructures which is also an integral part of the civil society. For the urban infrastructure network, the network modeling and extended analysis will be applied for interdependency analysis and safety assessment. Same kinds of analyses will be applied into the floodplain case; additionally, frequency analysis of hazard and a vulnerability assessment of the main supporting infrastructure will be performed; results from these analyses will be integrated for predicting the overall vulnerability of infrastructures.

3.1 Modeling framework

The basic Petri-Net analysis will be applied for qualitative evaluation of infrastructure interdependency; dynamic network analysis will be performed with extended analysis of developed Petri-Net which will be converted into the Markov Chain. Properties and characteristics of this Markov Chain will be determined to simulate the safety of the network infrastructures. The flowchart of the modeling of systems is provided below (Fig. 3.1):

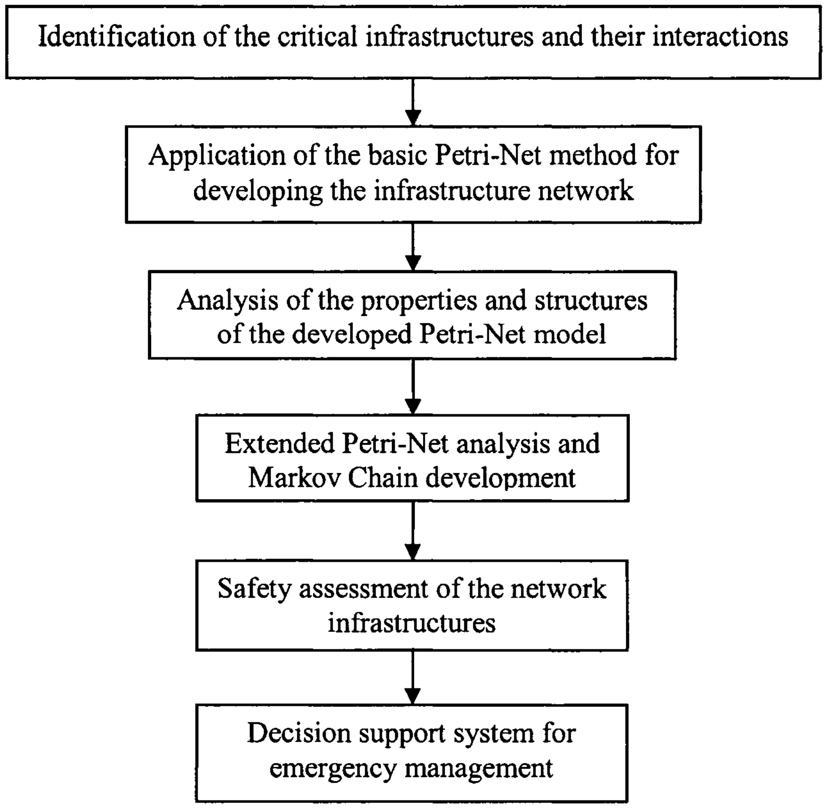

Fig. 3.1: Modeling of infrastructure interdependency

The above figure represents a general flowchart which can be applied in any network of infrastructure systems. This modeling framework will be applied for California electricity outage case study. Furthermore, few other relevant factors such as hazard frequency analysis, fragility assessment, etc. have also contributions into overall vulnerability, inclusion of which makes the model more realistic. In this study, the floodplain infrastructure network is concerned for this purpose. The flood frequency analysis will be performed for predicting certain flood levels. For the structural vulnerability assessment, fragility curves development approach will be applied. The assessed risks from flood frequency analysis and fragility analysis will be integrated with the evaluated safety of the network infrastructures. The flowchart is as below (Fig. 3.2):

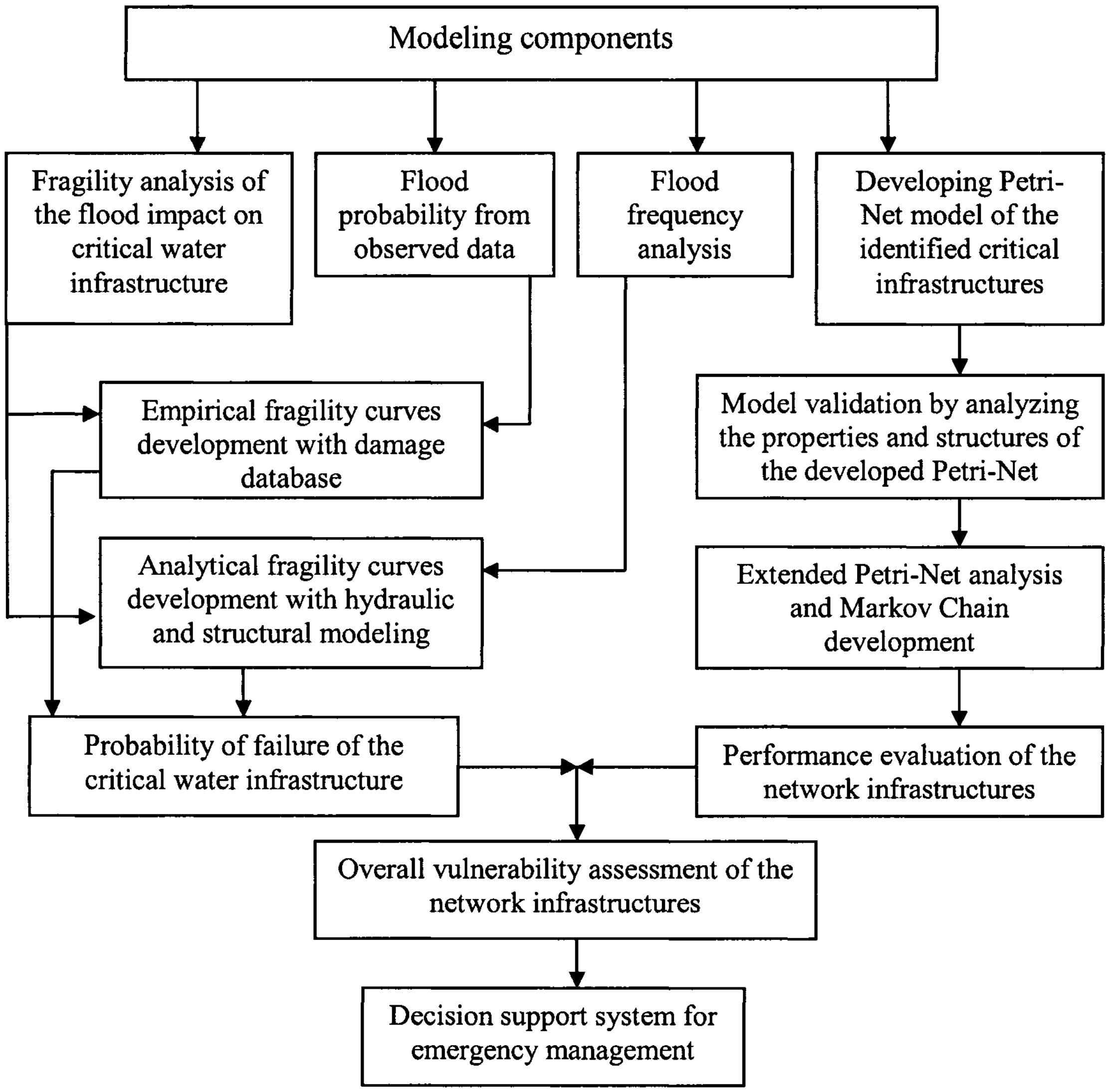

Fig. 3.2: Modeling of floodplain infrastructure interdependency

3.2 Theoretical background of the modeling components

Before applying the modeling tools, pertinent theories will be stated briefly in this section to get familiarized with their applicability and understand the modeling steps. As shown in Figure 3.1 and Figure 3.2, the modeling elements include the hazard frequency analysis, fragility curves development, Petri-Net development and its extended analysis, and development and analysis of Markov Chain. These are discussed below.

3.2.1 Flood frequency analysis

In hydrology, statistical frequency analysis is applied for predicting extreme flood events. Magnitude and frequency of extreme flood events are estimated from the highest flood event recorded in each year over a series of years. Chow (1951) showed that in hydrological study, most frequency distribution functions can be expressed by a general hydrologic frequency analysis equation:

$$x_T = \bar{x} + K\sigma \quad (3.1)$$

where, x_T = random hydrologic series data with a return period T; $\bar{x}$ = mean value; σ_x = standard deviation of the variate x; K = frequency factor which depends on the return period T and assumed frequency distribution. Return period T is the inverse of the probability of occurrence P. That is, $P = \frac{1}{T}$. The most commonly used frequency distribution functions are discussed below:

3.2.1.1 Gumbel's distribution method

Here, the highest flood level in a given year is the variate and the flood annual series constitutes a series of highest flood levels. The value of X with a return period T,

$$x_T = \bar{x} + K\sigma_{n-1} \quad (3.2)$$

where, $\sigma_{n-1} = \sqrt{\frac{\sum(x-\bar{x})^2}{N-1}}$;

K is the frequency factor which is expressed as, $K = \frac{(y_T - \bar{y}_n)}{s_n}$.

For a given T, value of X, $y_T = -\ln\left[\ln\frac{T}{T-1}\right]$

Here, $\bar{y}_n$ = reduced mean; s_n = reduced standard deviation, both of these parameters are the function of sample size N and are determined from the Gumbel's extreme value distribution chart (Subramanya 2001).

3.2.1.2 Log Pearson type III distribution method

This method of flood frequency analysis is recommended and widely used in United States for projects sponsored by the government (Subramanya 2001). In this method, the variate is first transformed into 10 based logarithmic form and the transformed dataset are analyzed. If X is the variate of a random hydrologic series, then the series Z variate for any recurrence interval is,

$$z_T = \bar{z} + K_z \sigma_z \tag{3.3}$$

where, $z = \log x$, $\sigma_z = \sqrt{\frac{\sum(z-\bar{z})^2}{N-1}}$; K_z = a frequency factor which is a function of T and the coefficient of skew C_s; it is determined from a specified table (Subramanya 2001). C_s is determined from the equation,

$$C_s = \frac{N\sum(z-\bar{z})^3}{(N-1)(N-2)(\sigma_z)^3} \tag{3.4}$$

where, the terms carry the usual meanings. Then,

$$x_T = anti\log(z_T) \tag{3.5}$$

3.2.2 Fragility curves development

Fragility curve is defined as a mathematical expression that represents the conditional probability of reaching or exceeding a certain damage state of an infrastructure at a given hazard level. Fragility curves convey the information about the vulnerability of an infrastructure through the probability distribution for various levels of hazard. These curves can be developed empirically and analytically. Both types are discussed below.

3.2.2.1 Empirical fragility curves

For developing empirical fragility curves, huge observed damage database for a particular hazard is essential. This study deals with the flood hazard for which the fragility curves development steps are as follows:

[i] Classifying the damage states, e.g. slight, moderate, severe or extensive, and complete damage and setting the characteristics of each state according to the observed data; say, slight damage indicates minor cracking, and so on.

[ii] Collecting the historical records of the number of events of the water levels (WL) exceeding certain levels and corresponding damage states (DS).

[iii] Calculating the conditional probability of the damage levels for a given exceeding water level according to the following equation,

$$P[DS|WL] = \frac{P[DS \cap WL]}{P[WL]} \tag{3.6}$$

where, $P[DS|WL]$ = conditional probability or fragility of the damage state;

$P[WL]$ = probability of water level exceeding a certain level =

$$\left(\frac{\textit{number of events of the occurrence of water level exceeding a certain level}}{\textit{number of total observations}} \right);$$

$P[DS \cap WL]$ = probability of occurrence of the water level and damage state =

$$\left(\frac{\textit{number of events of the occurrence of exceeding water level and damage state}}{\textit{number of total observations}} \right).$$

[iv] Constructing the empirical fragility curves with exceeding water levels in X-axis and corresponding probability of exceedence on Y-axis.

3.2.2.2 Analytical fragility curves

Availability of a huge observed damage database is often critical. In this case, analytical fragility curves are developed with the structural modeling of infrastructure for any hazard. The outputs of the structural failure modeling are used as the inputs for generating analytical fragility curves. In this study, failure modes of the hydraulic dam are analyzed for flood water levels. The steps of the analysis include,

[i] Modeling of infrastructure failure modes for a certain flood water level with the Monte Carlo simulation of the uncertain design parameters.

[ii] Classifying the damage states.

[iii] Determining the probability of exceedence of the damage states.

[iv] Repeating the steps for different water levels, and

[v] Developing fragility curves with exceeding water levels in X-axis and corresponding probability of exceedence on Y-axis.

Monte Carlo simulation process is applied into a system to address its uncertainties. For developing fragility curves of any structure due to the occurrence of a hazard, the uncertain parameters of structural modeling can be taken as the random variables for which a number of data are generated and the corresponding damage states are checked if these conditions are reached for that hazard level.

(A) Hydraulic modeling of critical water infrastructure (Dam)

In this study, a detailed hydraulic modeling will be performed for the analytical fragility curves development. Detailing of the model is discussed briefly with the main equations (Linsley and Franzini 1992). Here, for performing the model calculations, unit thickness of the dam is considered.

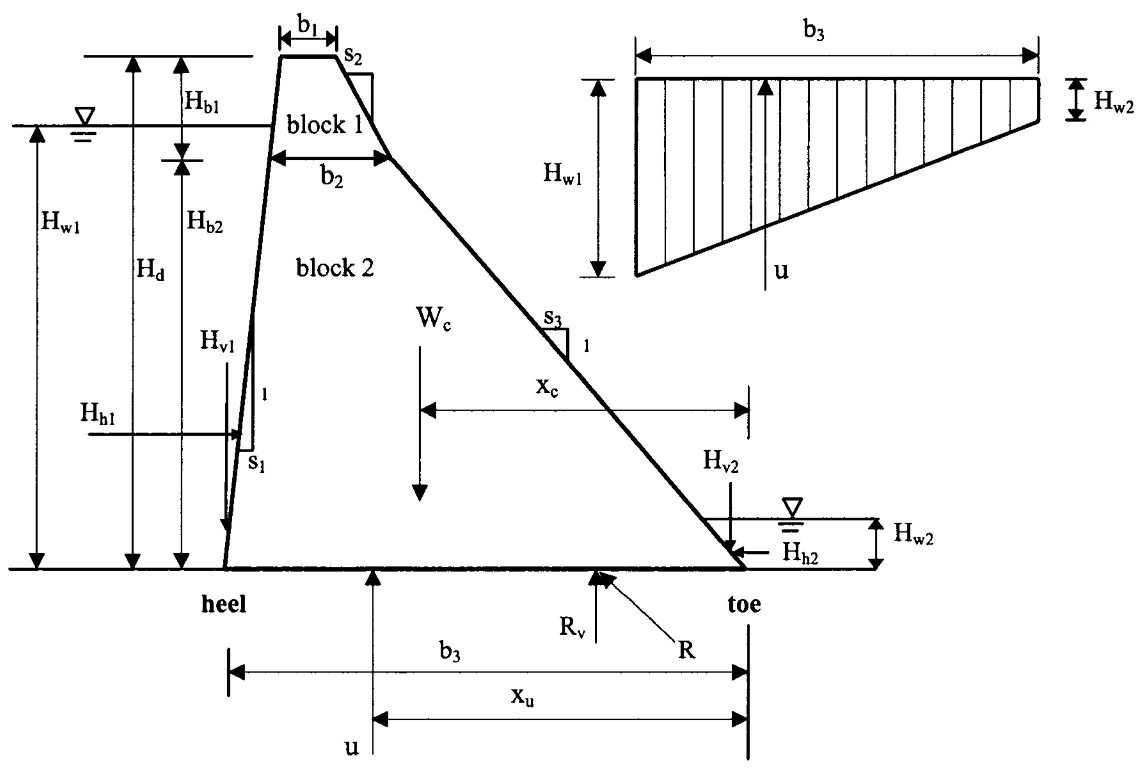

Fig. 3.3: Schematic of a dam (Linsley and Franzini 1992)

Concrete weight of the dam, $W_c = \gamma_c A_c$ (3.7)

Acting pressures on the dam, $H_{h1} = 0.5\gamma_w H_{w1}{}^2$ (3.8)

$$H_{h2} = 0.5\gamma_w H_{w2}{}^2 \quad (3.9)$$

$$H_{v1} = 0.5\gamma_w H_{w1} b_{b1} \quad (3.10)$$

$$H_{v2} = 0.5\gamma_w H_{w2} b_{b2} \quad (3.11)$$

$$u = \gamma_w \frac{H_{w1} + H_{w2}}{2} b_3 \quad (3.12)$$

Factor of safety (overturning):

$$FS_o = \frac{M_r}{M_o} \quad (3.13)$$

where, $M_r = W_c x_c + H_{v1}(b_3 - \frac{b_{b1}}{3}) + H_{h2}\frac{H_{w2}}{3} + H_{v2}\frac{b_{b2}}{3}$ (3.14)

$$M_o = H_{h1}\frac{H_{w1}}{3} + u x_u \quad (3.15)$$

Factor of safety (sliding):

It is assumed that there is no bond between the dam material and foundation material. Hence, the factor of safety against shear failure can be expressed as following,

$$FS_s = \frac{F_f}{(H_{h1} - H_{h2})} \quad (3.16)$$

where, $F_f = \mu R_v$ (3.17)

$$R_v = W_c + H_{v1} + H_{v2} - u \quad (3.18)$$

Inverse factor of safety:

$$IFS_o = \frac{1}{FS_o} \quad (3.19)$$

$$IFS_s = \frac{1}{FS_s} \quad (3.20)$$

Determination of the downstream water level

The downstream water level of the overflowing weir is the function of the design of weir, stream discharge and head above the weir, etc. In this study, it is assumed that when the dam is over flown, it can be considered as an overflow spillway. The steps of deriving the downstream water level for a flood flow are not straightforward. The methodology had been discussed by a number of researchers (Linsley and Franzini 1992, Graph 1998, Methods et al. 2003). For an ogee shape spillway,

$$q = \frac{Q}{L} = K_D \sqrt{g} (H_{w1} - H_d)^{\frac{3}{2}} \quad \text{[Graph 1998]} \tag{3.21}$$

where, q = stream discharge per flow length; Q = stream discharge; L = length of flow over the weir; H_{w1} = upstream water level; H_d = weir height; K_D = coefficient of discharge. Here, the approach velocity head is neglected. For determining the discharge coefficient, specified curves are used. Mainly, the values of the coefficients are read from the graph for a given ratio, $\left[\frac{H_{w1} - H_d}{H_d}\right]$.

Now, applying Bernoulli's energy equation and neglecting the approach velocity,

$$H_{w1} = H_{w2} + \frac{q^2}{2gH_{w2}^2} \tag{3.22}$$

For SI unit, the equation can be rewritten as,

$$19.62H_{w2}^3 - 19.62H_{w1}H_{w2}^2 + q^2 = 0 \tag{3.23}$$

This equation can be solved by a trial and error method. Equation (3.21) and equation (3.23) are used to determine the downstream water level at the dam for the upstream flood levels. The solution steps can be summarized as,

(i) Determining the ratio, $\left[\frac{H_{w1}-H_d}{H_d}\right]$.

(ii) Choosing the discharge coefficient from the graph.

(iii) Calculating the value of q using equation (3.21).

(iv) Determining H_{w2} from equation (3.23) with a trial and error method.

Here, A_c = area of dam cross section (m^2); b_1 = top width of dam (m); b_2 = width of the intersection line of block 1 and block 2 (m); b_3 = base width of dam (m); b_{b1}, b_{b2} = width of the acting area of vertical hydrostatic pressure at upstream and downstream sides, respectively (m); F_f = friction force along the contact plane (kN/m); FS_o = factor of safety for overturning against the toe of dam; FS_s = factor of safety against sliding along the contact plane of the dam and foundation; H_{b1}, H_{b2} = height of block 1 and block 2, respectively (m); H_d = height of dam (m); H_h = Horizontal projection of hydrostatic pressure (kN/m); H_v = vertical projection of hydrostatic pressure (kN/m); H_{w1}, H_{w2} = upstream and downstream water levels, respectively (m); IFS_o = inverse of FS_o; IFS_s = inverse of FS_s; M_o = overturning moment (kN-m/m); M_R = righting moment (kN-m/m); R, R_v = reaction force and vertical projection, respectively, at the base of dam (kN/m); u = uplift pressure (kN/m); W_c = weight of gravity dam (kN/m); x_{b1}, x_{b2}, x_c, x_u = distance of the center of gravity of block 1, block 2, dam concrete weight, acting of uplift pressure, respectively, from the toe of dam (m); γ_c = unit weight of dam (kN/m^3); γ_w = unit weight of water (kN/m^3); μ = coefficient of friction along contact plane.

(B) Calculation steps of the model

The conditional damage state probability or fragility of the hydraulic structure is determined for the given upstream water levels. The downstream water level is determined with trial and error method. The uncertain parameters are identified and enough random values within representative lower and upper bounds are generated. All the model inputs except upstream and downstream water levels are constant for each model simulation. Also, the random values are different for each simulation. For determining the conditional probability of damage states at a certain hazard level, the upper and lower bounds are set accordingly. The equations (3.7) - (3.20) are executed throughout the model simulation to find the intended risk level probability. The steps are summarized below:

[i] Giving inputs of the model: b_1, s_1, s_2, s_3, H_{b1}, H_{b2}, H_{w1}, γ_w, γ_c, μ.

[ii] Generating random values of uncertain parameters with Monte Carlo simulation.

[iii] Calculating output parameters (IFS_o and IFS_s) in each model simulation for the input values; the model calculates these values for the generated random numbers of the uncertain parameters in each simulation.

[iv] Calculating mean and standard deviation values of these calculated IFS_o and IFS_s.

[v] Generating the probability distribution with the mean and standard deviation determined in one simulation.

[vi] Determining the exceeding probability of the output parameters from the generated probability distribution.

[vii] Running the model for different upstream and downstream water levels (H_{w1}, H_{w2}) to generate the probabilities for drawing the analytical fragility curves.

3.2.3 Petri-Net analysis

Petri-Net is a graphical tool for representing and analyzing systems network. It is applied to study the behavior of concurrent, asynchronous, distributed, parallel, non deterministic, and/or stochastic systems (Murata 1989). A Petri-Net structure *(C)* is basically a four-tuple, $C = (P, T, I, O)$, where, P stands for places, T for transitions, I for input functions and O for output functions. Furthermore, tokens are assigned in places which is called network 'marking' indicating the existing condition of the network. Any Petri-Net has an initial distribution of the tokens which is called initial marking.

The definition of Petri-Net has evolved time to time in different ways to respond with the prevailing research demands. When any concept was added in the Petri-Net, the number of tuple had been increased to describe the Petri-Net representatively. In this study, the most conventional definition of Petri-Net will be discussed.

A Petri-Net structure C can be described as a seven-tuple, $C = (P, T, I, O, A, w, B)$. Here, the additional tuple such as A stands for arcs, w for arc weight, and, B for inhibitory places. More specifically,

$P = \{p_1, p_2, p_3, ..., p_m\}$, is a finite set of places, $m \geq 0$;

$T = \{t_1, t_2, t_3, ..., t_n\}$, is a finite set of transitions, $n \geq 0$;

I = a mapping from a transition t_j to a collection of input places $I(t_j)$;

O = a mapping of a transition t_j to a collection of output places $O(t_j)$;

A = a set of directed arcs which connect places with transitions and transitions with places, $A \subseteq P \times T \cup T \times P$;

w = a weight function which assigns a positive integer 'weight' to each arc in the net;

B = a set of inhibitor arcs, $B \subseteq P \times T$, and A and B are disjoint sets.

If the token number is too large, they are represented by numbers instead of dots. A transition is enabled if each of its input places has a minimum number of tokens equal to the weighting of arcs from the place to the transition. The transition fires by removing tokens from its input places and creates new tokens which are distributed to its output places (Murata 1989). Firing can continue as long as there exists at least one enabled transition, otherwise, the execution will be stopped. If an initial marking is given, a Petri-Net can be executed by successive firings of transitions. Petri-Net can be analyzed by reachability graph analysis where the possible reachable conditions are achieved by successive firing of the transitions and by matrix analysis when reachability tree analysis is not achievable. A network of systems can be represented by Petri-Net with the following example,

$C = (P, T, I, O, A, w, B)$;

$P = \{p_1, p_2, \ p_4\}$; $T = \{t_1, t_2, t_3\}$;

$I(t_1) = \{p_1\}$; $O(t_1) = \{p_2, \ p_3\}$; $I(t_2) = \{p_2, \ p_3, \ p_4\}$; $O(t_2) = \{p_4\}$; $I(t_3) = \{p_3\}$; $O(t_3) = \{p_2\}$;

$B = \{p3, t2\}$.

The initial marking of this Petri-Net is, [1, 2, 0, 1]. The arc from *p2* to *t2* has the multiplicity of three which means, at least three tokens should be available in *p2* and the other input places of *t2* should also have enough tokens to enable *t2* to fire. In this network, *p3* is the inhibitory place for *t2*; so, if there is a token in *p3, t2* cannot fire. Graphically, these network elements can be represented as follows:

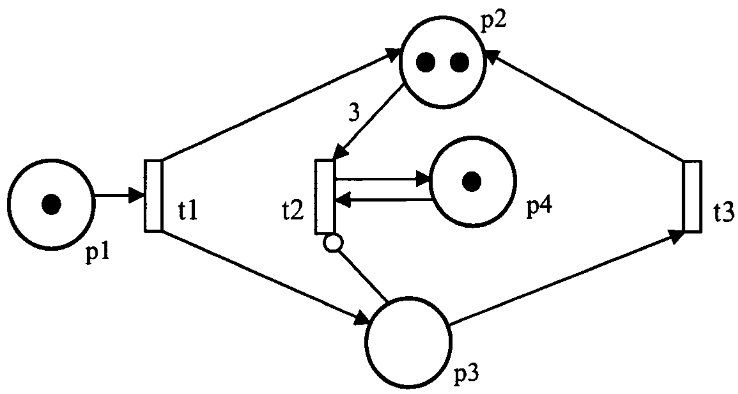

Fig. 3.4: Typical Petri-Net graph

In this Petri-Net, only transition t1 is enabled initially; when it fires, the output places p2 and p3 gain tokens. In this condition, as p3 is the inhibitory place for t2, it will be the input of t3, and t2 is now friable as there is no token in its inhibitory place and there are enough tokens in its input places, t3 will also fire to give one token to p2.

In the network analysis, with the interactions information, the places and transitions are defined accordingly. The conditions or states of the network are denoted as 'places', the events as 'transitions', occurrence of an event as 'firing', and holding of a condition as the 'token'.

(A) Structural properties of Petri-Net: invariant analysis

Invariant analyses such as place *(P)* invariants and transition *(T)* invariants are determined to check the structural properties of Petri-Net, which are independent of the initial marking (Murata 1989). A *P*-invariant indicates the set of places in which the weighted sum of the tokens remain constant for all markings; and, a *T*-invariant indicates the sequence of transitions whose firings cause the network to return to its initial condition.

A set of 'dummy places' are introduced in the Petri-Net if required to determine the place invariants and for maintaining the real condition of the network at the same time (Murata 1989). For determining the P-invariants, incidence matrix is determined first. If the numbers of places and transitions are m and n, respectively, then the incidence matrix $[C]$ has the dimension $m \times n$, which means, the transitions and places are placed in columns and rows, respectively. To refer the flow of tokens from and to a place in the network, -1 and 1 are assigned, respectively. More specifically, if p_i is the input of j^{th} transition and $p_{i\pm k}$ is the output of this transition, then C_{ij} will be -1 and $C_{(i\pm k)j}$ will be 1. The procedure of assigning tokens in the remaining columns of the matrix is same. In this study, the T-invariant analysis is not performed as the recovery strategy of the infrastructures is not considered. From the discussion, it can be shown that, the incidence matrix,

$$C = \begin{array}{c|cccccc} & t_1 & \cdots & t_j & \cdots & t_n \\ p_1 & \cdots & \cdots & \cdots & \cdots & \cdots \\ \cdots & \cdots & \cdots & \cdots & \cdots & \cdots \\ p_{i-k} & \cdots & \cdots & C_{(i-k)j} & \cdots & C_{(i-k)n} \\ \cdots & \cdots & \cdots & \cdots & \cdots & \cdots \\ p_i & \cdots & \cdots & C_{ij} & \cdots & C_{in} \\ \cdots & \cdots & \cdots & \cdots & \cdots & \cdots \\ p_{i+k} & \cdots & \cdots & C_{(i+k)j} & \cdots & C_{(i+k)n} \\ \cdots & \cdots & \cdots & \cdots & \cdots & \cdots \\ p_m & \cdots & \cdots & C_{mj} & \cdots & C_{mn} \end{array}$$

where, $i = 1, 2, \ldots \ldots, m;\ j = 1, 2, \ldots \ldots, n;\ and,\ k = 1, 2, \ldots \ldots, m-1.$

If the P-invariants 'y' is a $m \times 1$ column vector, then, the solution of 'y' is given by,

$$C^T \times y = 0 \qquad (3.24)$$

where, C^T is the transpose matrix of C.

(B) Behavioral properties of Petri-Net

These initial marking dependent behavioral properties enable to check the network characteristics (Murata 1989). Such properties are reachability, boundedness, liveness, reversibility, conservation and the like. Some of them are briefly discussed below (Peterson 1981, Murata 1989, Bobbio 1990):

Safeness: A place in a Petri-Net is safe if the number of token never exceeds 1 in that place throughout the simulation; and a Petri-Net is safe if all its places are safe.

Boundedness: A place is *k*-safe or *k*-bounded if the number of tokens in that place never exceeds an integer *k*.

Conservation: The total number of tokens in the network remains constant. Also, the weighted sum of tokens of all reachable markings should be constant which means there is no loss or gain of the tokens in the network.

Liveness: When a Petri-Net model cannot proceed, it becomes deadlocked which is the opposite of liveness. Usually, when some common resources are shared by events, if the resource is used by one transition and the resource is not released to become available for other transition, then the net becomes deadlock.

Reversibility: If there is any sequence in the Petri-Net that successive firing of a series of transitions again results in the initial marking, that Petri-Net is called reversible.

3.2.4 Extended analysis of Petri-Net

The basic Petri-Net doesn't consider firing time of the transitions. To account for the required time of the occurrence of an event, it is assumed that the firing time of each transition is exponentially distributed random variable. Thus, the extended Petri-Net is called Stochastic Petri-Net (SPN). The reachability graph of the SPN can be compared with the inherent Markov Chain which can be solved analytically to determine the probabilities of the states of the network (Murata 1989, Bobbio 1990).

In the following example, failure process of two components in parallel redundancy is shown; *t*1 and *t*2 are two failure events of components 1 and 2 whose failure rates are λ_1 and, λ_2, respectively. The reachability graph and corresponding Markov Chain are represented. Bobbio (1990) stated that, if *p* denotes probability, then,

After time *t*, *p* (state 4) of Markov Chain = *p* (M_4) of Petri-Net.

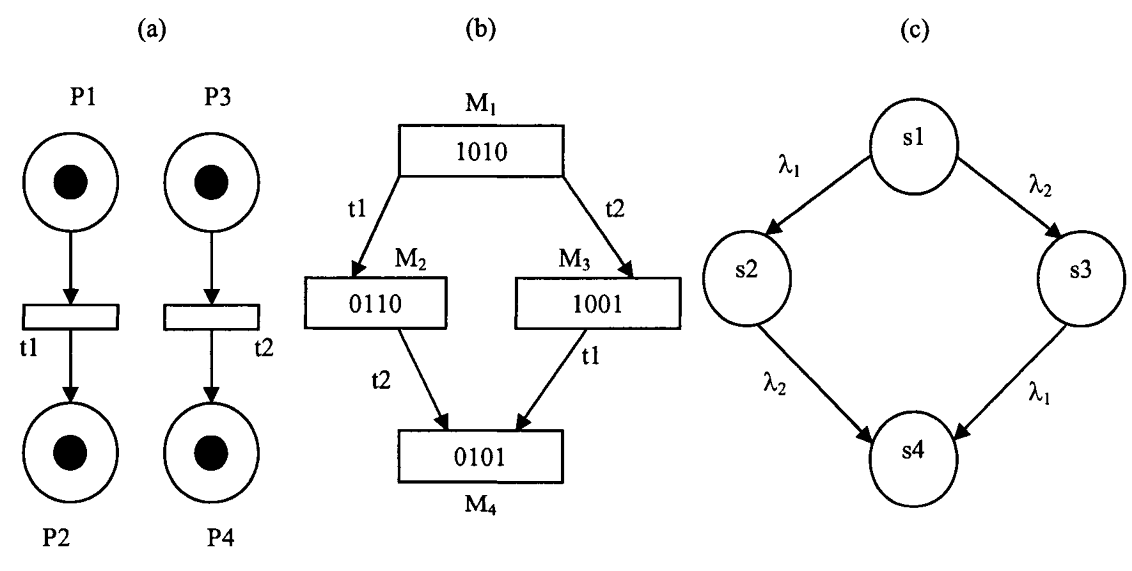

Fig 3.5: Petri-Net of two parallel systems (a), reachability tree (b), and Markov Chain (c) (Bobbio 1990)

Concept of Stochastic Petri-Net (SPN)

Zuberek (1985, 1991) has defined the characteristics of the timed Petri-Net. The basic concept is that, in timed Petri-Net, each transition takes a positive time to fire and the firing time is exponential random variable. Once a transition is enabled, firing is initiated by removing tokens from its input places; throughout the duration of firing, tokens remain in this transition. When firing is terminated, the tokens are distributed in the output places of that transition. If a transition is enabled while it fires, a new independent firing can be initiated. In this study, two types of Petri-Net will be analyzed. One kind of Petri-Net contains all the stochastically timed transitions which is called 'M-timed Petri-Net'; the other one contains both immediate and timed (stochastic) transitions, which is called 'Enhanced timed Petri-Net'. Theoretically, the transitions which take no time to fire are termed as the 'immediate' transitions. If the firing time of a set of transitions is too fast compared to the rest of the transitions in the net, then these fast firing transitions are also called 'immediate' transitions (Bobbio 1990).

Theories of both kinds of extended Petri-Net have been discussed in a series of articles by Zuberek (1980, 1985, 1987, 1988, 1991). Especially, this study adapts related theories from Zuberek (1991) which will not be repeated here. Instead, following the modeling equations, a flowchart of model execution is given in Figure 3.6.

State transition probability

If state s_j is directly t_k reachable from state s_i, transition probability,

$$q(s_i, s_j) = \frac{r(t_k) * n_i(t_k)}{\sum_{t \in T} r(t) * n_i(t)} \tag{3.25}$$

where, r = a firing rate function which assigns firing rate $r(t)$ to each transition 't' in the net, and firing time of 't' is a random variable $x(t)$ with the distribution function,

$$P(x(t) > y) = e^{-r(t)y}, \; y > 0 \qquad (3.26)$$

n = a firing-rank function indicating the number of active firings for each transition, i.e., the number of firings which have been initiated but are not terminated yet.

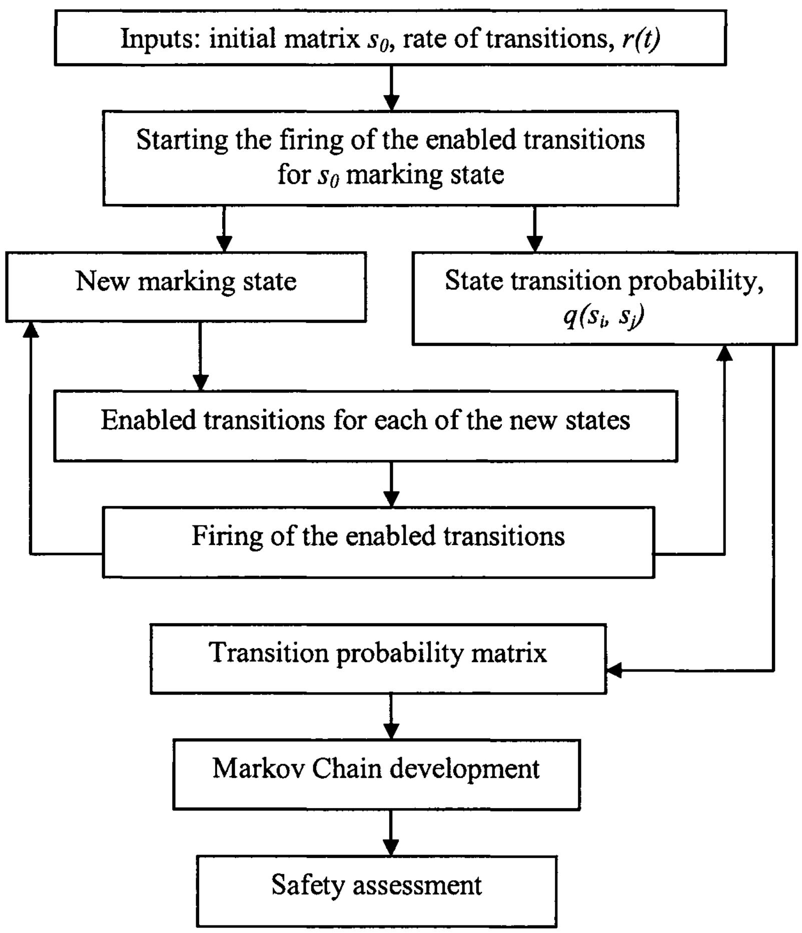

Fig. 3.6: Algorithm of the SPN analysis and safety assessment

3.2.5 Markov Chain analysis

Markov Chain analysis is applied to predict future probability of the occurrence of an event based on the current situation. Thus, this modeling approach can simulate the long term trend of an event. Related theories have been addressed frequently by a number of researchers (Howard 1971, Kennedy et al. 1974, Grimstead and Snell 1997).

Markov Chain is developed with 'transition probability vector' T_r with non negative entries adding upto 1, which come from the equation (3.25). It represents a sequence of probability vectors $p_0, p_1, p_2, \ldots$ with a stochastic matrix T_r such that,

$$p_1 = p_0 T_r,\ p_2 = p_1 T_r = p_0 T_r^2,\ p_3 = p_2 T_r = p_0 T_r^3 \ldots,$$

$$i.e.,\ p_n = p_0 T_r^n; \quad n = 1, 2, 3, \ldots\ldots\ldots \tag{3.27}$$

The probability vector p is called a steady state vector for the Markov Chain if the state vectors p_n get closer and closer to p as n increases. The entries of p are the long term probabilities of the Markov Chain.

Extended analysis of Markov Chain

Markov Chain may contain the transient state and absorbing state. Absorbing states are those states from which there is no output, which means, these states are absorbed within themselves. This Markov Chain can be separated into transient and absorbing states according to the following canonical form:

$$T_r = \begin{array}{ccc} Q & \vdots & R \\ \cdots & \vdots & \cdots \\ 0 & \vdots & I \end{array}$$

where, I is the identity matrix of absorbing states, 0 is a zero matrix, Q is the transient matrix, and R is the remaining matrix. The fundamental matrix is,

$$N = (I - Q)^{-1} \tag{3.28}$$

where, N indicates the expected number of times in transient states for starting at the different states before being absorbed. If t_i be the expected number of steps before the chain is absorbed, given that the chain starts in state s_i, and let t be the column vector whose i^{th} entry is t_i, then,

$$t = N \times c \tag{3.29}$$

where, c is a column vector all of whose entries are 1. If b_{ij} is the probability that an absorbing chain will be absorbed in the absorbing state s_j if it starts in the transient state s_i, and, B is the matrix with entries b_{ij}, then,

$$B = N \times R \tag{3.30}$$

3.3 Summary

In this chapter, pertinent theories of infrastructure fragility analysis, network analysis, and flood frequency analysis have been demonstrated which were proposed previously by the researchers from these fields. However, the fragility analysis steps in this study for vulnerability assessment are quite different from the conventional methods.

Basic Petri-Net is applied to capture the interdependency relationships among critical infrastructures. Application of the extended stochastic Petri-Net analysis for infrastructure interdependency analysis is quite compatible in a sense that the occurrence of the events representing the 'transition firing' is not deterministic, rather being stochastic. For example, if the electricity outage occurs, the emergency shutdown might take two hours, or eight hours, or a day, depending on the duration of electricity outage (reported by Energy Information Administration, Department of Energy, United States, 2001). Similarly, remaining events can also be thought as stochastic events.

Also, the methodology of the integrations stated in Figure 3.1 and Figure 3.2 has been proposed in this study which will be applied into two case studies in following chapters. One case study demonstrates the urban infrastructure interdependency with the case example of California electricity outage 2001; another case study of Canyon Ferry dam area will be discussed to illustrate the floodplain infrastructure interdependency.

Overall, a new kind of integrated modeling methodology has been introduced in this study for examining the infrastructure interdependency which may contribute to the emergency management to safeguard the critical infrastructures. The modeling steps can be shown with the following flowchart (Fig. 3.7):

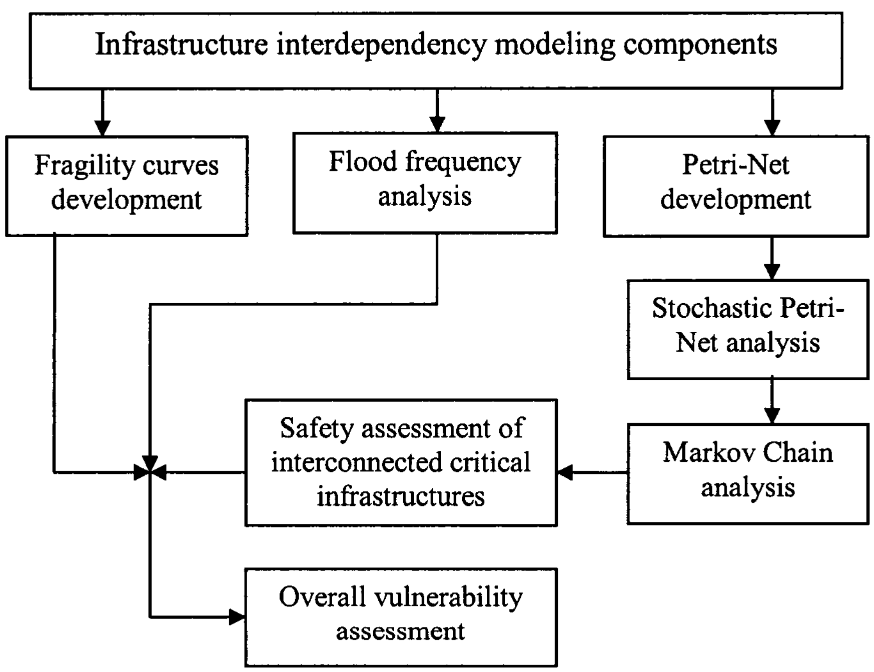

Fig. 3.7: Integrated modeling of infrastructure interdependency

Chapter 4: Urban Infrastructure Interdependency – California Electricity Outage 2001

In California, electricity disruption emerged due to error in human decision (Rinaldi et al. 2001). A rolling electricity outage in 2001 has led to extensive investigations to find out the reasons of such disruption which didn't emerge within a short period of time; rather, long term planning to revive the California power market had led to this situation. The main characteristics of the infrastructure interdependencies for California case study with extended Petri-Net analysis will be conducted in this chapter.

4.1 Reasons behind the power disruption problem

Rinaldi et al. (2001) summarized the reasons of the electricity crisis in California. In 1996, a regulatory legislation was passed to reform the electricity power market that required the investor-owned utilities to sell off their power-generating assets and purchase electricity in the open market. Wolak (2003) discussed that this unrealistic regulatory enabled the power generating units to gain market-power for raising the market prices substantially in excess of the production cost through their unilateral action; on the other hand, the utilities had to sell the purchased electricity to the consumer within a price limit upon which the state imposed a control. Ultimately the utilities experienced bankruptcy and couldn't maintain the bond ratings upto investment grade. Such economic crisis resulted in severe electricity shortage during early 2001.

4.2 Interdependencies among power generation related infrastructures

A number of reports had been released since the occurrence of electricity outage during early 2001 (Connole 2001, Klare 2001). Rinaldi et al. (2001) summarized that electricity disruption affected oil and natural gas production, refinery operation, pipeline transport of gasoline and its fuel, water supply for irrigation, and other key infrastructures. Information on the interdependencies among the energy sectors and other associated infrastructures are adapted from the published report by 'Energy Information Administration' of 'Department of Energy' of California. The uses of the main urban infrastructures are discussed briefly in this section.

Power plant infrastructure

The California State environmental restrictions encourage the oil and gas producers to rely heavily on electricity supply for their plant operations. For electricity outage, oil refineries either will be forced to reduce or completely shut down the production activities. Electricity is not vital for drawing natural gas from well storage, but its processing requires uninterrupted power supply. Electricity is vital for supervisory control and data acquisition (SCADA) systems operations. The fuel carrying pipe network consisting of a series of pumping stations has a greater exposure to electricity outage if different stations lie in different blocks; power failure in any block might sustain the whole delivery operation. Water pipes are highly vulnerable to power failure if there is no backup supply to operate the pumps and valves. Electricity outage doesn't have much impact on transports such as tank. However, electricity cannot be stored like other commodities; shedding of electricity affects the dependent infrastructures almost immediately (Shahidehpour and Wiedman 2005).

Oil refinery

Oil refineries produce gasoline and diesel fuel, asphalt or lubricating oil from crude oil. The power plant, transportations receive their major fuel supply from oil refinery. Additionally, oil lubricants are used in electric generator, natural gas compressor, and transportation.

Natural gas processing plant

Natural gas industry emerged in between 1991 and 2000 in response to the country's expanding economy, especially in California. Also, new demand had been produced for gas-fired power plants. Natural gas is processed as 'compressed natural gas (CNG)' and 'liquefied natural gas (LNG)'. Natural gas is also consumed as fuel by tank.

Fuel transporting pipelines

Pipelines are the integral part of the energy infrastructure systems where long pipelines network carry the fuel oil and CNG to the end recipients. The pipelines carry the products in large batches; any pipeline disruption compels the plants to store the product; when the capacity is surpassed, the production units have to be shut down immediately. If same pipelines carry the products from different refineries, the problems become more intense.

Fuel and lubricant transporting tanker

Other than the delivery pipelines, refined fuel oil and LNG are also carried by tanker. This transportation can be used as an alternative of the pipelines for fuel supply. But for lubricant supply, tanker is the only option.

Water supplying infrastructure

For power plant, water is used for cooling the generator, emission control, etc. In oil and natural gas plants, water is mainly used for production activities as well as cooling and controlling of temperature and pressure of the processing units.

Telecom industry

Today, telecom technology is being widely applied especially in industrial sectors to make automation and computerization of the systems. Rinaldi et al. (2001) classified the telecom industry as e-commerce, operation and repair crew communication, SCADA and EMS (energy management systems). Sauver (2004) discussed the roll of SCADA in today's civil life. SCADA is a realtime industrial process control systems used to centrally monitor and control the remote or local operational. It is used to control oil-gas pipelines, electricity generation and transmission equipments, manufacturing facilities, water distribution systems, etc. The computerized networks can acquire immediate data of utility flow, pressure, temperature or volume. Telecom disruption can not only shut down the whole operation of the supported infrastructures, also, there is a danger of severe accidents. Like electricity, telecom disruption can halt the operation of the supported infrastructures almost immediately. According to Rinaldi et al. (2001), although the advanced automated technology enhances the overall efficiency and reliability of the infrastructures, but extensive reliance on this technology has dramatically increased cyber interdependencies and complexities across all infrastructures leading to increased risks and greater requirements for security.

4.3 Development of the conceptual model using Petri-Net

To model the interdependencies among the above discussed infrastructures, their interactions need to be captured. In the case study network of infrastructures, oil refinery plant receives crude oil and processes it into fuels and lubricants; natural gas processing plant receives raw gas from the gas wells and processes it into fuels; power plant supplies electricity to the oil and natural gas plant and to the telecom industry; fuels are transported by the pipelines and tank transport, and, lubricant is transported by tank; water pipelines supply cooling and processing water to the power, oil and natural gas plant; all the infrastructures except tank, enjoy the telecom facilities. Tank transport and fuel carrying pipelines are also used to carry the crude oil to the refinery. In this network, few assumptions are made, such as, the natural gas processing plant is located near the gas well, and, telecom has underground water supply for its backup generator. So, the network of the infrastructures consists of following three kinds of infrastructures:

i) Energy infrastructures
   - Power plant
   - Oil refinery plant
   - Natural gas processing plant

ii) Transporting infrastructures
   - Fuel transporting pipeline networks
   - Fuel and lubricant transporting tanker
   - Water supplying pipeline network

iii) Telecom infrastructure
   - SCADA (Supervisory Control and Data Acquisition) communication

From the above discussions, the infrastructures network and their interactions can be depicted as in Figure 4.1. Here, 'P' stands for 'power plant'; 'O' for 'oil plant'; 'NG' for 'natural gas plant'; 'Ft' for 'fuel transporting pipelines; 'W' for 'water transporting pipelines'; 'Ta' for 'tank transport'; and, 'Tc' for 'telecommunication'.

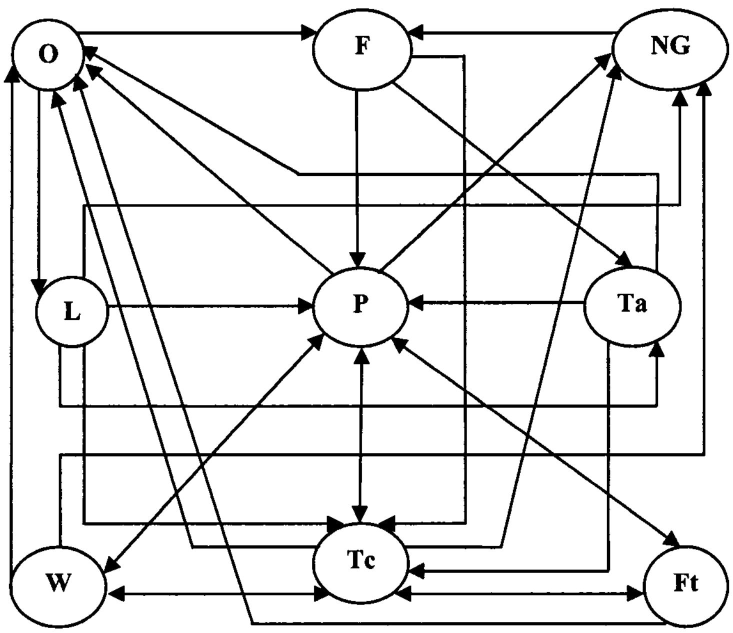

Fig. 4.1: Infrastructure interactions (California State)

This study intends to model the interdependencies among the stated infrastructures due to power failure using the Petri-Net modeling theory. In this case, 'place' indicates the prevailing condition of an infrastructure, and 'transition' indicates the occurrence of disruption. With these places and transitions (Tables 4.1 and 4.2), the Petri-Net model is developed as shown in Figure 4.2. In this network, the double arc from any place indicates that the place is both the input and output of the linked transition.

Table 4.1: List of places (California electricity outage)

Place	Description
p1	Power plant is in service
p2	Power failure
p3	Oil plant is out of service
p4	Natural gas plant is out of service
p5	Fuel transporting pipe is disrupted
p6	Water infrastructure is disrupted
p7	Tank is out of service
p8	Telecom service is not available
p9	Power failure (dummy place for oil plant)
p10	Power failure (dummy place for natural gas plant)
p11	Power failure (dummy place for fuel transporting pipe)
p12	Power failure (dummy place for water transporting pipe)
p13	Lubricant oil production stop (dummy place for power plant)
p14	Lubricant oil production stop (dummy place for natural gas plant)
p15	Lubricant oil production stop (dummy place for tank)
p16	Lubricant oil production stop and power failure (dummy place for telecom)
p17	Oil and natural gas fuels production stop (dummy place for power plant)
p18	Oil and natural gas fuels production stop (dummy place for tank)
p19	Oil and natural gas fuels production stop and power failure (dummy place for telecom)
p20	Tank disruption (dummy place for power plant)
p21	Tank disruption (dummy place for natural gas plant)
p22	Tank disruption and power failure (dummy place for telecom)
p23	Fuel transporting pipe and tank disruption (dummy place for power plant)
p24	Fuel transporting pipe and tank disruption (dummy place for oil plant)
p25	Fuel transporting pipe, tank and power disruption (dummy place for telecom)
p26	Water infrastructure disruption (dummy place for power plant)
p27	Water infrastructure disruption (dummy place for oil plant)
p28	Water infrastructure disruption (dummy place for natural gas plant)
p29	Telecom service is not available (dummy place for power plant)
p30	Telecom service is not available (dummy place for oil plant)
p31	Telecom service is not available (dummy place for natural gas plant)
p32	Telecom service is not available (dummy place for fuel transporting pipe network)
p33	Telecom service is not available (dummy place for water transporting pipe network)

Table 4.2: List of transitions (California electricity outage)

Transition	Description
t1	'Electric power' is disrupted
t2	'Power failure' affects oil plant
t3	'Power failure' affects natural gas plant
t4	'Power failure' affects fuel transporting pipe
t5	'Power failure' affects water infrastructure
t6	'Oil plant disruption' affects power plant
t7	'Oil plant disruption' affects natural gas plant
t8	'Oil plant disruption' affects tank transportation
t9	'Oil plant disruption and power failure' affect telecom
t10	'Oil and natural gas plant disruption' affects power plant
t11	'Oil and natural gas plant disruption' affects tank transportation
t12	'Oil and natural gas plant disruption and power failure' affect telecom
t13	'Tank disruption' affects power plant
t14	'Tank disruption' affects natural gas plant
t15	'Tank disruption and power failure' affects telecom
t16	'Fuel transporting pipe and tank disruption' affect power plant
t17	'Fuel transporting pipe and tank disruption' affect oil plant
t18	'Fuel transporting pipe, tank and power disruption' affect telecom
t19	'Water infrastructure disruption' affects power plant
t20	'Water infrastructure disruption' affects oil plant
t21	'Water infrastructure disruption' affects natural gas plant
t22	'Telecom disruption' affects power plant
t23	'Telecom disruption' affects oil plant
t24	'Telecom disruption' affects natural gas plant
t25	'Telecom disruption' affects fuel transporting pipe network
t26	'Telecom disruption' affects water transporting pipe network

In this network (Fig. 4.2), the double arc from any place shows that the place is both the input and output of the linked transition. For example, p2 is the input and output of the transition t2. The darkened transitions are immediate transitions and the rest are timed transitions.

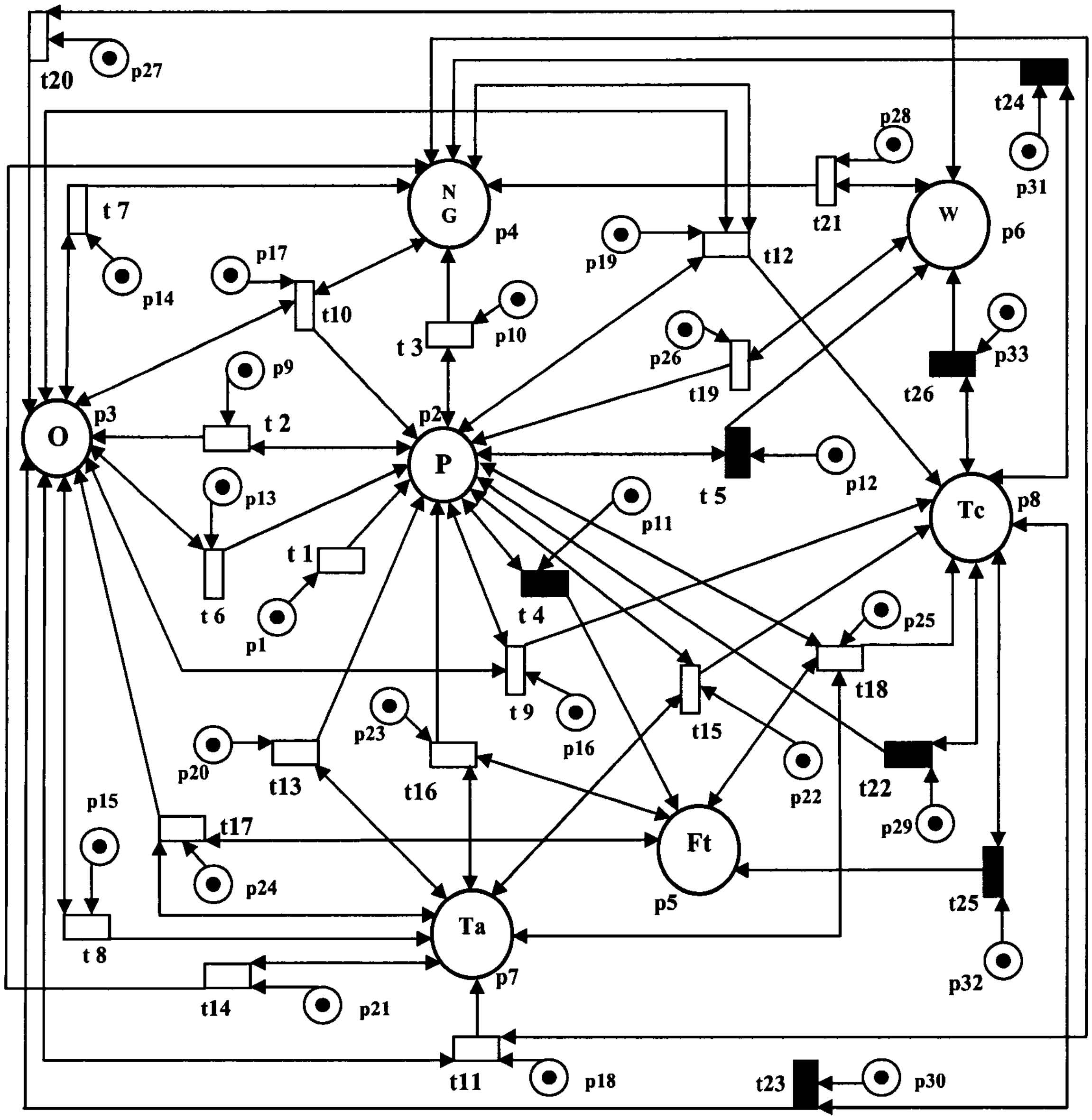

Fig 4.2: Petri-Net model of the urban infrastructure interdependency

4.3.1 Model execution and analysis

Before executing the model, it is assumed that there is no disturbance in the nodal infrastructures, expressed by the place 1 (p1). So, the initial marking of the network is,

$$M_0 = 1\ 0\ 0\ 0\ 0\ 0\ 0\ 0\ 1\ 1\ 1\ 1\ 1\ 1\ 1\ 1\ 1\ 1\ 1\ 1\ 1\ 1\ 1\ 1\ 1\ 1\ 1\ 1\ 1\ 1\ 1\ \ 1\ 1$$

The model execution starts with the firing of transition 1 (t1), that is, electric power is disrupted. As a result, place 2 (p2) gains one token, which indicates the occurrence of power failure. For this marking, the transitions expressing the occurrences of the disruptions of the power dependent infrastructures become enable. After firing these transitions, the marking becomes,

$$M = 0\ 1\ 1\ 1\ 1\ 1\ 0\ 0\ 0\ 0\ 0\ 0\ 1\ 1\ 1\ 1\ 1\ 1\ 1\ 1\ 1\ 1\ 1\ 1\ 1\ 1\ 1\ 1\ 1\ 1\ 1\quad 1\ 1$$

In this way, firings of transitions are performed until there is no enabled transition which indicates that all the interlinked infrastructures have been disrupted.

4.3.2 Structural properties: invariant analysis

The minimal *P*-invariants are capable of representing the interdependencies among the interconnected infrastructures (Gursesli and Desrochers 2003). For this model, the incidence matrix is,

$C =$

	t1	t2	t3	t4	t5	t6	t7	t8	t9	t10	t11	t12	t13	t14	t15	t16	t17	t18	t19	t20	t21	t22	t23	t24	t25	t26
p1	–1	0	0	0	0	0	0	0	0	0	0	0	0	0	0	0	0	0	0	0	0	0	0	0	0	0
p2	1	0	0	0	0	1	0	0	0	1	0	0	1	0	0	1	0	0	1	0	0	1	0	0	0	0
p3	0	1	0	0	0	0	0	0	0	0	0	0	0	0	0	0	1	0	0	1	0	0	1	0	0	0
p4	0	0	1	0	0	0	1	0	0	0	0	0	0	1	0	0	0	0	0	0	1	0	0	1	0	0
p5	0	0	0	1	0	0	0	0	0	0	0	0	0	0	0	0	0	0	0	0	0	0	0	0	1	0
p6	0	0	0	0	1	0	0	0	0	0	0	0	0	0	0	0	0	0	0	0	0	0	0	0	0	1
p7	0	0	0	0	0	0	0	1	0	0	1	0	0	0	0	0	0	0	0	0	0	0	0	0	0	0
p8	0	0	0	0	0	0	0	0	1	0	0	1	0	0	1	0	0	1	0	0	0	0	0	0	0	0
p9	0	–1	0	0	0	0	0	0	0	0	0	0	0	0	0	0	0	0	0	0	0	0	0	0	0	0
p10	0	0	–1	0	0	0	0	0	0	0	0	0	0	0	0	0	0	0	0	0	0	0	0	0	0	0
p11	0	0	0	–1	0	0	0	0	0	0	0	0	0	0	0	0	0	0	0	0	0	0	0	0	0	0
p12	0	0	0	0	–1	0	0	0	0	0	0	0	0	0	0	0	0	0	0	0	0	0	0	0	0	0
p13	0	0	0	0	0	–1	0	0	0	0	0	0	0	0	0	0	0	0	0	0	0	0	0	0	0	0
p14	0	0	0	0	0	0	–1	0	0	0	0	0	0	0	0	0	0	0	0	0	0	0	0	0	0	0
p15	0	0	0	0	0	0	0	–1	0	0	0	0	0	0	0	0	0	0	0	0	0	0	0	0	0	0
p16	0	0	0	0	0	0	0	0	–1	0	0	0	0	0	0	0	0	0	0	0	0	0	0	0	0	0
p17	0	0	0	0	0	0	0	0	0	–1	0	0	0	0	0	0	0	0	0	0	0	0	0	0	0	0
p18	0	0	0	0	0	0	0	0	0	0	–1	0	0	0	0	0	0	0	0	0	0	0	0	0	0	0
p19	0	0	0	0	0	0	0	0	0	0	0	–1	0	0	0	0	0	0	0	0	0	0	0	0	0	0
p20	0	0	0	0	0	0	0	0	0	0	0	0	–1	0	0	0	0	0	0	0	0	0	0	0	0	0
p21	0	0	0	0	0	0	0	0	0	0	0	0	0	–1	0	0	0	0	0	0	0	0	0	0	0	0
p22	0	0	0	0	0	0	0	0	0	0	0	0	0	0	–1	0	0	0	0	0	0	0	0	0	0	0
p23	0	0	0	0	0	0	0	0	0	0	0	0	0	0	0	–1	0	0	0	0	0	0	0	0	0	0
p24	0	0	0	0	0	0	0	0	0	0	0	0	0	0	0	0	–1	0	0	0	0	0	0	0	0	0
p25	0	0	0	0	0	0	0	0	0	0	0	0	0	0	0	0	0	–1	0	0	0	0	0	0	0	0
p26	0	0	0	0	0	0	0	0	0	0	0	0	0	0	0	0	0	0	–1	0	0	0	0	0	0	0
p27	0	0	0	0	0	0	0	0	0	0	0	0	0	0	0	0	0	0	0	–1	0	0	0	0	0	0
p28	0	0	0	0	0	0	0	0	0	0	0	0	0	0	0	0	0	0	0	0	–1	0	0	0	0	0
p29	0	0	0	0	0	0	0	0	0	0	0	0	0	0	0	0	0	0	0	0	0	–1	0	0	0	0
p30	0	0	0	0	0	0	0	0	0	0	0	0	0	0	0	0	0	0	0	0	0	0	–1	0	0	0
p31	0	0	0	0	0	0	0	0	0	0	0	0	0	0	0	0	0	0	0	0	0	0	0	–1	0	0
p32	0	0	0	0	0	0	0	0	0	0	0	0	0	0	0	0	0	0	0	0	0	0	0	0	–1	0
p33	0	0	0	0	0	0	0	0	0	0	0	0	0	0	0	0	0	0	0	0	0	0	0	0	0	–1

Applying equation 3.24, seven place invariants are found in the network which are as follows:

Table 4.3: Place invariants (California electricity outage)

	Place invariants							
	I_{p1}	I_{p2}	I_{p3}	I_{p4}	I_{p5}	I_{p6}	I_{p7}	Sum of invariants
p1	0	0	1	0	0	0	0	1
p2	0	0	1	0	0	0	0	1
p3	0	0	0	1	0	0	0	1
p4	0	0	0	0	1	0	0	1
p5	0	0	0	0	0	1	0	1
p6	0	0	0	0	0	0	1	1
p7	1	0	0	0	0	0	0	1
p8	0	1	0	0	0	0	0	1
p9	0	0	0	1	0	0	0	1
p10	0	0	0	0	1	0	0	1
p11	0	0	0	0	0	1	0	1
p12	0	0	0	0	0	0	1	1
p13	0	0	1	0	0	0	0	1
p14	0	0	0	0	1	0	0	1
p15	1	0	0	0	0	0	0	1
p16	0	1	0	0	0	0	0	1
p17	0	0	1	0	0	0	0	1
p18	1	0	0	0	0	0	0	1
p19	0	1	0	0	0	0	0	1
p20	0	0	1	0	0	0	0	1
p21	0	0	0	0	1	0	0	1
p22	0	1	0	0	0	0	0	1
p23	0	0	1	0	0	0	0	1
p24	0	0	0	1	0	0	0	1
p25	0	1	0	0	0	0	0	1
p26	0	0	1	0	0	0	0	1
p27	0	0	0	1	0	0	0	1
p28	0	0	0	0	1	0	0	1
p29	0	0	1	0	0	0	0	1
p30	0	0	0	1	0	0	0	1
p31	0	0	0	0	1	0	0	1
p32	0	0	0	0	0	1	0	1
p33	0	0	0	0	0	0	1	1

4.3.3 Model properties

Boundedness: Taking the summation of all the P-invariants,

$I_1 + I_2 + I_3 + ... + I_7 =$ 1 1 1 1 1 1 1 1 1 1 1 1 1 1 1 1 1 1 1 1 1 1 1 1 1 1 1 1 1 1 1   1 1

The weighted sum of the tokens in the places is constant for all reachable markings. So, the developed Petri-Net model is bounded.

Liveness: The model is a deadlock model.

4.3.4 Result interpretation

Interpretations of the invariant analysis are described based on the listed characteristics of the places and transitions.

[1] P-invariant 1 gives, M(p7) + M(p15) + M(p18) = 2

This simulation gives the interpretation that, tank disruption occurs when the lubricant and fuel production stop. Or, in other words, oil and natural gas production disruption induce the tank disruption.

[2] P-invariant 2 gives, M(p8) + M(p16) + M(p19) + M(p22) + M(p25) = 4

Telecom service outage occurs due to the lubricant production stop and power failure, fuel production stop and power failure, tank disruption and power failure, and, pipelines, tank and power disruptions.

[3] P-invariant 3 gives, M(p1) + M(p2) + M(p13) + M(p17) + M(p20) + M(p23) + M(p26) + M(p29) = 7

This place invariant shows that, power failure is induced by the hazard occurrence; also, power production is halted if there is no lubricant oil, no fuel for the generator, tank is not available for carrying the lubricants, fuel transporting pipes, tanks are not available for carrying the fuels to the plant, water is not available for cooling and emission control in the generator, and, if the telecom doesn't work, the plant cannot continue its production activities.

[4] P-invariant 4 gives, M(p3) + M(p9) + M(p24) + M(p27) + M(p30) = 4

Oil plant is disrupted if no power is available for the production activities, the fuel pipelines and tanks are not available for carrying the crude oil to the plant, water is not available for the production activities, and telecom outage hampers the plant operation.

[5] P-invariant 5 gives, M(p4) + M(p10) + M(p14) + M(p21) + M(p28) + M(p31) = 5

Natural gas plant becomes out of service when, there no power to run the compressor, no lubricant oil is available for its compressor, tank is disrupted and lubricants cannot be supplied to the plant, there is no water for production activities, and telecom disruption halts the plant operations.

[6] P-invariant 6 gives, M(p5) + M(p11) + M(p32) = 2

Fuel transporting pipes cannot carry the fuels if there is no power available for operating the pumps-valves for the movement of fuels, and if the telecom is out of service, the plant needs to shut down its activities.

[7] P-invariant 7 gives, M(p6) + M(p12) + M(p33) = 2

Water distribution pipes are disrupted when there is no power for the pumps and valves, and when the telecom is disrupted, the infrastructure has to shut down the all the activities to avoid hazard risks.

4.4 Safety assessment with extended Petri-Net analysis

The methodology of extended Petri-Net analysis has been described in Chapter 3 which will be applied in the part of the developed Petri-Net for this case study. Here, the network will be executed for the following three scenarios for a comparative study:

[i] The network contains only the energy infrastructures, that is, the power plant, oil refinery, and the natural gas plant. It is assumed that the oil plant only serves the fuel supply purposes. For the lubricants, the power plant and natural gas plant are not dependent on that particular refinery.

[ii] The network contains the same three energy infrastructures, power plant, oil refinery, and natural gas plant; in this case, natural gas plant and power plant depend on the lubricants supply from the refinery for their compressor and generator, respectively.

[iii] The network consists of the energy and transporting infrastructures.

4.4.1 Scenario 1

In this case, the power plant depends on the oil refinery and natural gas plant for its fuel supply. The oil and natural gas supply depend on the power plant for their production activities. It is assumed that the power plant generator and natural gas compressor receive their lubricants supply from any source outside the concerned network. The place and transitions of the network are described below (Tables 4.4 and 4.5).

Table 4.4: List of places (scenario 1)

Place	Description
p1	Power plant is in service
p2	Power failure
p3	Oil plant is out of service
p4	Natural gas plant is out of service
p5	Power failure (dummy place for oil plant)
p6	Power failure (dummy place for natural gas plant)
p7	Oil and natural gas (fuel) production stop (dummy place for power plant)

Table 4.5: List of transitions (scenario 1)

Transition	Description	Firing rate
t1	'Electric power' is disrupted	Deterministic
t2	'Power failure' affects oil plant	100
t3	'Power failure' affects natural gas plant	90
t4	'Oil and natural gas (fuel) production stop' affects power plant	40

With these listed places and transitions, the corresponding Petri-Net can be developed (Fig. 4.3) and the reachability graph can be constructed (Table 4.6) for the initial marking, $M_0 = \begin{bmatrix} 1 & 0 & 0 & 0 & 1 & 1 & 1 \end{bmatrix}$. Here, s_i = previous state; s_j = next state; $r(t)$ = firing rate; q = transition probability determined from equation (3.25); t_k = firing transition.

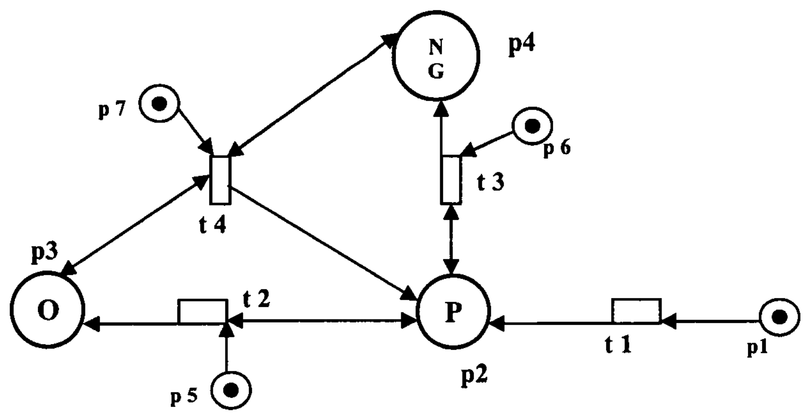

Fig. 4.3: Petri-Net model of the energy infrastructures (no lubricants)

Table 4.6: Reachability graph (scenario 1)

s_i	*Track*	t_k	*r(t)*	s_j	*Damaged infrastructures*	*q*
s_0		1	Deterministic	s1	P	1
s1	1	2	100	s2	P+O	.526
		3	90	s3	P+NG	.474
s2	1,2	3	90	s4	P+O+NG	1
s3	1,3	2	100	s4	P+NG+O	1
s4	1,2,3	4	40	s5	P+O+NG+P	1

This reachability graph shows the steps how all the infrastructures are disrupted one by one. The electricity disruption is the deterministic event (s1) in this network. The oil and natural gas plant will not be affected immediately, as they have backup power supplying generator with limited capacity for temporary use. After a certain period, the allocated fuel for these temporary generators will be consumed and the processing activities no longer can be continued. In this network, firing rate of oil disruption due to electricity outage is higher than that of natural gas plant. As a result, probability of oil plant disruption (s2) first is higher than that of natural gas plant (s3). If either oil or natural gas plant disrupts, the power plant will still has the backup fuel supply from the other. When both oil and natural gas plants disrupt, the power plant production activities will deteriorate due to the lack of fuel availability (s4). However, disruptions of the oil or natural gas plant have no impacts on each other in this network.

4.4.2 Scenario 2

In addition to the scenario 1, the power plant and natural gas plant depend on the oil refinery in the network for their generator and compressor lubricants supply, respectively. The places, transitions of the network are shown below (Tables 4.7 and 4.8) with which the Petri-Net can be developed (Fig 4.4). The corresponding reachability graph is constructed (Table 4.9) for the initial marking, $M_0 = 1\ 0\ 0\ 0\ 1\ 1\ 1\ 1\ 1$.

Table 4.7: List of places (scenario 2)

Place	Description
p1	Power plant is in service
p2	Power failure
p3	Oil plant is out of service
p4	Natural gas plant is out of service
p5	Power failure (dummy place for oil plant)
p6	Power failure (dummy place for natural gas plant)
p7	Oil (lubricant) production stop (dummy place for power plant)
p8	Oil (lubricant) production stop (dummy place for natural gas plant)
p9	Oil and natural gas (fuel) production stop (dummy place for power plant)

Table 4.8: List of transitions (scenario 2)

Transition	Description	Firing rate
t1	'Electric power' is disrupted	Deterministic
t2	'Power failure' affects oil plant	100
t3	'Power failure' affects natural gas plant	90
t4	'Oil (lubricant) production stop' affects power plant	20
t5	'Oil (lubricant) production stop' affects natural gas plant	25
t6	'Oil and natural gas (fuel) production stop' affects power plant	40

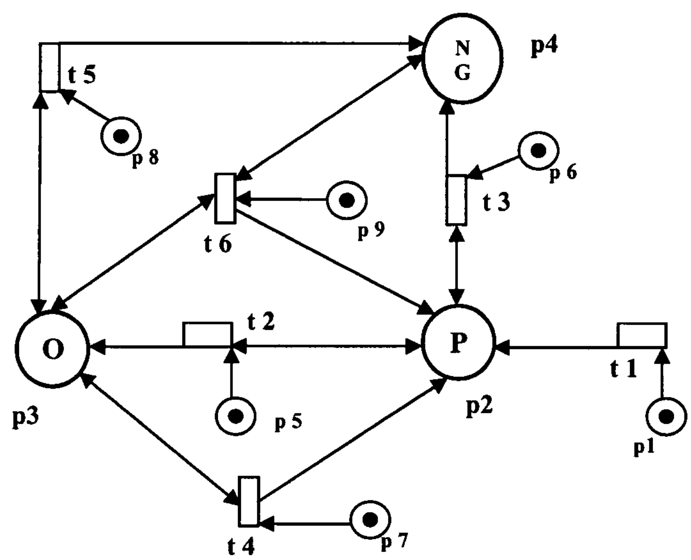

Fig. 4.4: Petri-Net model of the energy infrastructures (with lubricants)

Table 4.9: Reachability graph (scenario 2)

s_i	*Track*	t_k	*r(t)*	s_j	*Damaged infrastructures*	*q*
s_0		1	Deterministic	s1	P	1
s1	1	2	100	s2	P+O	.526
		3	90	s3	P+NG	.474
s2	1,2	3	90	s4	P+O+NG	.667
		4	20	s5	P+O+P	.148
		5	25	s6	P+O+NG	.185
s3	1,3	2	100	s4	P+NG+O	1
s4	1,2,3	4	20	s7	P+O+NG+P	.235
		5	25	s8	P+O+NG+NG	.294
		6	40	s9	P+O+NG+P	.471
s5	1,2,4	3	90	s7	P+O+P+NG	.783
		5	25	s10	P+O+P+NG	.217
s6	1,2,5	3	90	s8	P+O+NG+NG	.6
		4	20	s10	P+O+NG+P	.133
		6	40	s11	P+O+NG+P	.267
s7	1,2,3,4	5	25	s12	P+O+NG+P+NG	.385
		6	40	s13	P+O+NG+P+P	.615
s8	1,2,3,5	4	20	s12	P+O+NG+NG+P	.333
		6	40	s14	P+O+NG+NG+P	.667
s9	1,2,3,6	4	20	s13	P+O+NG+P+P	.444
		5	25	s14	P+O+NG+P+NG	.556
s10	1,2,4,5	3	90	s12	P+O+P+NG+NG	.692
		6	40	s15	P+O+P+NG+P	.308
s11	1,2,5,6	3	90	s14	P+O+NG+P+NG	.818
		4	20	s15	P+O+NG+P+P	.182
s12	1,2,3,4,5	6	40	s16	P+O+NG+P+NG+P	1
s13	1,2,3,4,6	5	25	s16	P+O+NG+P+P+NG	1
s14	1,2,3,5,6	4	20	s16	P+O+NG+NG+P+P	1
s15	1,2,4,5,6	3	90	s16	P+O+P+NG+P+NG	1

The reachability graph of this scenario shows how the network analysis becomes highly complex due to the inclusion of lubricants supply from the oil plant in the same network as the scenario 1. Here also, the electricity disruption is the deterministic event. In this case, if the oil plant is out of service due to electricity outage (s2), the lubricants supply to the power plant and natural gas plant will be stopped (s5, s6). Also, the fuel contribution from oil plant cannot be expected; moreover, the natural gas plant will be disrupted in course of time as it has no lubricants for its compressor, and consequently, fuel supply will also not be available (s4) which may also happen if electricity outage hampers natural gas production (s3) and oil refining activities. In this stage, all the infrastructures are disrupted; consequently, their conditions are deteriorated due to the interactions among each other which have been shown in the reachability graph above. For example, when both oil and natural gas processing stops (s4), consequently, the network infrastructures face significant impacts, such as the power plant will deteriorate due to the lack of lubricants and fuels (s7, s9); natural gas compressor cannot have lubricants (s8). When all the possible interactions occur, the network execution stops. It can be said form the network analysis that only oil plant disruption will pose the cascading impacts in the network. In this case, the energy infrastructures are more coupled and more vulnerable than that in scenario 1.

4.4.3 Scenario 3

This scenario also adds another feature in the network of scenario 1. In this case, the nodal infrastructures in the network are the energy infrastructures power plant, oil refinery, natural gas plant, and the fuel transporting infrastructures. The lubricants supply from the same refinery is not considered. The fuel transporting infrastructures such as tank and pipelines are included in the network. The places and transitions of the network are given at Tables 4.10 and 4.11, respectively. The developed Petri-Net is shown in Figure 4.5. The initial marking of the network is,

$$M_0 = 1\ 0\ 0\ 0\ 0\ 0\ 1\ 1\ 1\ 1\ 1\ 1\ 1$$

Table 4.10: List of places (scenario 3)

Place	Description
p1	Power plant is in service
p2	Power failure
p3	Oil plant is out of service
p4	Natural gas plant is out of service
p5	Fuel transporting pipe is disrupted
p6	Tank is out of service
p7	Power failure (dummy place for oil plant)
p8	Power failure (dummy place for natural gas plant)
p9	Power failure (dummy place for fuel transporting pipe)
p10	Oil and natural gas fuels production stop (dummy place for power plant)
p11	Oil and natural gas fuels production stop (dummy place for tank transport)
p12	Fuel transporting pipe and tank disruption (dummy place for power plant)
p13	Fuel transporting pipe and tank disruption (dummy place for oil plant)

Table 4.11: List of transitions (scenario 3)

Transition	Description	Firing rate
t1	'Electric power' is disrupted	Deterministic
t2	'Power failure' affects oil plant	100
t3	'Power failure' affects natural gas plant	90
t4	'Power failure' affects fuel transporting pipe	immediate
t5	'Oil and natural gas (fuel) production stop' affects power plant	40
t6	'Oil and natural gas (fuel) production stop' affects tank transport	25
t7	'Fuel transporting pipe and tank disruption' affect power plant	50
t8	'Fuel transporting pipe and tank disruption' affect oil plant	60

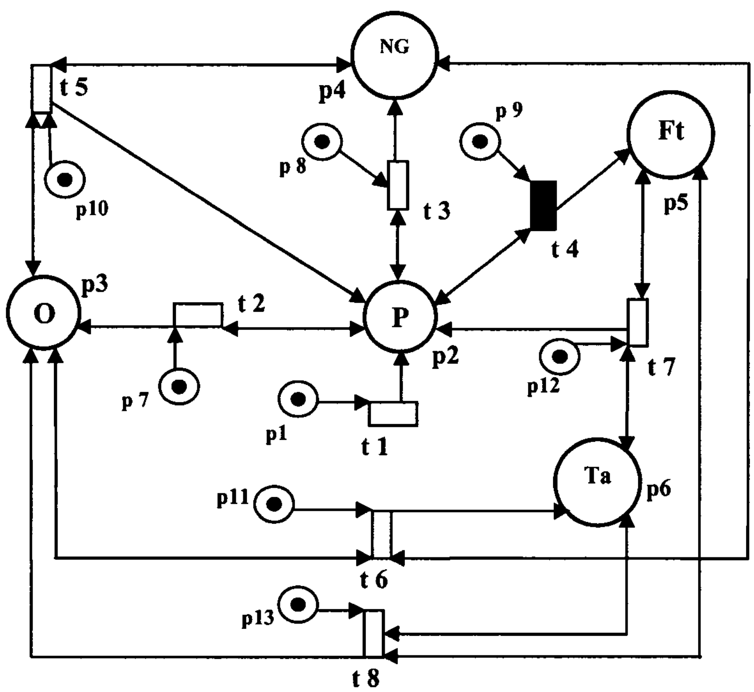

Fig. 4.5: Petri-Net model of the fuel transporting and energy infrastructures

Table 4.12: Reachability graph (scenario 3)

s_i	*Track*	t_k	*r(t)*	s_j	*Damaged infrastructures*	*q*
s_0		1	Deterministic	s1	P+Ft	1
s1	1,4	2	100	s2	P+Ft+O	.526
		3	90	s3	P+Ft+NG	.473
s2	1,4,2	3	90	s4	P+Ft+O+NG	1
s3	1,4,3	2	100	s4	P+Ft+NG+O	1
s4	1,4,2,3	5	40	s5	P+Ft+O+NG+P	.615
		6	25	s6	P+Ft+O+NG+Ta	.385
s5	1,4,2,3,5	6	25	s7	P+Ft+O+NG+P+Ta	1
s6	1,4,2,3,6	5	40	s7	P+Ft+O+NG+Ta+P	.267
		7	50	s8	P+Ft+O+NG+Ta+P	.333
		8	60	s9	P+Ft+O+NG+Ta+O	.4
s7	1,4,2,3,6,5	7	50	s10	P+Ft+O+NG+Ta+P+P	.455
		8	60	s11	P+Ft+O+NG+Ta+P+O	.546
s8	1,4,2,3,6,7	5	40	s10	P+Ft+O+NG+Ta+P+P	.4
		8	60	s12	P+Ft+O+NG+Ta+P+O	.6
s9	1,4,2,3,6,8	5	40	s11	P+Ft+O+NG+Ta+O+P	.445
		7	50	s12	P+Ft+O+NG+Ta+O+P	.555
s10	1,4,2,3,6,5,7	8	60	s13	P+Ft+O+NG+Ta+P+P+O	1
s11	1,4,2,3,6,5,8	7	50	s13	P+Ft+O+NG+Ta+P+O+P	1
s12	1,4,2,3,6,7,8	5	40	s13	P+Ft+O+NG+Ta+O+P	1

This network analysis addresses the role of fuel transporting pipes in the network. It is evident that when electricity outage occurs, the pipeline disruption will occur immediately compared to the other events in the network. So, the event of electricity outage and pipeline disruption (s1) is deterministic in the current analysis. Initially, the electricity outage will hamper the oil and natural gas processing activities. In this condition, fuel transporting pipes cannot hamper the fuel supply to the power plant or oil plant as there is tank as backup for fuel transportation. However, with time, the oil and natural gas plants have to be shutdown as the backup generator will consume the allocated fuel and there will be no electricity supply for continuing processing activities (s2, s3). The resulting fuel supply shutdown (s4) ultimately is going to deteriorate the power plant; the tank transport will also be disrupted when it finishes its fuel storage (s5, s6), which leads to s7 when both happen. For tank disruption (s6), it is not possible to carry the fuel to the power plant (s8) from oil and natural gas plant and crude oil to the oil refinery from the production site (s9) as both the tank and fuel transport pipes are not functional; s7 also pose the same impacts leading to the conditions s10 and s11. The state s8 consequently deteriorates the power plant to reach the state s10, and s12 which at the end, reach the absorbing state (s13) by deteriorating the oil and power plant from tank-fuel pipe disruption and fuel depletion, respectively which indicates that disruptions of all the infrastructures and interactions have been simulated for one run. State s9 reaches states s11 and s12 deteriorating the power plant resulting from fuel depletion and fuel transporting problem, respectively, and reaches the absorbing state s13 where deterioration from s11 comes from the fuel transporting problem for power plant. However, as there is no recovery strategy in the net, the network execution will stop here.

Comparing the above three scenarios, it is evident that, if the network infrastructures depend on the multiple services provided by the other infrastructures in the same network, their coupling will be higher and disruption in one infrastructure will cause cascading impacts on the interconnected infrastructures due to their interactions. The backup system in the network as well as receiving services from infrastructures outside the network will reduce the vulnerability. For example, the oil and natural gas plant should receive electricity supply from different grids, so that outage in one grid will not cause total shutdown of the plants. If the power plant and natural gas plant receive lubricants supply from the same oil refinery in the network, they should have access to the other sources in case of emergency to avoid disruptions.

4.5 Markov Chain development and analysis

In the previous section, the reachability graphs for three different scenarios have been determined using extended analysis of SPN. From the previous chapter, it is known that for timed Petri-Net, Markov Chain of the network can be developed from its reachability graph. For illustration, second scenario has been chosen for developing the Markov Chain. In this case, the Petri-Net consists of the three energy infrastructures, power, oil refinery and natural gas plants; the power plant receives its fuel supply from oil and natural gas plant, lubricants from same oil refinery, and oil-gas plants depend on power plant for the power supply for production and other activities. The developed Markov Chain for this scenario is shown below:

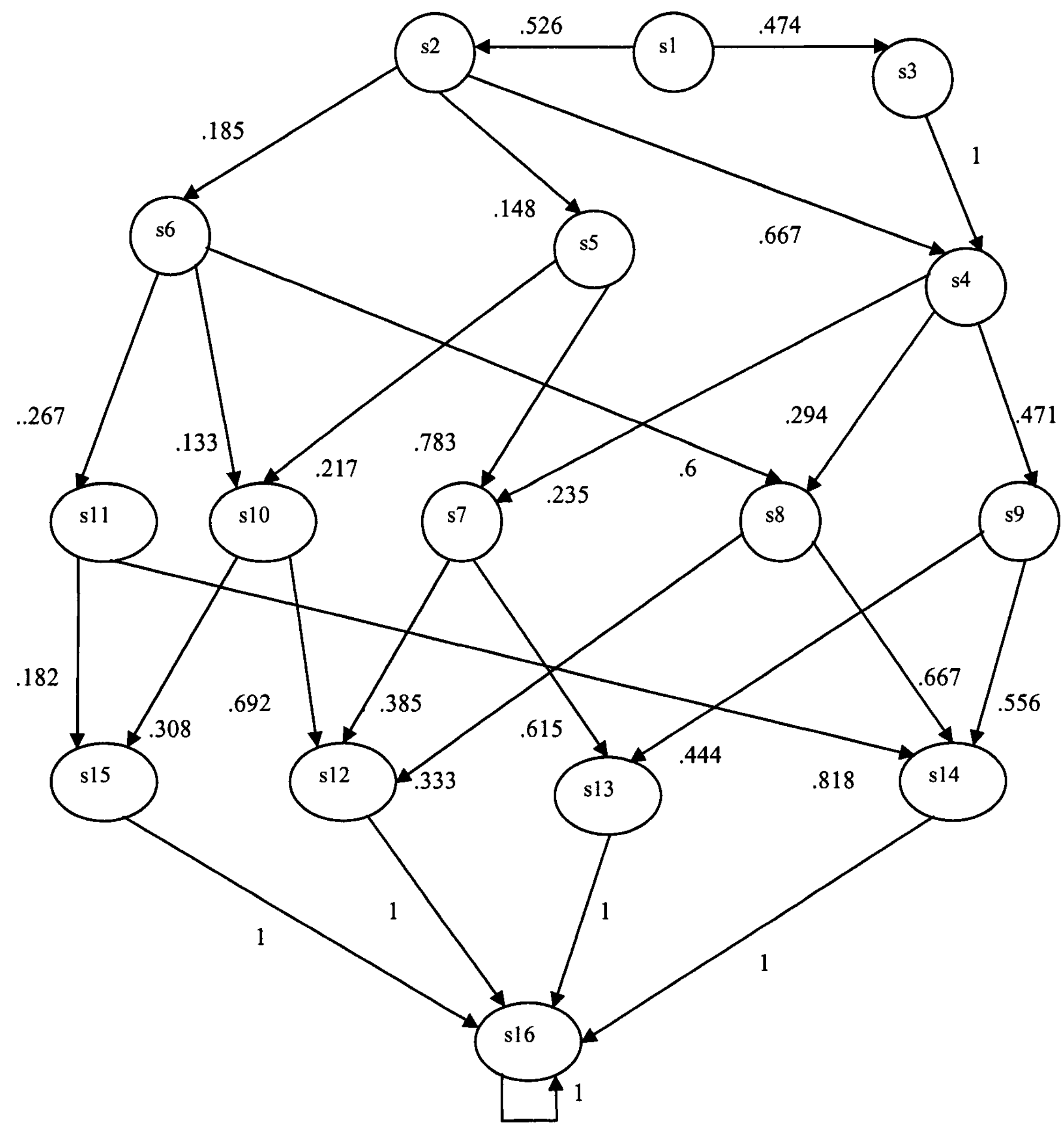

Fig. 4.6: Markov Chain (scenario 2)

4.5.1 Transition matrix

The transition matrix *(T_r)* can be generated from the above Markov Chain. The initial state matrix p is assigned with the assumption that, initially, the probability of state 1 is '1', and the probabilities of the remaining states are 'zero'. With these two parameters, T_r and p, the steady state probabilities of the states are calculated.

The transition matrix, T_r =

States	*s*1	*s*2	*s*3	*s*4	*s*5	*s*6	*s*7	*s*8	*s*9	*s*10	*s*11	*s*12	*s*13	*s*14	*s*15	*s*16
*s*1	0	.526	.474	0	0	0	0	0	0	0	0	0	0	0	0	0
*s*2	0	0	0	.667	.148	.185	0	0	0	0	0	0	0	0	0	0
*s*3	0	0	0	1	0	0	0	0	0	0	0	0	0	0	0	0
*s*4	0	0	0	0	0	0	.235	.294	.471	0	0	0	0	0	0	0
*s*5	0	0	0	0	0	0	.783	0	0	.217	0	0	0	0	0	0
*s*6	0	0	0	0	0	0	0	.6	0	.133	.267	0	0	0	0	0
*s*7	0	0	0	0	0	0	0	0	0	0	0	.385	.615	0	0	0
*s*8	0	0	0	0	0	0	0	0	0	0	0	.333	0	.667	0	0
*s*9	0	0	0	0	0	0	0	0	0	0	0	0	.444	.556	0	0
*s*10	0	0	0	0	0	0	0	0	0	0	0	.692	0	0	.308	0
*s*11	0	0	0	0	0	0	0	0	0	0	0	0	0	.818	.182	0
*s*12	0	0	0	0	0	0	0	0	0	0	0	0	0	0	0	1
*s*13	0	0	0	0	0	0	0	0	0	0	0	0	0	0	0	1
*s*14	0	0	0	0	0	0	0	0	0	0	0	0	0	0	0	1
*s*15	0	0	0	0	0	0	0	0	0	0	0	0	0	0	0	1
*s*16	0	0	0	0	0	0	0	0	0	0	0	0	0	0	0	1

Initial state matrix, p = 1 0 0 0 0 0 0 0 0 0 0 0 0 0 0 0

Now, for calculating the steady state probabilities, p will be multiplied with successive powers of T_r until the steady state is reached. The calculations are as follows:

Table 4.13: Steady state probability (scenario 2)

	*s*1	*s*2	*s*3	*s*4	*s*5	*s*6	*s*7	*s*8	*s*9	*s*10	*s*11	*s*12	*s*13	*s*14	*s*15	*s*16
p	1	0	0	0	0	0	0	0	0	0	0	0	0	0	0	0
$p*T_r$	0	.526	.474	0	0	0	0	0	0	0	0	0	0	0	0	0
$p*T_r^2$	0	0	0	.825	.078	.097	0	0	0	0	0	0	0	0	0	0
$p*T_r^3$	0	0	0	0	0	0	.255	.301	.388	.03	.026	0	0	0	0	0
$p*T_r^4$	0	0	0	0	0	0	0	0	0	0	0	.219	.329	.438	.014	0
$p*T_r^5$	0	0	0	0	0	0	0	0	0	0	0	0	0	0	0	1
$p*T_r^6$	0	0	0	0	0	0	0	0	0	0	0	0	0	0	0	1

Here, $p* T_r^5 = p* T_r^6$. So, the Markov Chain attains the steady state at $p* T_r^5$.

The above result shows that the state s16 will be attained at steady state, which is compatible as it indicates that all the infrastructures are disrupted in the course of time. The model result also shows that disruption of all the infrastructures in the network are induced even by single infrastructure disruption. In this model, the recovery strategy is not considered which means the infrastructures do not recover if they are disrupted once. For this reason, the steady state should indicate that all the infrastructures are disrupted which has been captured from the model result.

4.5.2 Extended analysis of Markov Chain

In this Markov Chain, there is only one absorbing state, s16. The behavior of the network can further be analyzed with the analysis of the effects of the existence of the absorbing state in the network. First, the transition matrix, T_r can be divided into transient state and absorbing state in the canonical form,

$$T_r = \begin{array}{ccc} Q & \vdots & R \\ \cdots & \vdots & \cdots \\ 0 & \vdots & I \end{array}$$

Here '*I*' is 1-by-1 identity matrix, *0* is a 1-by-15 zero matrix, *R* is a 15-by-1 matrix, and Q is a 15-by-15 matrix. In this case,

$Q =$

0	.526	.474	0	0	0	0	0	0	0	0	0	0	0	0
0	0	0	.667	.148	.185	0	0	0	0	0	0	0	0	0
0	0	0	1	0	0	0	0	0	0	0	0	0	0	0
0	0	0	0	0	0	.235	.294	.471	0	0	0	0	0	0
0	0	0	0	0	0	.783	0	0	.217	0	0	0	0	0
0	0	0	0	0	0	0	.6	0	.133	.267	0	0	0	0
0	0	0	0	0	0	0	0	0	0	0	.385	.615	0	0
0	0	0	0	0	0	0	0	0	0	0	.333	0	.667	0
0	0	0	0	0	0	0	0	0	0	0	0	.444	.556	0
0	0	0	0	0	0	0	0	0	0	0	.692	0	0	.308
0	0	0	0	0	0	0	0	0	0	0	0	0	.818	.182
0	0	0	0	0	0	0	0	0	0	0	0	0	0	0
0	0	0	0	0	0	0	0	0	0	0	0	0	0	0
0	0	0	0	0	0	0	0	0	0	0	0	0	0	0
0	0	0	0	0	0	0	0	0	0	0	0	0	0	0

$R^T = 0 \ 0 \ 0 \ 0 \ 0 \ 0 \ 0 \ 0 \ 0 \ 0 \ 0 \ 1 \ 1 \ 1 \ 1$

(i) The fundamental matrix is, $N = (I - Q)^{-1}$, or, $N =$

$N =$

states	*s*1	*s*2	*s*3	*s*4	*s*5	*s*6	*s*7	*s*8	*s*9	*s*10	*s*11	*s*12	*s*13	*s*14	*s*15
*s*1	1	.526	.474	.825	.078	.097	.255	.301	.388	.03	.026	.219	.329	.438	.014
*s*2	0	1	0	.667	.148	.185	.273	.307	.314	.057	.049	.246	.307	.42	.026
*s*3	0	0	1	1	0	0	.235	.294	.471	0	0	.188	.354	.458	0
*s*4	0	0	0	1	0	0	.235	.294	.471	0	0	.188	.354	0	0
*s*5	0	0	0	0	1	0	.783	0	0	.217	0	.451	.482	0	.067
*s*6	0	0	0	0	0	1	0	.6	0	.133	.267	.292	0	.619	.09
*s*7	0	0	0	0	0	0	1	0	0	0	0	.385	.615	0	0
*s*8	0	0	0	0	0	0	0	1	0	0	0	.333	0	.667	0
*s*9	0	0	0	0	0	0	0	0	1	0	0	0	.444	.556	0
*s*10	0	0	0	0	0	0	0	0	0	1	0	.692	0	0	.308
*s*11	0	0	0	0	0	0	0	0	0	0	1	0	0	.818	.182
*s*12	0	0	0	0	0	0	0	0	0	0	0	1	0	0	0
*s*13	0	0	0	0	0	0	0	0	0	0	0	0	1	0	0
*s*14	0	0	0	0	0	0	0	0	0	0	0	0	0	1	0
*s*15	0	0	0	0	0	0	0	0	0	0	0	0	0	0	1

The first row of the above result indicates that if we start in state 1, then the expected number of times in states 1, 2, 3,...,15 before being absorbed are 1, .526, .474,......., .0139 . The remaining rows imply the same interpretations.

(ii) If t_i be the expected number of steps before the chain is absorbed in state 16, given that the chain starts in state s_i, and let 't' be the 15-by-1 column vector whose i^{th} entry is t_i, then, $t = N * c$, where, c is a 15-by-1 column vector all of whose entries are 1,

$c^T =$ 1 1 1 1 1 1 1 1 1 1 1 1 1 1 1

Then,

$t^T =$

s1	s2	s3	s4	s5	s6	s7	s8	s9	s10	s11	s12	s13	s14	s15
5	4	4	3	3	3	2	2	2	2	2	1	1	1	1

(iii) B_{ij} is the probability that an absorbing chain will be absorbed in the absorbing state s_j if it starts in the transient state s_i. Let B be the matrix with entries B_{ij}. Then, $B = N * R$

or,

$B =$

s1	s2	s3	s4	s5	s6	s7	s8	s9	s10	s11	s12	s13	s14	s15
1	1	1	1	1	1	1	1	1	1	1	1	1	1	1

As, there is only one absorbing state in the network, the result shows that from each transient state, the probability of reaching at the absorbing state s16 is 1.

4.6 Summary

This chapter illustrates the urban infrastructure interdependency with a case study of California electricity outage in 2001 which occurred due to the myopic financial planning of reviving the electricity market. However, the plan made the market unrest in the long run. Only five years after the implementation of the plan of competitive electricity generation and selling, it triggered a serious electricity crisis in the state which consequently hampered the operation of the other energy infrastructures, e.g. oil and natural gas plant, energy transporting systems, e.g. tank and pipelines, municipal water system, telecom, etc. The problem was propagated more as the electricity sector itself is dependent on the services provided by these infrastructures for its power generation activities.

A basic Petri-Net model was developed for this case study to capture the interdependencies among these infrastructures. The place invariants of the constructed Petri-Net captured their interactions accurately. Later, extended network analysis was applied into the part of the basic Petri-Net model for a comparative study of three different case scenarios. One scenario demonstrated the interdependencies among the energy infrastructures, such as electricity, oil, and natural gas. In this scenario, it was assumed that the electricity sector depends on the other two infrastructures only for its generator fuel supply; oil and natural gas sectors depend on the electricity supply for their production activities; the power plant and natural gas plant receive their lubricants supply from other sources outside the network. The second scenario deals with the same infrastructures and same interdependencies; additionally, it was assumed that the oil plant supplies the required lubricants to the power plant generator and natural gas compressor. The third scenario is an extension of scenario one where, additionally, the energy transporting infrastructures, e.g. tank and pipelines, were included in the network. Comparison of the reachability graphs of these three scenarios showed how the network analysis becomes more complicated with the addition of either infrastructures or interdependencies in the network. The results also indicate that interdependencies among the infrastructures in the same network should be reduced to minimize the vulnerability. For example, in the first case, if only the oil plant is disrupted, neither the power plant nor the natural gas plant has to stop their production activities. On the other hand, in the second case, if only oil production stops, electricity outage will occur after a certain time as the power plant is dependent on oil lubricants for its generator; also, the natural gas plant has to be shut down as its compressor lubricants deplete with time. When the crude oil, refined oil, liquefied and compressed natural gas carrying tank and pipelines are disrupted, the power plant and oil plant cannot continue their production activities as the power plant has no fuel to run its generator, and the oil plant has no crude oil to refine. However, in most cases, the natural gas plant is near its production site and outage of the energy transporting infrastructures has no direct impacts on it.

The three scenarios accounted for the cascading deterioration of the infrastructures once a single infrastructure is disrupted. Markov Chain was applied in scenario 2 to show how to determine the steady state probability of the possible states of the network. The results showed that in course of time, all the infrastructures will be disrupted as they are interconnected. The results are compatible in the sense that the recovery strategy was not included in the network, and at steady state, all the infrastructures will be disrupted. It was discussed that reducing the degree of coupling between the infrastructures and ensuring the backup systems could significantly reduce the infrastructure vulnerability.

Chapter 5: Integration of the Modeling of Infrastructure Interdependency with Vulnerability Assessment - Canyon Ferry Floodplain Area

Flood occupies the highest rank among natural disasters in respect of their adverse impacts (Isomina et al. 2005). Most of the flood in a floodplain area starts its primary impact with the failure of a dam or levee. For example, flooding from levee failures due to Hurricane Katrina set in motion an unanticipated failure of multiple infrastructure systems in the City of New Orleans that resulted from the complex interactions among interdependent infrastructures (Leavitt and Kiefer 2006).

This chapter presents the application of the integrated approach of modeling flood-related infrastructure interdependency in a case study of the Canyon Ferry Dam at the Missouri Basin in Montana with the other surrounding infrastructures (U.S. Department of the Interior 2007). It is intended to examine the vulnerabilities of critical water infrastructures for emergency management in this region. Related theories and methodologies have been discussed in Chapter three which comprises of the flood frequency analysis, fragility curves analysis, development of Petri-Net model and its extended analysis, Markov Chain development and analysis, and their integration. Flood frequency analysis is done with both Gumbel's method and Log Pearson Type III method with 52 years water level data in Canyon Ferry reservoir, vulnerability of the Canyon Ferry Dam due to flood is quantified through fragility curves development; the consequent cascading effects on infrastructures are simulated using Petri-Net and its extended analysis; for predicting the long term conditions of the infrastructures, Markov

Chain analysis will be performed. Both empirical and analytical fragility curves will be developed using observed flood hazard information, hydraulic modeling of dam failure, and Monte Carlo simulation.

5.1 Flood frequency analysis

The statistical methods are applied widely for flood frequency analysis. Mostly, the Gumbel method and Log Pearson Type III (LP III) method are used. The Canyon Ferry Dam of the case study area was built in between 1949 to 1954. The reservoir started filling up from the year 1953, and attained a steady state in 1955. A 52-year reservoir forebay peak elevation data is available from the United States Bureau of Reclamation which is updated everyday. The streambed elevation near the dam is 1108.68 m. The peak water levels are given in Table 5.1. Flood frequency analysis will be performed with both the Gumbel's method and LP III method.

Table 5.1: Reservoir forebay elevation data from 1955 to 2006 at Canyon Ferry Lake, Missouri River near Helena, Montana

Year	Peak value of gauge elevation (ft)	Peak value of gauge height (ft)	Peak value of gauge height, x (m)	Year	Peak value of gauge elevation (ft)	Peak value of gauge height (ft)	Peak value of gauge height, x (m)
1955	3800	163.5	49.848	1981	3799.66	163.16	49.744
1956	3800	163.5	49.848	1982	3798.81	162.31	49.485
1957	3799.23	162.73	49.613	1983	3798.28	161.78	49.323
1958	3798.9	162.4	49.512	1984	3799.14	162.64	49.585
1959	3799.88	163.38	49.811	1985	3791.66	155.16	47.305
1960	3799.94	163.44	49.829	1986	3797.25	160.75	49.009
1961	3788.43	151.93	46.32	1987	3792.89	156.39	47.68
1962	3800	163.5	49.848	1988	3791.91	155.41	47.381
1963	3799.7	163.2	49.756	1989	3785.88	149.38	45.543
1964	3800	163.5	49.848	1990	3794.37	157.87	48.131
1965	3799.93	163.43	49.826	1991	3798.02	161.52	49.244
1966	3798.58	162.08	49.415	1992	3786.79	150.29	45.82
1967	3798.3	161.8	49.329	1993	3797.92	161.42	49.213
1968	3797.14	160.64	48.976	1994	3794.73	158.23	48.241
1969	3797.63	161.13	49.125	1995	3798.83	162.33	49.491
1970	3797.14	160.64	48.976	1996	3797.85	161.35	49.192
1971	3797.47	160.97	49.076	1997	3798.49	161.99	49.387
1972	3797.34	160.84	49.037	1998	3799.38	162.88	49.659
1973	3796.55	160.05	48.796	1999	3796.8	160.3	48.872
1974	3798.65	162.15	49.436	2000	3790.12	153.62	46.835
1975	3799.93	163.43	49.826	2001	3789.5	153	46.646
1976	3798.22	161.72	49.305	2002	3796.49	159.99	48.777
1977	3797.09	160.59	48.96	2003	3797.66	161.16	49.134
1978	3797.93	161.43	49.216	2004	3786.27	149.77	45.662
1979	3796.19	159.69	48.686	2005	3798.51	162.01	49.393
1980	3799.18	162.68	49.598	2006	3796.36	159.86	48.738

5.1.1 Gumbel's distribution

The mean and standard deviation of the peak water level are 48.833 and 1.156, respectively. With these values and using equation (3.2), the predicted flood levels are found to be as follows (Table 5.2):

Table 5.2: Flood frequency analysis by Gumbel's method

T (year)	P = 1/T	T/(T-1)	y_T	y_n	s_n	K	Gauge height, x_T = mean x + $K*S_n$
2	0.5	2	0.3665	0.5493	1.1638	-0.1570	48.6512
10	0.1	1.111	2.2503			1.4616	50.5226
25	0.04	1.041	3.1985			2.2764	51.4645
50	0.02	1.020	3.9019			2.8808	52.1633
100	0.01	1.010	4.6001			3.4807	52.8569
200	0.005	1.005	5.2958			4.0785	53.5480
1000	0.001	1.001	6.9072			5.4631	55.1488

5.1.2 Log Pearson Type III distribution

The same data are used to simulate the flood frequency by LP III method. Here the calculations are carried out taking the 10 based logarithms of water levels. Using the equation (3.4), the value of skew coefficient C_s is found to be -1.6734. The value of K is interpolated. The calculated flood levels with equation (3.5) are given at Table 5.3.

Table 5.3: Flood frequency analysis by LP III method

T (year)	P = 1/T	Upper value of C_s	Lower value of C_s	Upper value of K	Lower value of K	K_z	K_z*Std	z_T	x_T
2	0.5	-1.4	-1.8	0.282	0.225	0.243	0.0025	1.691	49.106
10	0.1	-1.4	-1.8	1.041	0.945	0.9754	0.0102	1.698	49.982
25	0.04	-1.4	-1.8	1.198	1.035	1.0866	0.0114	1.700	50.116
50	0.02	-1.4	-1.8	1.27	1.069	1.1326	0.0119	1.700	50.172
100	0.01	-1.4	-1.8	1.318	1.087	1.1601	0.0122	1.700	50.205
200	0.005	-1.4	-1.8	1.351	1.097	1.1774	0.0123	1.700	50.226
1000	0.001	-1.4	-1.8	1.465	1.13	1.236	0.013	1.701	50.297

The above results show that the Gumbel's method is more conservative than LP III method for this case. Difference between the predicted water levels by these two methods is well below than 20 % for each predicted water levels, which indicates that the results are quite satisfactory (ConnDOT Drainage Manual, 2000). The available water data shows no anomaly or unexpected high water levels. It should be noted that the dam had been operating for 52 years only, and in future, any kind of extreme event might happen which could change the prediction results.

5.2 Fragility analysis of Canyon Ferry Dam

The Canyon Ferry dam is a concrete gravity dam with 52.5 m height above the streambed, top width is 6 m, base width is 40 m, the crest length is 305 m, the upstream face is vertical, and the downstream face slope is 1: 1.3 (H:V). The dam is more than 50 years old. Both empirical and analytical fragility curves developments will be demonstrated in this chapter.

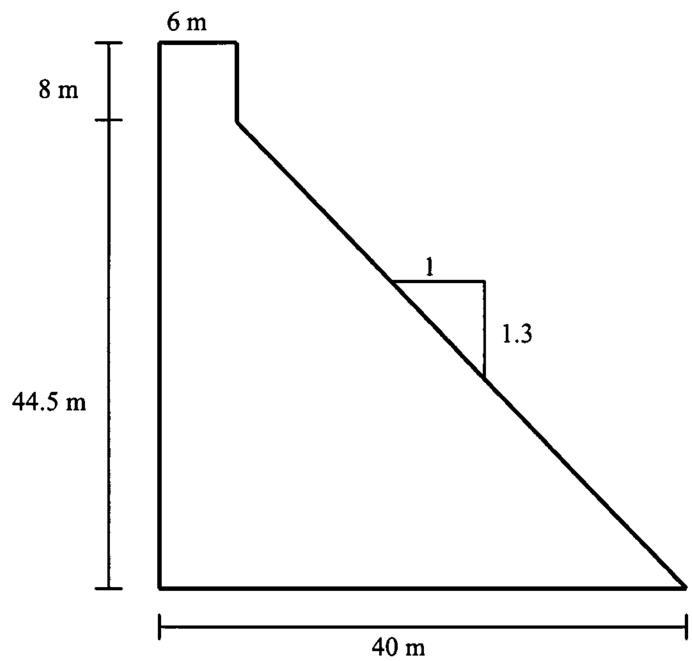

Fig. 5.1: Cross section of the Canyon Ferry dam

5.2.1 Empirical fragility curves

Deteriorated conditions of a dam are considered as 'damage' and flood levels are denoted as 'hazard'. Four damage states of infrastructures are specified by HAZUS (Multihazard Loss Estimation Methodology) as, slight, moderate, severe or extensive, and complete or collapse (O'Rourke et al. 2000). In this study, these four damage classifications are extended according to the hypothetical damage conditions of the structure. Several failure modes of a concrete gravity dam were observed, which have been discussed before (Malla and Wieland 1999, Shayan and Grimstad 2006).

There are different failure scenarios of a dam. If the impacts on a dam are severe enough, minor cracks are developed initially; if no remedial action is taken, the cracks spread out through the dam and become more prominent. Gradually, the concrete sloughs especially from the upstream side of the dam under higher level of hazard. When the damage level reaches at the extreme, fissures can be created through which seepage can take place. Therefore, the damage states can be classified in this study as,

[i] Slight damage state (D1) = minor cracks,

[ii] Moderate damage state (D2) = prominent cracks,

[iii] Severe or extensive damage state (D3) = concrete sloughing, and,

[iv] Collapsed damage state (D4) = seepage through dam.

With the above analysis and following the steps described in the section 3.2.2.1 of Chapter 3, the probability data of different damage states are generated. For example, out of 624 observations, the number of the occurrence of a water level of 44 m or more at the upstream of a dam is 563, and the number of incidents that the dam experiences minor cracks is 187; the occurrence number of other damage states is zero; then, following the equation (3.6), the probability of reaching at the damage state of minor cracks is:

$$P[damage|WL] = \frac{P[damage \bigcap WL]}{P[WL]} = \frac{\frac{187}{624}}{\frac{562}{624}} = \frac{187}{562} = 0.333$$

In the similar way, a set of damage states probabilities dataset are generated for water levels upto 50 m (Table 5.4).

Table 5.4: Generated probability from hypothetical data

Water level	Minor cracks	Prominent cracks	Concrete sloughing	Seepage
38	0	0	0	0
38.5	0	0	0	0
39	0	0	0	0
39.5	0	0	0	0
40	0	0	0	0
40.5	0	0	0	0
41	0	0	0	0
41.5	0	0	0	0
42	0	0	0	0
42.5	0.035	0	0	0
43	0.1	0	0	0
43.5	0.2	0	0	0
44	0.333	0	0	0
44.5	0.475	0	0	0
45	0.67	0	0	0
45.5	0.84	0.03	0	0
46	0.968	0.08	0	0
46.5	1	0.16	0.02	0
47	1	0.3	0.062	0
47.5	1	0.473	0.13	0
48	1	0.64	0.25	0.0445
48.5	1	0.757	0.4	0.125
49	1	0.843	0.57	0.267
49.5	1	0.91	0.7	0.412
50	1	0.95	0.79	0.53

With this dataset, a set of empirical fragility curves of dam are developed for the four damage states (i.e., D1 – D4) as provided in Figure 5.2. It indicates that, probability of 'minor cracks' initiates at 42.5 m water level and reaches to 1 after 46.5 m. The other damage states don't reach to a probability 1 upto the 50 m water level. Probability of damage state 'prominent cracks' starts at 45.5 m and reaches to a probability of 0.95, the concrete sloughing probability starts at 46.5 m and reaches a probability of 0.79, and seepage probability starts at 48 m and reaches to 0.53 at 50 m water level.

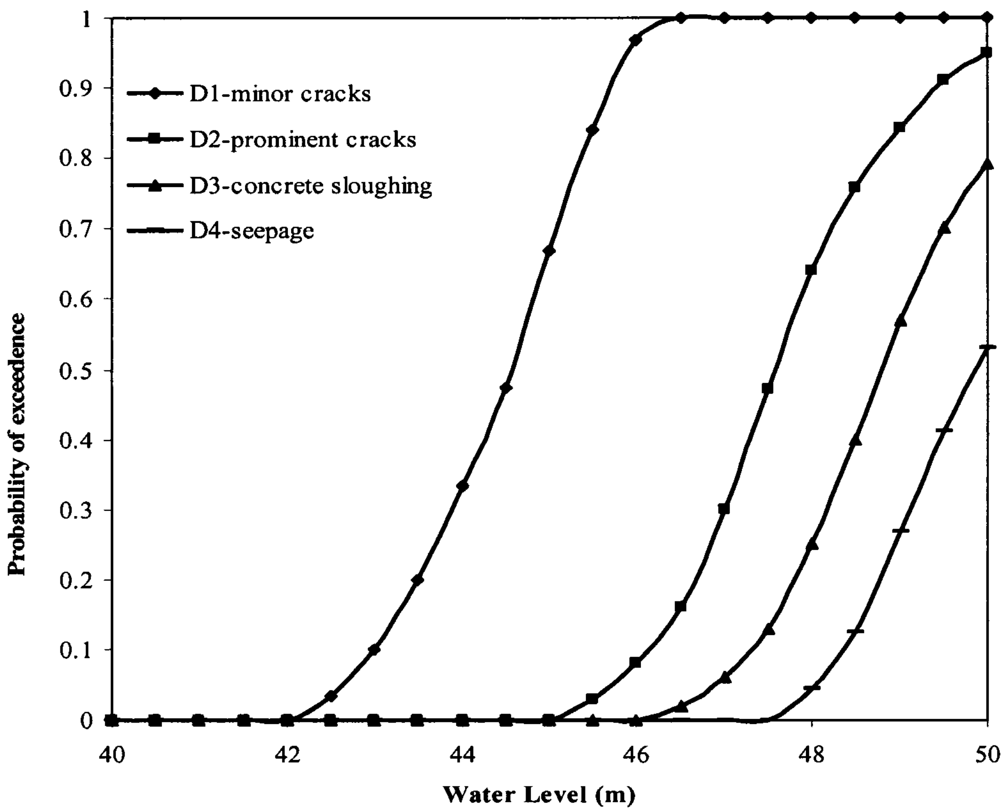

Fig. 5.2: Empirical fragility curves of dam

5.2.2 Analytical fragility curves

For developing the analytical fragility curves of the dam, first the hydraulic modeling of dam failure is performed, then, the probability data of different damage states are generated from the model outputs. The dam is analyzed to determine its failure modes for different water levels. In the structural failure modeling of the dam, two failure modes are considered in this study which are,

[i] Dam is failed due to overturning with respect to its toe; and

[ii] Dam is failed from sliding due to the shear failure along the intersection of the dam and the foundation.

For both types of failures, the factor of safety with a value greater than 1 is desirable. The inverse of the factor of safety is used in this study for the ease of analysis. If the corresponding probability of inverse factor of safety exceeds 1, a deteriorated condition of the dam is implied. Applying the steps in section 3.2.2.2, the analytical fragility curves development for the study case follows the steps,

[i] Classifying the damage states of the dam.

Here, we have two failure modes; two other damage states are also considered where the undesirable design conditions are matter of concern. From the literature, the overturning factor of safety is accepted for the value of around 2, the value for sliding factor of safety is 1 - 1.5 (Linsley and Franzini, 1992). In this study, overturning factor of safety at 1.5 and sliding factor of safety at 1.25 are checked where the values of IFS_o and IFS_s values are 0.667 and 0.8, respectively.

[ii] Hydraulic modeling of dam to determine IFS_o and IFS_s for a set of water levels.

[iii] Calculating the exceeding probabilities of these damage states.

[iv] Determining the analytical fragility curves with these values.

In this study, the Monte Carlo simulation is applied in the model where the random variables have been chosen as the specific weight of dam material, γ_c, which is selected as that, with the dam age, concrete strength might not be as strong as the initial condition and there are a lot of uncertainties associated with this parameter; the other parameter is the coefficient of friction μ which might vary at a certain range depending on the geological characteristics of the foundation material. In this analysis, 10,000 values of the both variables are generated; for the specific weight parameter, the range is 21-23.6 kN/m^3, and for friction coefficient, the range is 0.65 - 0.7. The damage conditions are checked if they are attained or exceeded for different water levels; thus, the exceedence probability of occurrences of the damage states are found with which the analytical fragility curves are generated. Applying the methodology described in section 3.2.2.8, the sample probability calculations for one run will be shown. For this, it is intended to check the exceeding probability of IFS_o = 0.667 and IFS_s = 1. The calculation steps of one model run are illustrated below:

(A) Sample calculation (IFS_o = 0.667)

[i] Inputs of the model: b_1=6.1; s_1=0; s_2=0; s_3=1/1.3; h_{b1} = 8, h_{b2} = 44.5, h_{w1} = 48; h_{w2} = 0; γ_w = 9.81, γ_c = 21 - 23.6.

For each run, 10,000 values are generated for the parameters related to the random variable such as weight of dam, righting moment. The output parameters of the model are calculated using the provided equations in section 3.2.2.2 of Chapter 3. For each run, 10,000 results are generated for the damage state parameter, IFS_o.

[ii] From these 10,000 values, the calculated mean, *'M'* and standard deviation *'S'* of IFS_o are 0.6677, and 0.0226, respectively.

[iii] With these two parameters *(M, S)*, the probability distribution is generated.

[iv] In this model run, it is checked whether the value of IFS_o reaches or exceeds 0.667. For this, the lower bound is given as '0.667' and the upper bound is 'infinity' in the model to find the probability. For this trial, the model results shows the probability, p = 0.51142 (Fig. 5.3).

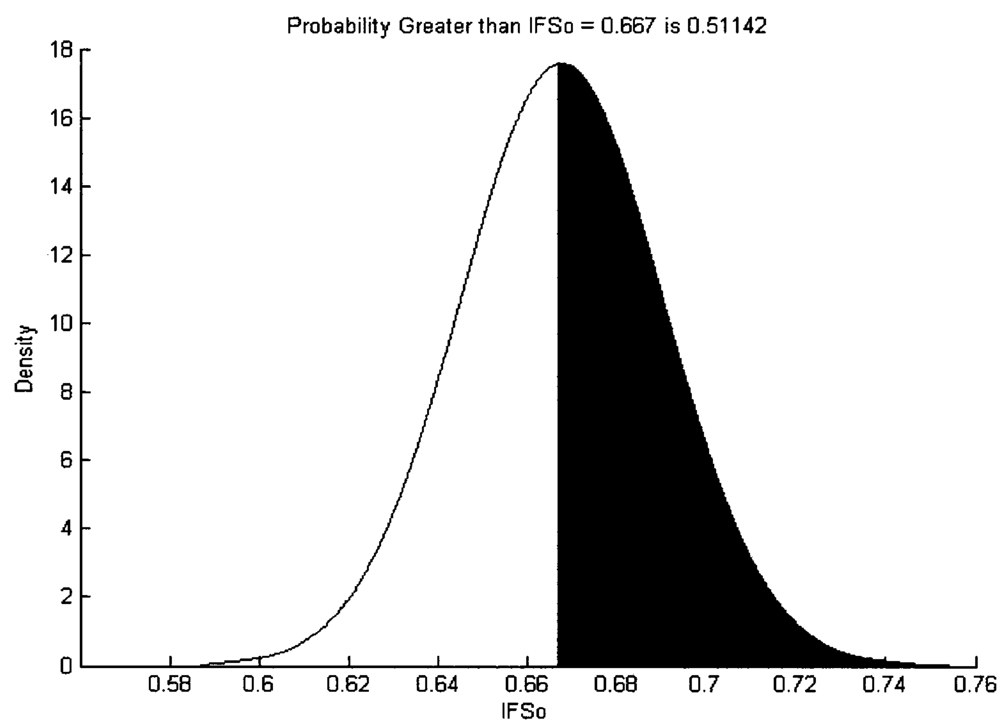

Fig. 5.3: Exceeding probability of IFS_o = 0.667

(B) Sample calculation (IFS_s = 1)

[i] Inputs of the model: b_1=6.1; s_1=0; s_2=0; s_3=1/1.3; h_{b1} = 8, h_{b2} = 44.5, h_{w1} = 45; h_{w2} = 0; γ_w = 9.81, γ_c = 21 - 23.6, μ = 0.65 - 0.7.

For each run, 10,000 values are generated for the parameters related to the random variables such as weight of dam, frictional force, and, reaction force at foundation. The output parameters of the model are calculated as before. For each run, 10,000 results are generated for the damage parameter, IFS_s.

[ii] From these 10,000 values, the calculated mean, *'M'* and standard deviation *'S'* of IFS_s are 0.969, and 0.056, respectively.

[iii] With these two parameters *(M, S),* the probability distribution is generated.

[iv] In this model, it is aimed to check whether the value of IFS_s reaches or exceeds 1. So, the lower bound is given as '1' and the upper bound is 'infinity' in the model. For this trial, the model result shows the probability, $p = 0.2902$ (Fig. 5.4).

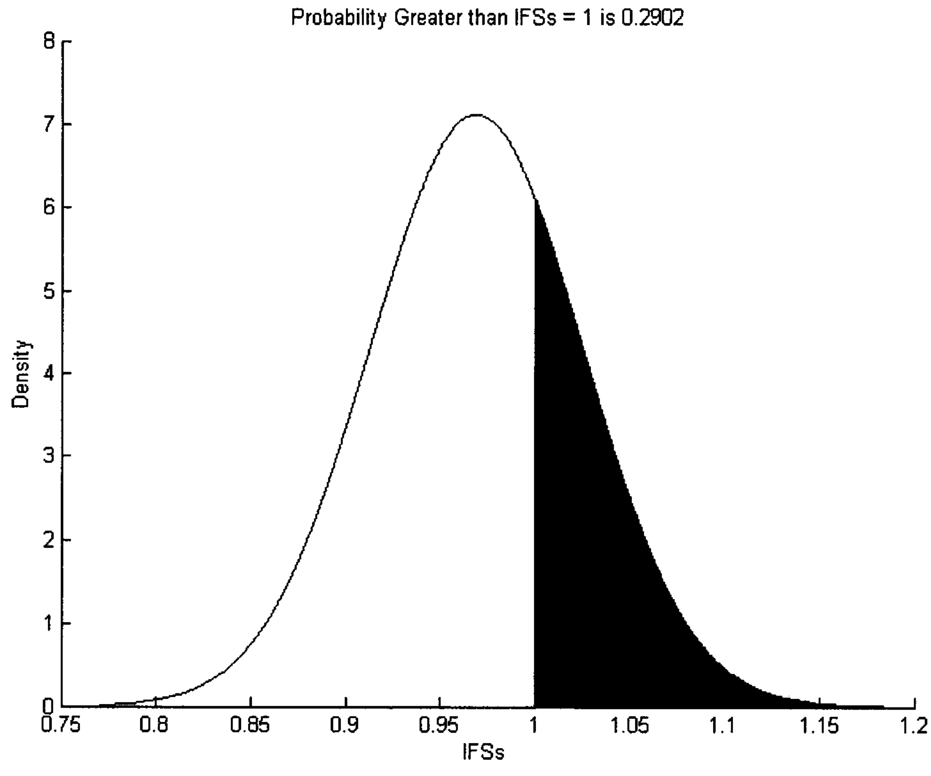

Fig. 5.4: Exceeding probability of $IFS_s = 1$

Table 5.5: Generated probability from hydraulic modeling

Water level	IFSO>0.667	IFSO>1	IFSS>0.8	IFSS>1
38	0	0	0	0
38.5	0	0	0	0
39	0	0	0	0
39.5	0	0	0.0031	0
40	0	0	0.0199	0
40.5	0	0	0.0747	0
41	0	0	0.2027	0
41.5	0	0	0.3989	0
42	0	0	0.6145	0
42.5	0	0	0.7901	0
43	0	0	0.9008	0.0022
43.5	0	0	0.961	0.0136
44	0	0	0.9865	0.0503
44.5	0	0	0.9957	0.1428
45	0	0	0.9988	0.2902
45.5	0.0015	0	0.9997	0.4855
46	0.0098	0	0.9999	0.6728
46.5	0.0411	0	1	0.8148
47	0.1294	0	1	0.9087
47.5	0.2944	0	1	0.9601
48	0.5114	0	1	0.9854
48.5	0.7214	0	1	0.9944
49	0.868	0	1	0.9982
49.5	0.9502	0	1	0.9994
50	0.9847	0	1	0.9998
50.5	0.9967	0	1	1
51	0.9993	0	1	1
51.5	0.9999	0	1	1
52	1	0	1	1
52.5	1	0	1	1
53	1	0	1	1
53.5	1	0	1	1
54	1	0	1	1
54.5	1	0	1	1
55	1	0	1	1
55.5	1	0	1	1
56	1	0	1	1
56.5	1	0.0026	1	1

57	1	0.0125	1	1
57.5	1	0.0480	1	1
58	1	0.1335	1	1
58.5	1	0.2911	1	1
59	1	0.4841	1	1
59.5	1	0.6825	1	1
60	1	0.8324	1	1
60.5	1	0.9297	1	1
61	1	0.9744	1	1
61.5	1	0.9924	1	1
62	1	0.9982	1	1
62.5	1	0.9996	1	1
63	1	0.9999	1	1
63.5	1	1	1	1
64	1	1	1	1
64.5	1	1	1	1
65	1	1	1	1
65.5	1	1	1	1
66	1	1	1	1

With these dataset, analytical fragility curves are developed (Fig. 5.5).

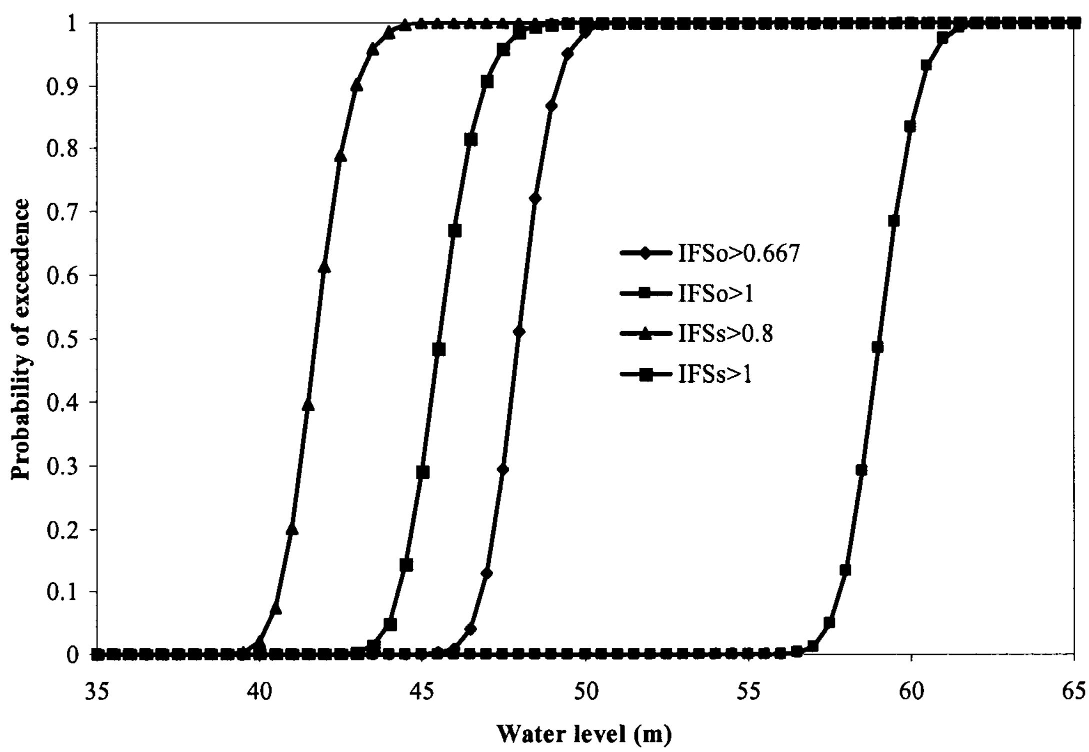

Fig. 5.5: Analytical fragility curves of dam

As shown in Figure 5.5, probability of the damage state 'IFS_o > 0.667' starts at the 45.5 m water level and reaches to 1 at the 52 m water level; for 'IFS_o > 1', probability starts at 56.5 m and reaches to 1 at the 63.5 m; for 'IFS_s > 0.8', the corresponding range is 39.5 - 46.5 m; and, for 'IFS_s > 1', the range is 43 - 50.5 m.

It is noted that the dam is under a higher risk for sliding than overturning of the dam based on the results from the hydraulic and fragility curves analysis. Overturning failure probability starts at 4 m flood level and reaches to full probability at the flood level of 11 m above the dam, whereas, sliding failure probability starts at the 9.5 m free board below the dam and has the full probability at 2 m of free board. In this case, from the result analysis, it is expected that for the flood hazard, first the sliding failure will occur before overturning failure which gives the serious hazard indication, then, preparedness for the overturning failure can be made to avoid the consequent failure.

While performing the fragility analysis, the restrictive approach has been taken. In this model, load of water sheet above the crest and downstream face for overflow condition is not included. The flood frequency analysis and fragility assessment indicate that, highly likely, the dam will overflow in extreme cases, rather than failing. But even if the dam is overtopped, it will cause huge deteriorating impacts on the adjacent infrastructures in the floodplain area.

5.3 Petri-Net model of the interactions among floodplain infrastructures

The multiple purpose Canyon Ferry Dam was constructed for flood control, supplying huge amounts of water for producing hydroelectricity, and irrigation mainly. There is also an intake pipe which meets part of the required municipal water used for drinking and industrial purposes. Several other additional infrastructures used for the operation of the main infrastructures are also included in the study system to illustrate the interdependencies among the critical infrastructures in floodplain area. The concerned infrastructures network in this study consists of the concrete gravity dam, penstock, hydraulic power plant, electric substation, intake pipeline and pumping infrastructure, irrigation system, municipal water infrastructure, and telecom. Interrelationships among the study system components are briefly stated below towards the development of a Petri-Net model for this study area. Some additional information are taken from the study by Robert (2004).

Gravity dam

Concrete gravity dam is used for storing reservoir water to use it for various purposes. Huge amount of water is received from the storage reservoir with the pipelines from the dam. When dam is overflown or collapsed due to a high flood flow, it causes the invasion of floodwater into the adjacent flood plain area. High pressure from floodwater leads to the rupture of penstock. Inundation from flood water causes malfunction or failure of the power plant, transformer substation, intake pipes, irrigation lands, water carrying pipes, and telecom infrastructures.

The Canyon Ferry dam was constructed in between 1949 to 1954 and it started its operation from early 1955. Its main function is to store enough water for hydroelectricity generation, irrigation and flood control. Also, it meets part of the required municipal water. Moreover, the dam site is famous for recreational activities.

Penstock

A penstock is a pipe conduit or tunnel with large diameter to carry rapid flow of water to the hydroelectric power plant. The large diameter pipe throws the received water maintaining enough head to the system of turbines to rotate them. It consists of gates for controlling the water flow from the reservoir. The service penstocks in Canyon Ferry area are embedded through the dam and they run upto the above ground power plant. If penstock does not function properly, for example, gate is shut down suddenly, water elevation will then rise up which consequently results in flooding of hydroelectric dam. Upstream portion of the penstock usually runs through the dam; rupture of the penstock could induce dam collapse. Also, malfunction of the penstock leads to the shutdown of the power plant.

Power plant

The power plant consists of the turbines, shafts, and generators for producing electricity. The water from the penstock from a high head falls to the turbine and the turbine rotates with a high speed. The turbine is connected to a shaft which is connected to generator. As the turbine rotates, the shaft also rotates to move the generator with a high speed. The electric coils in the generator gain energy to produce electricity energy. The produced electricity is transmitted to the transformer substation to adjust the voltage and to make it appropriate for sending to the recipients. Any damage or failure of the generators makes it impossible to supply the electricity energy to the substation. Again, if the generators are not capable of receiving the rotation, the penstock operation has to be stopped down. Thus, the downstream failure also induces the upstream infrastructure shutdown.

Transformer substation

The substation infrastructure contains transformer and overhead lines. The main functions of the transformer substation are to adjust the voltage of the produced electricity received from the power plant and to send this electricity to the recipients. Electricity from the station is used to meet the local and remote requirements.

In the study case network, dam operation and maintenance requires availability of electricity. Electric winches control the spillway valves or gates for controlling the flow between the upstream and downstream of the dam. In case the substation cannot supply electricity, the spillway has a greater chance to be blocked which haults the flood water evacuation and upstream water level will be increased to cause dam overflow. Electricity is also vital for operating the penstock valve and gates; the pump and flow controlling valves of the intake infrastructure also depend on the electricity service. In irrigation sector, the pump operation uses electricity to distribute the water to the croplands. Municipal water carrying pipes and treatment plant need to use electricity for their functioning. If the transformer substation equipments are damaged or failed, it will not be able to absorb the produced electricity; consequently, the turbines have to be stopped to avoid any accidental risks.

Intake infrastructure

In the floodplain area of the study system, the intake infrastructure consists of the water receiving pipes and pumping station. The large diameter intake pipes are carried under the ground and run through upto a receiving canal. For receiving the reservoir water, valves are opened to allow the flow through the pipes. There is a separate pumping station which pumps this water and throws to a canal from which irrigation system takes the water through pipes. Also, the municipal water is received from this station. Intake infrastructure plays very important role in the network. In case, the pipes are blocked and not able to receive water from the reservoir, the water level in the reservoir will increase. Additionally, if the pumps are inactive, the irrigation sector and municipal water sector will receive no water for their uses.

Irrigation system

This system has distribution pipelines to distribute the water to the croplands. The required water is received from the storage canal which is supplied by the intake infrastructure. In this study network, no impacts of the irrigation system outage is addressed, though it has a greater contribution in the agricultural economy which has a big role in constructing and maintaining of rural floodplain infrastructures.

Municipal Water infrastructure

Canyon Ferry reservoir supplies part of the required municipal water. This infrastructure consists of the water distributing pipelines and the treatment facility. The system not only depends on the water supply, electricity is also vitally required for operating pipe valves and treatment activities. However, outage of this infrastructure is not included in the study which has economic impacts on national finances.

Telecom

Telecom is used extensively for automated infrastructures. Specially, it is vital when large pipe networks have to run through inaccessible areas. In this study, it is assumed that the water pressure in the penstock, intake and water distributing pipes are monitored and controlled remotely as it is not practically possible to perform these activities by only engaging personnel. If telecom is out of service, it will not be possible to get the pressure data and control the valves and gates. In this case, these infrastructures have to be shut down on an emergency basis to avoid any spilling or rupture accidents. Telecom is also used in other infrastructures for monitoring purposes. However, in this study, only the pipelines telecom services are addressed.

Development and analysis of basic Petri-Net model

Using the infrastructure interactions information above, the network of infrastructure systems can be shown as in Figure 5.6. Here, 'D' stands for gravity dam, 'Ps' stands for 'penstock', 'PP' is 'power plant', 'S' is transformer substation, 'In' is the intake pipeline and pumping infrastructure, 'Ir' is irrigation system, 'W' is municipal water carrying infrastructure, and 'Tc' is telecom.

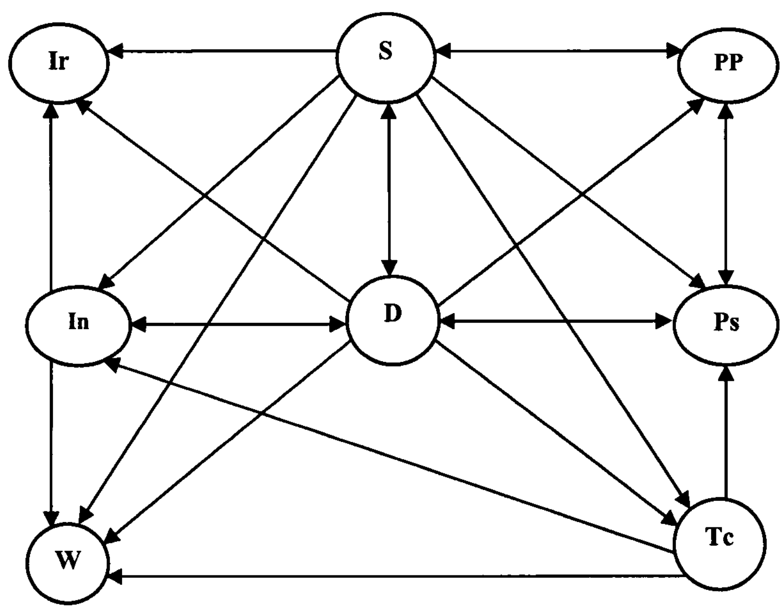

Fig. 5.6: Infrastructure interactions (Canyon Ferry floodplain area)

For developing the Petri-Net model of the study system, the places and transitions are defined accordingly. The conditions or states of the infrastructure components are denoted as 'places', the events of impacts or disruptions as 'transitions', occurrence of an event as 'firing', and holding of a condition as the 'token'. For the study system (Fig. 5.6), the places and transitions of the model are listed in Tables 1 and 2. The developed Petri-Net model for the study system is shown in Figure 5.7.

Table 5.6: List of places (Canyon Ferry floodplain)

Place	Description
p1	No hazard
p2	Dam overflow
p3	Penstock disruption
p4	Power plant disruption
p5	Substation disruption
p6	Intake infrastructure disruption
p7	Irrigation system disruption
p8	Municipal water treatment plant disruption
p9	Telecom disruption
p10	Dam overflow (dummy place for penstock)
p11	Dam overflow (dummy place for power plant)
p12	Dam overflow (dummy place for substation)
p13	Dam overflow (dummy place for intake infrastructure)
p14	Dam overflow (dummy place for irrigation system)
p15	Dam overflow (dummy place for water plant)
p16	Dam overflow (dummy place for telecom)
p17	Penstock disruption (dummy place for dam)
p18	Penstock disruption (dummy place for power plant)
p19	Power plant disruption (dummy place for penstock)
p20	Power plant disruption (dummy place for substation)
p21	Substation disruption (dummy place for dam)
p22	Substation disruption (dummy place for penstock)
p23	Substation disruption (dummy place for power plant)
p24	Substation disruption (dummy place for intake infrastructure)
p25	Substation disruption (dummy place for irrigation system)
p26	Substation disruption (dummy place for water plant)
p27	Substation disruption (dummy place for telecom)
p28	Intake infrastructure disruption (dummy place for dam)
p29	Intake infrastructure disruption (dummy place for irrigation system)
p30	Intake infrastructure disruption (dummy place for water plant)
p31	Telecom disruption (dummy place for penstock)
p32	Telecom disruption (dummy place for intake infrastructure)
p33	Telecom disruption (dummy place for water plant)

Table 5.7: List of transitions (Canyon Ferry floodplain)

Transition	Description
t1	Dam is flooded
t2	Dam overflow affects penstock
t3	Dam overflow affects power plant
t4	Dam overflow affects substation
t5	Dam overflow affects intake infrastructure
t6	Dam overflow affects irrigation system
t7	Dam overflow affects water plant
t8	Dam overflow affects telecom
t9	Penstock disruption affects dam
t10	Penstock disruption affects power plant
t11	Power plant disruption affects penstock
t12	Power plant disruption affects substation
t13	Substation disruption affects dam operation
t14	Substation disruption affects penstock
t15	Substation disruption affects power plant
t16	Substation disruption affects intake infrastructure
t17	Substation disruption affects irrigation system
t18	Substation disruption affects water plant
t19	Substation disruption affects telecom
t20	Intake infrastructure disruption affects dam
t21	Intake infrastructure disruption affects irrigation system
t22	Intake infrastructure disruption affects water plant
t23	Telecom disruption affects penstock
t24	Telecom disruption affects intake infrastructure
t25	Telecom disruption affects water plant

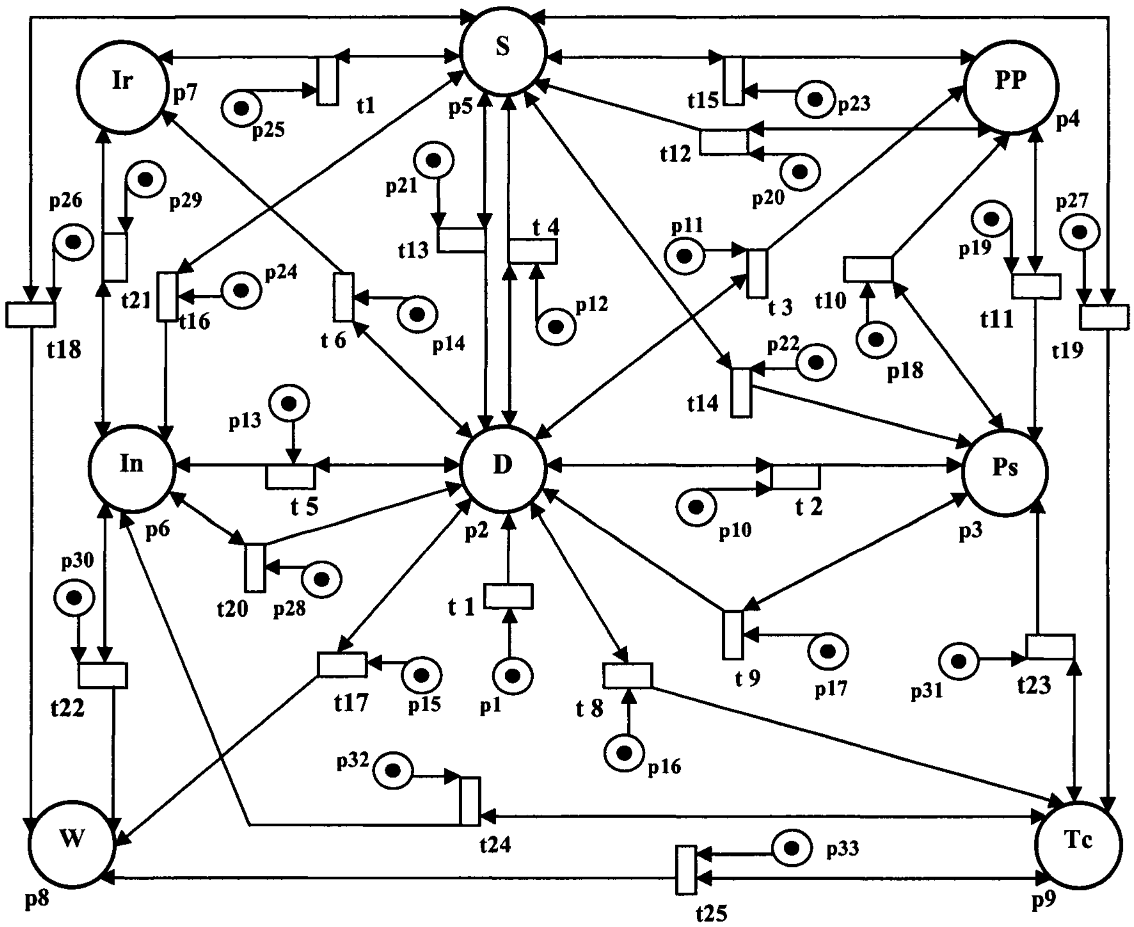

Fig 5.7: Petri-Net model of the floodplain infrastructure interdependency

5.3.1 Model execution and analysis

Initially, there is no flood and all the infrastructures are functioning properly in the Petri-Net model. In this case, the initial marking of the network is,

$M_0 =$ 1 0 0 0 0 0 0 0 0 1 1 1 1 1 1 1 1 1 1 1 1 1 1 1 1 1 1 1 1 1 1 1 1

The model execution starts with firing of t1, i.e. dam overflow occurs. Thus, the token in p1 flows to p2, which is available for firing the transitions t2 through t8. The total sum of the tokens is 18.

5.3.2 Structural properties: invariant analysis

For this model, the incidence matrix is, C =

	*t*1	*t*2	*t*3	*t*4	*t*5	*t*6	*t*7	*t*8	*t*9	*t*10	*t*11	*t*12	*t*13	*t*14	*t*15	*t*16	*t*17	*t*18	*t*19	*t*20	*t*21	*t*22	*t*23	*t*24	*t*25
*p*1	−1	0	0	0	0	0	0	0	0	0	0	0	0	0	0	0	0	0	0	0	0	0	0	0	0
*p*2	1	0	0	0	0	0	0	0	1	0	0	0	1	0	0	0	0	0	0	1	0	0	0	0	0
*p*3	0	1	0	0	0	0	0	0	0	0	1	0	0	1	0	0	0	0	0	0	0	0	1	0	0
*p*4	0	0	1	0	0	0	0	0	0	1	0	0	0	0	1	0	0	0	0	0	0	0	0	0	0
*p*5	0	0	0	1	0	0	0	0	0	0	0	1	0	0	0	0	0	0	0	0	0	0	0	0	0
*p*6	0	0	0	0	1	0	0	0	0	0	0	0	0	0	0	1	0	0	0	0	0	0	0	1	0
*p*7	0	0	0	0	0	1	0	0	0	0	0	0	0	0	0	0	1	0	0	0	1	0	0	0	0
*p*8	0	0	0	0	0	0	1	0	0	0	0	0	0	0	0	0	0	1	0	0	0	1	0	0	1
*p*9	0	0	0	0	0	0	0	1	0	0	0	0	0	0	0	0	0	0	1	0	0	0	0	0	0
*p*10	0	−1	0	0	0	0	0	0	0	0	0	0	0	0	0	0	0	0	0	0	0	0	0	0	0
*p*11	0	0	−1	0	0	0	0	0	0	0	0	0	0	0	0	0	0	0	0	0	0	0	0	0	0
*p*12	0	0	0	−1	0	0	0	0	0	0	0	0	0	0	0	0	0	0	0	0	0	0	0	0	0
*p*13	0	0	0	0	−1	0	0	0	0	0	0	0	0	0	0	0	0	0	0	0	0	0	0	0	0
*p*14	0	0	0	0	0	−1	0	0	0	0	0	0	0	0	0	0	0	0	0	0	0	0	0	0	0
*p*15	0	0	0	0	0	0	−1	0	0	0	0	0	0	0	0	0	0	0	0	0	0	0	0	0	0
*p*16	0	0	0	0	0	0	0	−1	0	0	0	0	0	0	0	0	0	0	0	0	0	0	0	0	0
*p*17	0	0	0	0	0	0	0	0	−1	0	0	0	0	0	0	0	0	0	0	0	0	0	0	0	0
*p*18	0	0	0	0	0	0	0	0	0	−1	0	0	0	0	0	0	0	0	0	0	0	0	0	0	0
*p*19	0	0	0	0	0	0	0	0	0	0	−1	0	0	0	0	0	0	0	0	0	0	0	0	0	0
*p*20	0	0	0	0	0	0	0	0	0	0	0	−1	0	0	0	0	0	0	0	0	0	0	0	0	0
*p*21	0	0	0	0	0	0	0	0	0	0	0	0	−1	0	0	0	0	0	0	0	0	0	0	0	0
*p*22	0	0	0	0	0	0	0	0	0	0	0	0	0	−1	0	0	0	0	0	0	0	0	0	0	0
*p*23	0	0	0	0	0	0	0	0	0	0	0	0	0	0	−1	0	0	0	0	0	0	0	0	0	0
*p*24	0	0	0	0	0	0	0	0	0	0	0	0	0	0	0	−1	0	0	0	0	0	0	0	0	0
*p*25	0	0	0	0	0	0	0	0	0	0	0	0	0	0	0	0	−1	0	0	0	0	0	0	0	0
*p*26	0	0	0	0	0	0	0	0	0	0	0	0	0	0	0	0	0	−1	0	0	0	0	0	0	0
*p*27	0	0	0	0	0	0	0	0	0	0	0	0	0	0	0	0	0	0	−1	0	0	0	0	0	0
*p*28	0	0	0	0	0	0	0	0	0	0	0	0	0	0	0	0	0	0	0	−1	0	0	0	0	0
*p*29	0	0	0	0	0	0	0	0	0	0	0	0	0	0	0	0	0	0	0	0	−1	0	0	0	0
*p*30	0	0	0	0	0	0	0	0	0	0	0	0	0	0	0	0	0	0	0	0	0	−1	0	0	0
*p*31	0	0	0	0	0	0	0	0	0	0	0	0	0	0	0	0	0	0	0	0	0	0	−1	0	0
*p*32	0	0	0	0	0	0	0	0	0	0	0	0	0	0	0	0	0	0	0	0	0	0	0	−1	0
*p*33	0	0	0	0	0	0	0	0	0	0	0	0	0	0	0	0	0	0	0	0	0	0	0	0	−1

Applying equation 3.24, eight place invariants are found in the network (Table 5.8).

Table 5.8: Place invariants (Canyon Ferry floodplain)

	Place invariants								
	I_{p1}	I_{p2}	I_{p3}	I_{p4}	I_{p5}	I_{p6}	I_{p7}	I_{p8}	Sum of the invariants
p1	0	0	0	1	0	0	0	0	1
p2	0	0	0	1	0	0	0	0	1
p3	0	0	0	0	0	1	0	0	1
p4	0	1	0	0	0	0	0	0	1
p5	1	0	0	0	0	0	0	0	1
p6	0	0	0	0	0	0	1	0	1
p7	0	0	0	0	1	0	0	0	1
p8	0	0	0	0	0	0	0	1	1
p9	0	0	1	0	0	0	0	0	1
p10	0	0	0	0	0	1	0	0	1
p11	0	1	0	0	0	0	0	0	1
p12	1	0	0	0	0	0	0	0	1
p13	0	0	0	0	0	0	1	0	1
p14	0	0	0	0	1	0	0	0	1
p15	0	0	0	0	0	0	0	1	1
p16	0	0	1	0	0	0	0	0	1
p17	0	0	0	1	0	0	0	0	1
p18	0	1	0	0	0	0	0	0	1
p19	0	0	0	0	0	1	0	0	1
p20	1	0	0	0	0	0	0	0	1
p21	0	0	0	1	0	0	0	0	1
p22	0	0	0	0	0	1	0	0	1
p23	0	1	0	0	0	0	0	0	1
p24	0	0	0	0	0	0	1	0	1
p25	0	0	0	0	1	0	0	0	1
p26	0	0	0	0	0	0	0	1	1
p27	0	0	1	0	0	0	0	0	1
p28	0	0	0	1	0	0	0	0	1
p29	0	0	0	0	1	0	0	0	1
p30	0	0	0	0	0	0	0	1	1
p31	0	0	0	0	0	1	0	0	1
p32	0	0	0	0	0	0	1	0	1
p33	0	0	0	0	0	0	0	1	1

5.3.3 Model properties

Boundedness: Taking the summation of all the P-invariants,

$$I_1 + I_2 + I_3 + \ldots + I_8 = 1\ 1\ 1\ 1\ 1\ 1\ 1\ 1\ 1\ 1\ 1\ 1\ 1\ 1\ 1\ 1\ 1\ 1\ 1\ 1\ 1\ 1\ 1\ 1\ 1\ 1\ 1\ 1\ 1\ 1\ 1\quad 1\ 1$$

The weighted sum of the tokens in the places is constant for all reachable markings. So, the developed Petri-Net model is bounded.

Liveness: The model is a deadlock model.

5.3.4 Result interpretation

From the P-invariant analysis of the developed Petri-Net model, eight minimal P-invariants (IP_1 through IP_8) are found, which simulates the infrastructure interdependency in the study system.

[1] IP_1 interprets that the number of tokens flowing among the places 5, 12 and 20 is always 2 throughout the simulation of the model, i.e.

$M(p5) + M(p12) + M(p20) = 2$

Examining the model, it is noticed that, substation is disrupted (place 5) due to the dam overflow inundation (place 12), or power plant is not supplying power to the substation (place 20).

[2] IP_2 gives, $M(p4) + M(p11) + M(p18) + M(p23) = 3$

This simulation implies that power plant disruption occurs due to the inundation from the flood water, penstock rupture, or, if the substation is unable to absorb the supplied energy from the plant.

[3] IP_3 gives, M(p9) + M(p16) + M(p27) = 2

Telecom service becomes unavailable if it is affected from flood water and if the substation cannot supply power to it.

[4] IP_4 gives, M(p1) + M(p2) + M(p17) + M(p21) + M(p28) = 4

Dam overflow results from the occurrence of high reservoir flow, increase in the upstream water elevation if the penstock and intake valves cannot be operated to allow the water flow through them, and substation cannot supply electricity to operate the spillway.

[5] IP_5 gives, M(p7) + M(p14) + M(p25) + M(p29) = 3

Here, the irrigation system service is disrupted if it is inundated by flood water, there is no electricity supply from the substation, and if the intake pipeline doesn't work properly to ensure enough water storage for irrigation.

[6] IP_6 gives, M(p3) + M(p10) + M(p19) + M(p22) + M(p31) = 4

Penstock can be ruptured by the thrust from the flood flow, if the power plant doesn't work, flow through the penstock has to be shut down, the valves cannot be operated due to the unavailability of electricity, and telecom service is not available to check the pipe pressure for avoiding rupture from overstress.

[7] IP_7 gives, M(p6) + M(p13) + M(p24) + M(p32) = 3

Intake infrastructure might rupture by the flood flow pressure, the valves cannot be operated due to the unavailability of electricity, and telecom service is not available to check the intake pipe pressure for avoiding rupture from overstress.

[8] IP_8 gives, $M(p8) + M(p15) + M(p26) + M(p30) + M(p33) = 4$

Water distributing pipes and the treatment plant get inundated from the flood water, substation electricity is required for operating their pumps and valves and for other production activities, proper functioning of the intake infrastructure is a must, and telecom service is necessary for observing and controlling the water systems.

5.4 Safety assessment with extended Petri-Net analysis

The methodology of extended Petri-Net analysis described in Chapter 3 will be applied in the part of the developed Petri-Net. Here, the network consists of the dam, penstock, power plant and the transformer substation. In this case, the operating conditions of each infrastructure such as either the infrastructure is shut down or operating will be simulated. For example, if the substation is flooded and the service is unavailable, the disrupted power plant cannot put the damage token to the substation as the substation is already out of service. Again, if the disrupted penstock cannot provide its service to the power plant, it has to be shut down, in this case, the damage token from flood flow is not considered as the plant is already shut down. In this study, the inhibitor arc has been used to imply the same phenomenon as assigning the infrastructure place with capacity 1. For the extended analysis, the net starts with the dam overflow event which is deterministic, further, the effects of dam overflow on the other power generating infrastructures will be simulated; contributions to the overflow increments from the penstock and spillway shutdown are not considered. The places and transitions can be tabulated as below (Tables 5.9 and 5.10):

Table 5.9: List of places (hydropower generating infrastructures)

Place	Description
p1	No hazard
p2	Dam overflow
p3	Penstock disruption
p4	Power plant disruption
p5	Substation disruption
p6	Dam overflow (dummy place for penstock)
p7	Dam overflow (dummy place for power plant)
p8	Dam overflow (dummy place for substation)
p9	Penstock disruption (dummy place for power plant)
p10	Power plant disruption (dummy place for penstock)
p11	Power plant disruption (dummy place for substation)
p12	Substation disruption (dummy place for penstock)
p13	Substation disruption (dummy place for power plant)

Table 5.10: List of transitions (hydropower generating infrastructures)

Transition	Description	Transition rate
t1	Dam is overtopped	Deterministic
t2	Dam overflow affects penstock	80
t3	Dam overflow affects power plant	70
t4	Dam overflow affects substation	50
t5	Penstock disruption affects power plant	45
t6	Power plant disruption affects penstock	85
t7	Power plant disruption affects substation	95
t8	Substation disruption affects penstock	90
t9	Substation disruption affects power plant	95

The Petri-Net with these places and transitions is as below (Fig. 5.8):

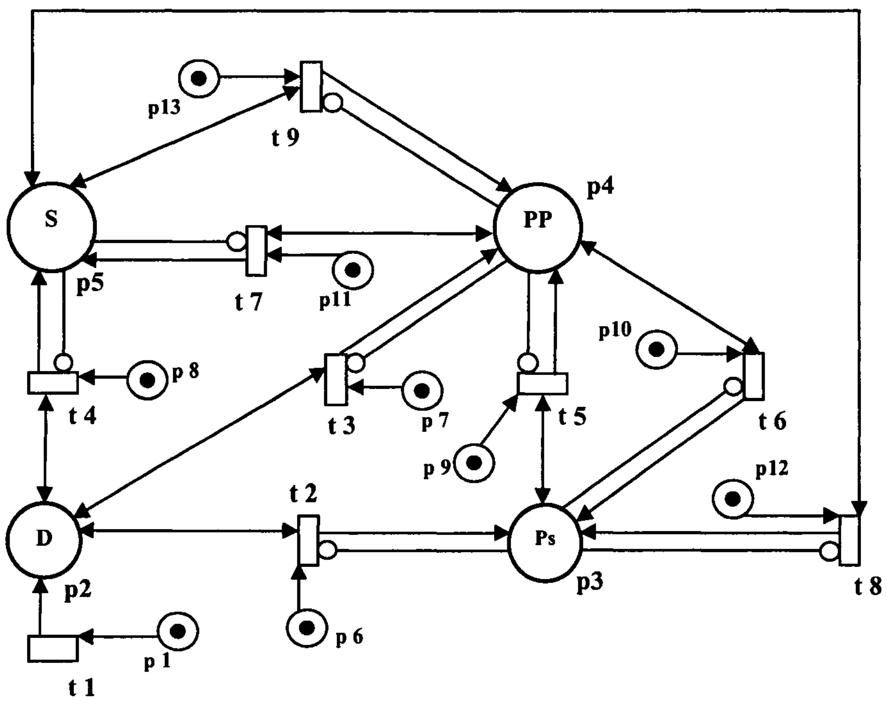

Fig. 5.8: Petri-Net model of the hydropower generating infrastructures

The network execution starts with the firing of the deterministic transition t1, that is, dam overflow occurs. Consequently, the token flow is captured to generate the reachability graph of the net. As before, s_i = previous state; s_j = next state; $r(t)$ = firing rate; q = transition probability determined from equation (3.25); t_k = firing transition. The reachability graph is provided at Table 5.11 for the initial marking,

$$M_0 = 1\ 0\ 0\ 0\ 0\ 1\ 1\ 1\ 1\ 1\ 1\ 1\ 1$$

Table 5.11: Reachability graph (hydropower generating infrastructures)

s_i	*Track*	t_k	*r(t)*	s_j	*Damaged infrastructure*	*q*
s_0		1	Deterministic	s1	D	1
s1	1	2	80	s2	D+P	.4
		3	70	s3	D+PP	.35
		4	50	s4	D+S	.25
s2	1,2	3	70	s5	D+P+PP	.424
		4	50	s6	D+P+S	.303
		5	45	s7	D+P+PP	.273
s3	1,3	2	80	s5	D+PP+P	.258
		4	50	s8	D+PP+S	.161
		6	85	s9	D+PP+P	.274
		7	95	s10	D+PP+S	.306
s4	1,4	2	80	s6	D+S+P	.239
		3	70	s8	D+S+PP	.209
		8	90	s11	D+S+P	.269
		9	95	s12	D+S+PP	.284
s5	1,2,3	4	50	s13	D+P+PP+S	.345
		7	95	s14	D+P+PP+S	.655
s6	1,2,4	3	70	s13	D+P+S+PP	.333
		5	45	s15	D+P+S+PP	.214
		9	95	s16	D+P+S+PP	.452
s7	1,2,5	4	50	s15	D+P+PP+S	.345
		7	95	s17	D+P+PP+S	.655
s8	1,3,4	2	80	s13	D+PP+S+P	.314
		6	85	s18	D+PP+S+P	.333
		8	90	s19	D+PP+S+P	.353
s9	1,3,6	4	50	s18	D+PP+P+S	.345
		7	95	s20	D+PP+P+S	.655
s10	1,3,7	2	80	s14	D+PP+S+P	.314
		6	85	s20	D+PP+S+P	.333
		8	90	s21	D+PP+S+P	.353
s11	1,4,8	3	70	s19	D+S+P+PP	.333
		5	45	s22	D+S+P+PP	.214
		9	95	s23	D+S+P+PP	.452
s12	1,4,9	2	80	s16	D+S+PP+P	.314
		6	85	s24	D+S+PP+P	.333
		8	90	s23	D+S+PP+P	.353

5.5 Markov Chain development and analysis

The Markov Chain for the reachability graph derived in the previous section can be developed with the calculated transition probabilities. The developed chain is as below:

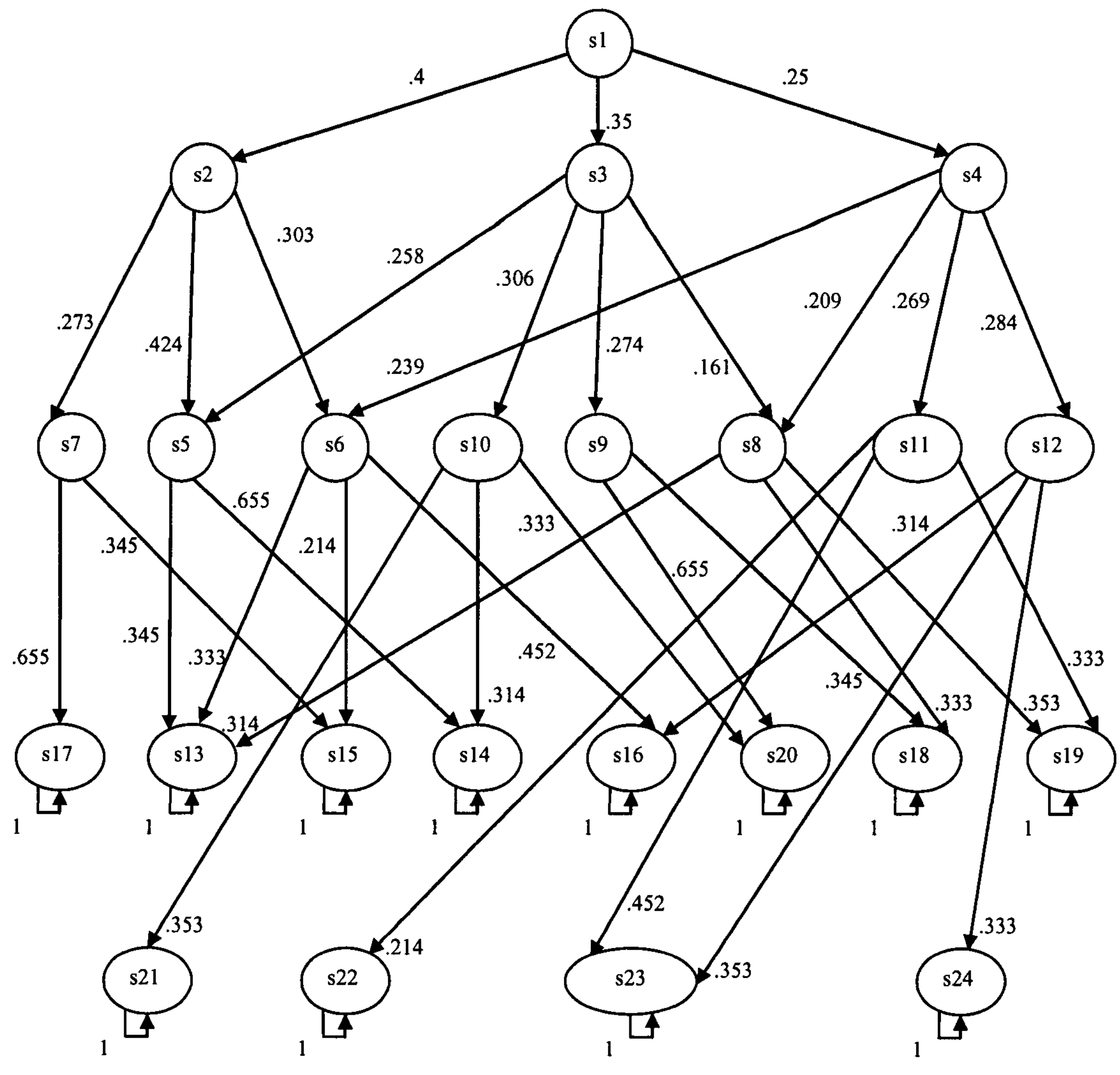

Fig. 5.9: Markov Chain (hydropower generating infrastructures)

5.5.1 Transition matrix

The transition matrix (T_r) can be generated from the above Markov Chain. The initial state matrix is assigned with the assumption that, initially, the probability of state 1 is '1', and the probabilities of the remaining states are 'zero'. With these two parameters, T_r and p, the steady state probabilities of the states are calculated.

The transition matrix, T_r =

states	*s1*	*s2*	*s3*	*s4*	*s5*	*s6*	*s7*	*s8*	*s9*	*s10*	*s11*	*s12*	*s13*	*s14*	*s15*	*s16*	*s17*	*s18*	*s19*	*s20*	*s21*	*s22*	*s23*	*s24*
s1	0	.4	.35	.25	0	0	0	0	0	0	0	0	0	0	0	0	0	0	0	0	0	0	0	0
s2	0	0	0	0	.424	.303	.273	0	0	0	0	0	0	0	0	0	0	0	0	0	0	0	0	0
s3	0	0	0	0	.258	0	0	.161	.274	.307	0	0	0	0	0	0	0	0	0	0	0	0	0	0
s4	0	0	0	0	0	.239	0	.209	0	0	.269	.283	0	0	0	0	0	0	0	0	0	0	0	0
s5	0	0	0	0	0	0	0	0	0	0	0	0	.345	.655	0	0	0	0	0	0	0	0	0	0
s6	0	0	0	0	0	0	0	0	0	0	0	0	.333	0	.214	.453	0	0	0	0	0	0	0	0
s7	0	0	0	0	0	0	0	0	0	0	0	0	0	0	.345	0	.655	0	0	0	0	0	0	0
s8	0	0	0	0	0	0	0	0	0	0	0	0	.314	0	0	0	0	.333	.353	0	0	0	0	0
s9	0	0	0	0	0	0	0	0	0	0	0	0	0	0	0	0	0	.345	0	.655	0	0	0	0
s10	0	0	0	0	0	0	0	0	0	0	0	0	0	.314	0	0	0	0	0	.333	.353	0	0	0
s11	0	0	0	0	0	0	0	0	0	0	0	0	0	0	0	0	0	0	.333	0	0	.214	.453	0
s12	0	0	0	0	0	0	0	0	0	0	0	0	0	0	0	.314	0	0	0	0	0	0	.353	.333
s13	0	0	0	0	0	0	0	0	0	0	0	0	1	0	0	0	0	0	0	0	0	0	0	0
s14	0	0	0	0	0	0	0	0	0	0	0	0	0	1	0	0	0	0	0	0	0	0	0	0
s15	0	0	0	0	0	0	0	0	0	0	0	0	0	0	1	0	0	0	0	0	0	0	0	0
s16	0	0	0	0	0	0	0	0	0	0	0	0	0	0	0	1	0	0	0	0	0	0	0	0
s17	0	0	0	0	0	0	0	0	0	0	0	0	0	0	0	0	1	0	0	0	0	0	0	0
s18	0	0	0	0	0	0	0	0	0	0	0	0	0	0	0	0	0	1	0	0	0	0	0	0
s19	0	0	0	0	0	0	0	0	0	0	0	0	0	0	0	0	0	0	1	0	0	0	0	0
s20	0	0	0	0	0	0	0	0	0	0	0	0	0	0	0	0	0	0	0	1	0	0	0	0
s21	0	0	0	0	0	0	0	0	0	0	0	0	0	0	0	0	0	0	0	0	1	0	0	0
s22	0	0	0	0	0	0	0	0	0	0	0	0	0	0	0	0	0	0	0	0	0	1	0	0
s23	0	0	0	0	0	0	0	0	0	0	0	0	0	0	0	0	0	0	0	0	0	0	1	0
s24	0	0	0	0	0	0	0	0	0	0	0	0	0	0	0	0	0	0	0	0	0	0	0	1

Initial state matrix,

$$p = 1\ 0\ 0\ 0\ 0\ 0\ 0\ 0\ 0\ 0\ 0\ 0\ 0\ 0\ 0\ 0\ 0\ 0\ 0\ 0\ 0\ 0\ 0\ 0$$

Now, for calculating the steady state probabilities, p will be multiplied with successive powers of T_r until the steady state is reached (Table 5.12):

Table 5.12: Steady state probability (hydropower generating infrastructures)

	s1	s2	s3	s4	s5	s6	s7	s8	s9	s10	s11	s12	s13	s14	s15	s16	s17	s18	s19	s20	s21	s22	s23	s24
p	1	0	0	0	0	0	0	0	0	0	0	0	0	0	0	0	0	0	0	0	0	0	0	0
$p*T_r$	0	.4	.35	.25	0	0	0	0	0	0	0	0	0	0	0	0	0	0	0	0	0	0	0	0
$p*T_r^2$	0	0	0	0	.26	.181	.109	.109	.096	.107	.067	.071	0	0	0	0	0	0	0	0	0	0	0	0
$p*T_r^3$	0	0	0	0	0	0	0	0	0	0	0	0	.184	.204	.076	.1	.072	.069	.061	.099	.038	.014	.055	.024
$p*T_r^4$	0	0	0	0	0	0	0	0	0	0	0	0	.184	.204	.076	.1	.072	.069	.061	.099	.038	.014	.055	.024

In this case, $p* T_r^3 = p* T_r^4$. So, the Markov Chain attains the steady state at $p* T_r^3$.

The above result shows that the states s13 through s24 will be attained at steady state, which is compatible as it indicates that all the infrastructures are disrupted in the course of time. In this model, the recovery strategy is not considered; it is assumed that the infrastructures do not recover if they are disrupted once. For this reason, the steady state should indicate that all the infrastructures are disrupted which have been captured from the model result.

5.5.2 Extended analysis of Markov Chain

In this Markov Chain, there are twelve absorbing states, s13 through s24. The behavior of the network can be further analyzed with the analysis of the effects of the existence of the absorbing states in the network. The analysis steps are shown below.

First, the transition matrix, T_r can be divided into transient state and absorbing state in the canonical form,

$$T_r = \begin{matrix} Q & \vdots & R \\ \cdots & \vdots & \cdots \\ 0 & \vdots & I \end{matrix}$$

In this case 'I' is 12-by-12 identity matrix; 0, R, and Q are 12-by-12 matrices, shown below:

$$
Q = \begin{matrix}
0 & .4 & .35 & .25 & 0 & 0 & 0 & 0 & 0 & 0 & 0 & 0 \\
0 & 0 & 0 & 0 & .424 & .303 & .273 & 0 & 0 & 0 & 0 & 0 \\
0 & 0 & 0 & 0 & .258 & 0 & 0 & .161 & .274 & .307 & 0 & 0 \\
0 & 0 & 0 & 0 & 0 & .239 & 0 & .209 & 0 & 0 & .269 & .283 \\
0 & 0 & 0 & 0 & 0 & 0 & 0 & 0 & 0 & 0 & 0 & 0 \\
0 & 0 & 0 & 0 & 0 & 0 & 0 & 0 & 0 & 0 & 0 & 0 \\
0 & 0 & 0 & 0 & 0 & 0 & 0 & 0 & 0 & 0 & 0 & 0 \\
0 & 0 & 0 & 0 & 0 & 0 & 0 & 0 & 0 & 0 & 0 & 0 \\
0 & 0 & 0 & 0 & 0 & 0 & 0 & 0 & 0 & 0 & 0 & 0 \\
0 & 0 & 0 & 0 & 0 & 0 & 0 & 0 & 0 & 0 & 0 & 0 \\
0 & 0 & 0 & 0 & 0 & 0 & 0 & 0 & 0 & 0 & 0 & 0 \\
0 & 0 & 0 & 0 & 0 & 0 & 0 & 0 & 0 & 0 & 0 & 0
\end{matrix}
$$

$$
R = \begin{matrix}
0 & 0 & 0 & 0 & 0 & 0 & 0 & 0 & 0 & 0 & 0 & 0 \\
0 & 0 & 0 & 0 & 0 & 0 & 0 & 0 & 0 & 0 & 0 & 0 \\
0 & 0 & 0 & 0 & 0 & 0 & 0 & 0 & 0 & 0 & 0 & 0 \\
0 & 0 & 0 & 0 & 0 & 0 & 0 & 0 & 0 & 0 & 0 & 0 \\
.345 & .655 & 0 & 0 & 0 & 0 & 0 & 0 & 0 & 0 & 0 & 0 \\
.333 & 0 & .214 & .453 & 0 & 0 & 0 & 0 & 0 & 0 & 0 & 0 \\
0 & 0 & .345 & 0 & .655 & 0 & 0 & 0 & 0 & 0 & 0 & 0 \\
.314 & 0 & 0 & 0 & 0 & .333 & .353 & 0 & 0 & 0 & 0 & 0 \\
0 & 0 & 0 & 0 & 0 & .345 & 0 & .655 & 0 & 0 & 0 & 0 \\
0 & .314 & 0 & 0 & 0 & 0 & 0 & .333 & .353 & 0 & 0 & 0 \\
0 & 0 & 0 & 0 & 0 & 0 & .333 & 0 & 0 & .214 & .453 & 0 \\
0 & 0 & 0 & .314 & 0 & 0 & 0 & 0 & 0 & 0 & .353 & .333
\end{matrix}
$$

With these matrices, the analysis can be continued as follows,

(i) The fundamental matrix, $N = (I - Q)^{-1}$, or,

$N =$

States	$s1$	$s2$	$s3$	$s4$	$s5$	$s6$	$s7$	$s8$	$s9$	$s10$	$s11$	$s12$
$s1$	1	.4	.35	.25	.26	.181	.109	.109	.096	.107	.067	.071
$s2$	0	1	0	0	.424	.303	.273	0	0	0	0	0
$s3$	0	0	1	0	.258	0	0	.161	.274	.307	0	0
$s4$	0	0	0	1	0	.239	0	.209	0	0	.269	.283
$s5$	0	0	0	0	1	0	0	0	0	0	0	0
$s6$	0	0	0	0	0	1	0	0	0	0	0	0
$s7$	0	0	0	0	0	0	1	0	0	0	0	0
$s8$	0	0	0	0	0	0	0	1	0	0	0	0
$s9$	0	0	0	0	0	0	0	0	1	0	0	0
$s10$	0	0	0	0	0	0	0	0	0	1	0	0
$s11$	0	0	0	0	0	0	0	0	0	0	1	0
$s12$	0	0	0	0	0	0	0	0	0	0	0	1

The first row of the above result indicates that if we start in state 1, then the expected number of times in states 1, 2, 3,…,12 before being absorbed are 1, .4, .35,……., .071. The remaining rows imply the same interpretations.

(ii) If t_i be the expected number of steps before the chain is absorbed, given that the chain starts in state s_i, and let 't' be the 12-by-1 column vector whose i^{th} entry is t_i, then, $t = N \times c$, where, c is a 12-by-1 column vector all of whose entries are 1,

$c^T =$ 1 1 1 1 1 1 1 1 1 1 1 1

Then, $t^T =$

$s1$	$s2$	$s3$	$s4$	$s5$	$s6$	$s7$	$s8$	$s9$	$s10$	$s11$	$s12$
3	2	2	2	1	1	1	1	1	1	1	1

(iii) B_{ij} is the probability that an absorbing chain will be absorbed in the absorbing state s_j if it starts in the transient state s_i. Let B be the matrix with entries B_{ij}. Then, $B = N \times R$, or,

$B =$

States	$s13$	$s14$	$s15$	$s16$	$s17$	$s18$	$s19$	$s20$	$s21$	$s22$	$s23$	$s24$
$s1$	.184	.204	.076	.104	.072	.069	.061	.099	.038	.014	.055	.024
$s2$	.247	.278	.159	.137	.179	0	0	0	0	0	0	0
$s3$	.14	.265	0	0	0	.148	.057	.282	.108	0	0	0
$s4$	.145	0	.051	.197	0	.07	.163	0	0	.058	.222	.094
$s5$	.345	.655	0	0	0	0	0	0	0	0	0	0
$s6$	.333	0	.214	.453	0	0	0	0	0	0	0	0
$s7$	0	0	.345	0	.655	0	0	0	0	0	0	0
$s8$	.314	0	0	0	0	.333	.353	0	0	0	0	0
$s9$	0	0	0	0	0	.345	0	.655	0	0	0	0
$s10$	0	.314	0	0	0	0	0	.333	.353	0	0	0
$s11$	0	0	0	0	0	0	.333	0	0	.214	.453	0
$s12$	0	0	0	.314	0	0	0	0	0	0	.353	.333

The generated matrix B above shows the probability of reaching the absorbing states from the transient states. For example, if the net starts at transient state 1, that is, the dam overflow occurs, then, the probability of reaching at states 13 though 24 are 0.184, 0.204, …, 0.055, and 0.024, which matches with the steady state results considering the occurrence of state 1 first. Similarly, if the net starts at the state 2 indicating the ruptured penstock from flood water pressure, the probability of reaching at the same absorbing states are 0.247, 0.278, …, 0. Checking the reachability graph of extended Petri-Net analysis, it is noticed that the states 18 through 24 are not reachable from state 2. The other results can also be checked from the reachability graph and found to be satisfactory.

The model results show that the network analysis could address the scenario correctly. In the extended analysis, the derived absorbing states s13 through s24 indicate the same condition, that is, all the infrastructures in the network are out of service, but they are attained in different ways. For example, s13 is attained by firing the transitions t1, t2, t3, and t4, that is, the floodwater inundates penstock, power plant and substation leading to the shutdown of these infrastructures. The state s14 is reached by firing t1, t2, t3, and t7, that is, the penstock and power plant are inundated by flood water and the their operations are halted, whereas, the shutdown of the substation results from the unavailability of the power supply from the power plant generators. Another absorbing state s22 is reached by firing t1, t4, t8, and t5, which means, the substation outage occurs from flood water inundation, subsequently, the electricity outage halts the penstock operation which finally disrupts the power plant operation. The steady state result shows the probability of being in state s14 has the highest probability of 0.204, and the state s22 has the lowest probability of 0.014.

5.6 Extended modeling results

Following the modeling methodology depicted in figure 3.2, it can be stated that, flood occurrence probability from frequency analysis, vulnerability from the fragility curves, and the predicted risk from the extended Petri-Net analysis can be integrated to forecast the overall vulnerability of any infrastructure.

For example, from the empirical fragility curves, the exceeding probability (p_{fc}) of minor crack is 0.68 at the 45 m water level, and from the observed data, the probability of occurrence of this water level, $p_f = \frac{444}{624} = .7115$

So, the overall vulnerability $= p_{fc} \times p_f = 0.68 \times 0.7115 = 0.4838$

In this case, the risk analysis result is not integrated with this probability, as it was done for dam overflow, and, there is no observed data about dam overflow yet.

The flood frequency analysis results can be used to predict the overflowing situation over the dam. For example, considering the more risky flood prediction, that is, from Gumbel's flood frequency analysis, a 200 year flood overflows the 52.5 m high dam with more than 1m of flood level over the dam with a probability of 0.005. From the analytical fragility curves analysis, it is noticed that the dam will experience sliding, but there is no overturning possibility. However, it can be predicted that in this condition, there will be enough flood flow to make the downstream infrastructures inactive.

Now, results from the extended network analysis can be integrated with this scenario to predict the overall vulnerability. In this case, if the network starts at state 1, that is, dam overflow occurs, then the steady state probability of state 13, that is, the flood water will first inactivate the power plant generator, then the substation will be flooded, and penstock will rupture is 0.184.

With the following notations,

p_{fc} = risk probability from fragility curves analysis;

p_f = Flood level probability from frequency analysis;

p_{ext} = steady state probability of any state from the extended network analysis.

Then, overall vulnerability = $p_{fc} \times p_f \times p_{ext}$ = 1 * 0.005 * 0.184 = 0.00092

Thus, vulnerability of the other states can be determined in a similar way.

5.7 Summary

In this chapter, an integrated infrastructure interdependency modeling study based on flood frequency analysis, fragility curves analysis, Petri-Net development, extended analysis of the part of the Petri-Net, Markov Chain generation, extended analysis of Markov Chain have been performed which in together simulated the overall safety of the critical floodplain infrastructures.

Flood frequency analysis has been done with Gumbel's method and Log Pearson Type III method. The results were consistent where the difference in the results by two methods was well below of 20 % for each prediction. The Canyon Ferry dam started its operation from 1955, and 52 years data of extreme water level at Canyon Ferry forebay or reservoir area upto 2006 were used in the study. In the observed data, the extreme water levels never flooded the dam.

The fragility analysis was done both empirically and analytically. The probability data for empirical fragility curves development are hypothetical to show the development methodology, as the availability of such kind of data is nearly impossible. However, the analytical fragility curves development is solely based on the structural modeling results where the model outputs are directly used for generating the analytical fragility curves. The model approached to a conservative design.

The Petri-Net model had been developed considering the most possible disaster scenario, that is, the dam is overflown. The interactions among the critical floodplain infrastructures, such as, power generating infrastructures comprising of penstock, power plant, and transformer substation, water intake infrastructure comprising of valve-pumping systems, irrigation system, and water distributing and treatment plants were simulated using the developed Petri-Net. The invariant analysis of the developed Petri-Net model simulated the interactions correctly.

The extended analysis of a part of the developed Petri-Net model helps us understand the dynamic behavior of the infrastructures network. This reachability graph from the analysis shows how the infrastructure damage states are attained; also, the corresponding probabilities of these states were captured. Markov Chain analysis showed the steady sate or long run condition of the network. The extended analysis of the developed chain tracked the extended Petri-Net analysis quite convincingly.

Integration of the above mentioned modeling tools and analyses provide a useful tool for predicting overall probability of infrastructure damage states which could lead to develop an efficient flood-related emergency management strategy.

Chapter 6: Conclusions and Future Directions

Currently, infrastructure interdependency issue has been raised as a serious concern worldwide, especially in North America to assess the interdependent vulnerabilities of the critical infrastructures for disaster preparedness. In this research, an integrated method has been developed and applied into two different kinds of case studies, urban and floodplain infrastructure systems networks. This chapter will present the summary of the current research, contributions to the filed of study, and future recommendations which are briefed in next sections.

6.1 Research summary

In this research, efforts have been employed to model the interdependencies among the critical infrastructures in a community. Current infrastructure problems in Canada have been identified in this study. A detailed literature review is carried out to investigate the methodologies applied to address the infrastructure interdependency issue. Summarizing the models and tools, and considering the limitations of the studies, a new modeling framework has been proposed. Theory of the modeling components such as fragility curves analysis, flood frequency analysis, basic Petri-Net model, extended Petri-Net model, Markov Chain development and analysis as well as the developed integrated modeling approach have been demonstrated clearly. The proposed methodology has been applied into urban and floodplain infrastructure systems.

For illustrating the urban infrastructure interdependency, a case study of California electricity outage in 2001 has been conducted. California electricity outage in

2001 occurred due to inconsistent regulatory imposed to restructure the electricity market. Resulting electricity crisis jeopardized the interconnected energy infrastructures, such as, oil and natural gas plants, fuel transportation systems, e.g. tank and pipelines, municipal water system, telecom, etc. A basic Petri-Net model was developed for this case study to capture the interdependencies among the above stated infrastructure systems. Extended Petri-Net analysis was applied into part of the basic Petri-Net for three different case scenarios. The reachability graphs of these scenarios revealed how the network analysis becomes more complicated with the addition of infrastructures or interdependencies in the network. It was discussed that interdependencies among the infrastructures in a network should be reduced to minimize the vulnerability. The three scenarios accounted for the deterioration of any infrastructure in case it is disrupted once. Markov Chain was developed for one scenario to show how to determine the steady state probabilities of the possible network states. The results showed that due to the inherent interconnectedness, all the infrastructures will be disrupted in the course of time as no recovery strategy was included in the network.

The study case for analyzing floodplain infrastructure interdependency was chosen as the Canyon Ferry reservoir area. The floodplain infrastructures network consists of reservoir water storing concrete gravity dam, water carrying penstock for power plant, electricity generating power plant, transformer substation, water intake pipe and pumping system for irrigation and municipal water supply, irrigation system, municipal water carrying pipeline and treatment facility, and telecom for monitoring and remotely controlling the pipelines.

The flood frequency analysis in the Canyon Ferry Lake adjacent to the Canyon Ferry dam was analyzed with both Gumbel's and LP III methods. Some differences in the results from both analyses were observed, but they were in acceptable limit. Between the two methods, Gumbel's analysis predicted higher water levels.

The empirical and analytical fragility curves development of the concrete gravity dam was shown in detail. However, for developing the empirical fragility curves, hypothetical data were used to demonstrate the applicability of the method as real data seems impossible to get. The obtained results appeared to be quite compatible which validates the applicability of the method. The analytical fragility curves were developed with the detailed hydraulic modeling to check the vulnerability of several damage states. Alongwith the two major failure criteria, overturning and sliding failures, other two damage states were taken as the undesirable design conditions. The results showed that there is a very low probability of dam overturning; dam sliding occurs at a water level which was never attained before. The hydraulic modeling was done in a conservative manner.

The basic Petri-Net model for this study case was developed and analyzed. The extended analysis was applied to the part of the developed Petri-Net as before, only with the exception that, in this case, it was intended to check only the inoperable conditions of the infrastructures network consisting of the gravity dam, penstock, power plant, and substation. In this analysis, the inhibitor arcs were introduced to simulate that the network places cannot absorb more than one token which indicated that if one infrastructure is already disrupted by any other infrastructure, it has to be shut down, deterioration due to the interactions with the other infrastructures are not included as it is intended to check only the inoperable conditions. Markov Chain was developed from the reachability graph and was analyzed; compatible results have been achieved.

In this study case, the overall vulnerability was determined by integrating the fragility curves analysis result, flood frequency result, and, results from extended Petri-Net and Markov Chain. The integration was shown with examples. Obtained results from all of these analyses and integration were reasonable. It indicates that a combined extended Petri-Net modeling and Fragility analysis approach is a useful decision tool for addressing flood-induced cascading impacts on critical infrastructures.

6.2 Contributions to the field of study

This research leads towards a new direction in the current field of study. The literature investigation shows that the infrastructure vulnerability had been assessed mostly for single and isolated infrastructure system; very few studies considered the interconnectedness of the infrastructures. When any infrastructure is disrupted due to an external hazard and if there is any other infrastructure connected to it, the second one will also be disrupted, and the disruption will be propagated to the first disrupted infrastructure. This research fully demonstrated how to capture this phenomenon.

In this study, fragility analysis was carried out for a gravity dam structure, for which there are very few studies or none like this one, as, mostly the fragility curves had been developed for earthquake impacted infrastructures.

Earlier, infrastructure interdependency was addressed with different methodologies. For example, Leontief input-output model (Haimes and Jiang, 2005) was applied to address this issue where the disruption is expressed in terms of inoperability percentage. In another study, Gursesli and Desrochers (2003) introduced the possibility of the application of the basic Petri-Net model and illustrated that with a case example. But that study only addressed qualitatively how the interdependencies in an infrastructures system can be expressed. This research carried out a dynamic analysis for quantitative assessment of the risk probabilities.

Extended Petri-Net and Markov Chain analysis is a dynamic tool to evaluate the safety of the components in a system. Before, the methodology had been applied for predicting the software performance and had never been used or introduced for possible application in infrastructure interdependency analysis. This study introduced and applied the methodology for addressing infrastructure interdependency for the very first time and the obtained results are quite satisfactory. Also, this study presents the integration of a number of different modeling tools such as flood frequency analysis, fragility curves analysis, basic and extended Petri-Net, Markov Chain application to simulate the overall vulnerability assessment of the interconnected infrastructures.

6.3 Future recommendations

This research could be continued with the inclusion of further works. For example, the fragility curves can be developed with a direct numerical optimization method where the flood water levels are randomly generated. In generating the Monte Carlo random numbers of the uncertain parameters, more data generation will give more accurate probability prediction.

Fragility analysis of more infrastructure systems can be performed. The analysis should be carried out by corresponding researchers. For example, a hydraulic engineer can assess the fragility of hydraulic dam, a bridge engineer can do that for a bridge, a building engineer can deal with structural buildings such as power plant, etc., and so on. Communication gap among the authorities of the different infrastructure sectors should be minimized. Interdisciplinary discussion and exchange of research output is vital for establishing an efficient infrastructure management system in a particular region.

In Petri-Net modeling, inclusion of the recovery strategy will make the system analysis more realistic. More critical infrastructures can be included in the study system. The extended Petri-Net analysis can be performed for the whole network, for which an extensive model and database can be developed.

Data collection is another vital point in addressing the current issue. Commonly, the infrastructure personnel are not willing to share any information for security purposes. But this practice makes the research advancement extremely difficult.

Overall, this research is a very good introduction in the infrastructure interdependency analysis field, which could be carried out further to include more dynamic analysis to make the methodology more robust and comprehensive.

References

Bao-hua, Y., Li-li, X., and En-jie, H. (2004). 'A comprehensive study method for lifeline system interaction under seismic conditions'. *Acta Seismologica Sinica*, 17(2), 211-221.

Bobbio, A. (1990). 'System modeling with Petri Nets'. *System Reliability Assessment*, Kluwer p.c., 102-143.

California Public Utilities Commission (2001). 'Energy Division Report on Interruptible Programs and Rotating Outages'. San Francisco, CA, Feb. 8, 2001.

Chang, S. E., Rose, A. Z., Shinozuka, M. and Tierney, K. J. (2000). 'Modeling earthquake impact on urban lifeline systems: advances and integration in loss estimation'. *Proceedings of the China-US Millennium Symposium of Earthquake Engineering: Earthquake Engineering Frontiers in the New Millennium*, November 8–11, Beijing, China.

Chock, G. Y. K. (2005). 'Modeling of hurricane damage for Hawaii Residential construction'. *Journal of Wind Engineering and Industrial Aerodynamics*, 93(8), 603–622.

Chow, V. T. (1959). 'Open Channel Hydraulics'. McGraw-Hill, New York, NY.

Cirado, G., and Lindemann, C. (1993). 'Analysis of deterministic and stochastic Petri Nets'. *Proceedings of the Fifth International Workshop on Petri-Nets and Performance Models (PNPM93),* Toulouse, France, October.

Connole, P. (2001). 'California power crisis may become national mess'. *Reuters*, Feb. 15.

Energy Information Administration, U. S. Department of Energy (2000). 'Natural Gas Annual 1999'. DOE/EIA-0131(99). Website: http://www.eia.doe.gov/pub/oil_gas/natural_gas/data_publications/natural_gas_annual/historical/1999/pdf/front_matter.pdf

Energy Information Administration, Department of Energy (2001). 'Electricity Shortage in California: Issues for Petroleum and Natural Gas Supply'. Website: www.eia.doe.gov

Erberik, M. A., and Elnashai, A. S. (2004). 'Fragility analysis of flat-slab structures'. *Engineering Structures,* 26, 937–948.

Ezell, B. C., Farr, J. V, and Wiese, I. (2000). 'Infrastructures risk analysis model'. *Journal of Infra. Systems*, 6(3), 114-117.

Filliben, J. J., Gurley, K., Pinelli, J.-P., and Simiu, E. (2002). 'Fragility curves, damage matrices, and wind induced loss estimation'. *3rd International Conference on Computer Simulation in Risk Analysis and Hazard Mitigation,* June 19-21, Sintra, Portugal, 119-126.

Graph, W. H. (1998). 'Fluvial hydraulics: Flow and transport processes in channels of simple geometry'. Altinakar, M. S. (Collaborator), John Wiley & Sons, U.K.

Grimstead, C. M., and Snell J. L. (1997). 'Introduction to probability'. An online textbook, published by American Mathematical Society. Website: http://www.dartmouth.edu/~chance/teaching_aids/books_articles/probability_book/amsbook.mac.pdf

Gursesli, O., and Desrochers, A. A. (2003). 'Modeling infrastructure interdependencies using Petri Nets'. *Systems, Man and Cybernetics*, IEEE International Conference, 2, 1506-1512.

Haimes, Y. Y., Horowitz, B. M., Lambert, J. H., Santos, J. R., Lian C. and Crowther, K. G. (2005). 'Inoperability input-output model for interdependent infrastructure sectors. I: Theory and methodology'. *Journal of Infra. Systems*, 11(2), 67-79.

Haimes, Y. Y., Horowitz, B. M., Lambert, J. H., Santos, J. R., Crowther, K. G., and Lian C. (2005). 'Inoperability input-output model for interdependent infrastructure sectors. II: Case studies'. *Journal of Infra. Systems*, 11(2), 80-92.

Haimes, Y. Y., and Jiang, P. (2005). 'Leontief-based model of risk in complex interconnected infrastructures'. *Journal of Infra. Systems,* 7(1), 1-12.

Hall, J. W., Dawson, R. J., Sayers, P. B., Rosu, C., Chatterton, J. B., and Deakin, R. (2003). 'A methodology for national-scale flood risk assessment'. *Proceedings of the Institution of Civil Engineers - Water Maritime and Engineering,* 156(3), 235-214.

Howard, R. A. (1971). 'Dynamic probabilistic systems'. Volume 1, NY: John Wiley Sons.

Hura, G. S. (1987). 'Petri net applications'. *IEEE Potentials,* 6(3), 25-28.

Hwang, H. H. M., and Chou, T. (1998). 'Evaluation of seismic performance of an electric substation using event tree/fault tree technique'. *Probabilistic Engineering Mechanics,* 13(2), 117-124.

Hwang, H., Jernigan, J. B., and Lin, Y. W. (2000). 'Evaluation of seismic damage to Memphis bridges and highway systems'. *Journal of Bridge Engineering,* 5(4), 322-330.

Istomina, M. N., Kocharyan, A. G., and Lebedeva, I. P. (2005). 'Floods: genesis, socioeconomic and environmental impacts'. *Water Resources*, 32(4), 349-358.

Jovanoska, E. D. (2000). 'Fragility curves for reinforced concrete structures in Skopje (Macedonia) region'. *Soil Dynamics and Earthquake Engineering*, 19(6), 455-466.

Kennedy, J. G., Snell, J. L., and Thompson, G. L. (1974). 'Introduction to finite mathematics'. 3rd edition, Englewood Cliffs, NJ: Prentice-Hall.

Kim, S. H., and Shinozuka, M. (2004). 'Development of fragility curves of bridges retrofitted by column jacketing'. *Probabilistic Engineering Mechanics*, 19(1-2), 105-112.

Klare, M. (2001). 'California's power crisis: A warning to all'. *Pacific News Service*, Feb. 7.

Koch, I., Junker,B. H. and Heiner, M. (2005). 'Application of Petri net theory for modelling and validation of the sucrose breakdown pathway in the potato tuber'. *Bioinformatics*, 21(7), 1219-1226.

Krings, A. and Oman, P. (2003). 'A simple GSPN for modeling common mode failures in critical infrastructures'. *Proceedings of the 36th Hawaii International Conference on System Sciences*, Hilton Waikoloa Village, Island of Hawaii, Jan 6-9.

Lambert, J. H., and Sarda, P. (2003). 'Risk analysis in disaster planning by superposition of infrastructures and societal networks'. *ASCE Conference Proceedings*, 1-11.

Leavitt, W. M., and Kiefer, J. J. (2006). 'Infrastructure interdependency and the creation of a normal disaster: the case of Hurricane Katrina and the City of New Orleans'. *Public Works Management & Policy,* 10(4), 306-314.

Lee, K. H., Rosowsky, D. V. (2005). 'Fragility assessment for roof sheathing failure in high wind regions'. *Engineering Structures*, 27(6), 857–868.

Linsley, R. K., and Franzini J. B. (1992). 'Water resources engineering'. 4th edition McGraw-Hill, NY.

Leonardo, D. O., Craig, J. I., and Goodno, B. G. (2004). 'Probabilistic response of interdependent infrastructure networks'. *2nd annual meting of the Asian-pacific network of centers for earthquake engineering research (ANCER),* Honolulu, Hawaii, July 28-30.

Leontief, W. W. (1966). 'Input-output economics'. Oxford University Press, NY.

Methods, H., Dyhouse, G., Hatchett, J., and Benn, J. (2003). 'Floodplain modeling using HEC-RAS'. 1st edition, Haestad Press, Waterbury, CT, USA.

Malla, S., and Wieland, M. (1999). 'Analysis of an arch-gravity dam with a horizontal crack'. *Computers and Structures*, 72(1), 267-278.

Manson, P. R. (1988). 'Petri net theory: a survey'. Technical report, no. 139, Univ. of Cambridge, Computer Laboratory, UK.

Mendonca, D., and Wallace, W. A. (2006). 'Impacts of the 2001 World Trade Center on New York City Critical Infrastructures'. *Journal of Infra. Systems*, 12(4), 260-270.

Moselhi,, O., Hammad, A., Alkass, C., Debbabi, M., and Haider, M. (2005). 'Vulnerability assessment of civil infrastructure systems: A network approach'. 1st

CSCE Specialty Conference on Infrastructure Technologies, Management and Policy, June, Toronto.

Murata, T. (1989). 'Petri Nets: properties, analysis and applications'. *Proceedings of the IEEE,* 77(4), 541-580.

North American Electric Reliability Council (2001). '2001 Summer Assessment'. Princeton, NJ.

Nozick, L.K., Turnquist, M.A., Jones, D.A., Davis, J.R. and Lawton, C.R. (2005). 'Assessing the performance of interdependent infrastructures and optimizing investments'. *International J. of Critical Infrastructures*, 1, (2-3), 144–154.

Office of Critical Infrastructure Protection and Emergency Preparedness, OCIPEP (2003). 'Threats to Canada's Critical Infrastructure'. *Government of Canada,* Number: TA03-001.

O'Rourke, M. J., Eeri, M., and So, P. (2000). 'Seismic fragility curves for on-grade steel tanks'. *Earthquake Spectra*, 16(4), 801-815.

Panzieri, S., Setola, R., and Ulivi, G. (2005). 'An approach to model complex interdependent infrastructures'. *16th IFAC World Congress,* Czech Republic.

Peterson, J. L. (1981). 'Petri net theory and the modeling of systems'. Prentice-Hall, Inc., *Englewood Cliffs*, N. J. 07632.

Petri, C. A. (1962). 'Communicating with Automata'. PhD thesis, Technical University Darmstadt, Germany.

President's Commission on Critical Infrastructure Protection, PCCIP (1997). 'Critical foundations: protecting America's infrastructures'. [Online]. Available: http://www.ciao.gov

Public Safety and Emergency Preparedness Canada, PSEPC (2005). 'Modernization of the Emergency Preparedness Act'. *Consultation paper*. Website: http://www.publicsafety.gc.ca/pol/em/fl/Modernization_EPA.pdf

Ramchandani, C. (1974). 'Analysis of asynchronous concurrent systems by timed Petri nets'. Project MAC Technical report MAC-TR-120, Massachusetts Institute of Technology, Cambridge, MA.

Raposo, A. B., Magalhães, L. P., and Ricarte, I. L. M. (2000). 'Petri nets based coordination mechanisms for multi-workflow environments'. *Computer Systems Science and Engineering*, 15(5), 315-326.

Rinaldi, S. M., Peerenboom, J. P., and Kelly, T. K. (2001). 'Critical infrastructure interdependencies'. *IEEE Control System Magazine*, 11-25.

Robert, B. (2004). 'A method for the study of cascading effects within lifeline networks'. *International J. of Critical Infrastructures*, 1(1), 86-99.

Sauver, J. S. (2004). 'SCADA security and critical infrastructure'. Eugene, Oregon Infraguard meeting, 308 Forum, LCC. Website: http://darkwing.uoregon.edu/~joe/scadaig/

Schiff, A. J. (2004). 'Documenting damage, disruption, interdependencies and the emergency response of power and communication systems after earthquakes'. *International J. of Critical Infrastructures*, 1(1), 100–107.

Shahidehpour, M., and Wiedman, T. (2005). 'Impact of natural gas infrastructure on electric power systems'. *Proceedings of IEEE*, 93(5), 1042-1056.

Shayan, A., and Grimstad, J. (2006). 'Deterioration of concrete in a hydroelectric concrete gravity dam and its characterization'. *Cement and Concrete Research*, 36(2), 371-383.

Shinozuka, M., Tanaka, S. and Koiwa, H. (1994). 'Interaction of lifeline systems under earthquake conditions'. *Proceedings of the 2nd China-US-Japan Trilateral Symposium on Lifeline Earthquake Engineering*, 43–52.

Simpson, D. M., Rockaway, T. D., Weigel, T. A., Coomes, P. A. and Holloman, C. O. (2005). 'Framing a new approach to critical infrastructure modeling and extreme events'. *International J. of Critical Infrastructures*, 1(2-3), 125-143.

Subramanya, K. (2001). 'Engineering Hydrology'. 2nd edition, McGraw Hall, New Delhi.

Tolone, W.J., Wilson, D., Raja, A., Xiang, W., Hao, H., Phelps, S., and Johnson, W. (2004). 'Critical infrastructure integration modeling and simulation'. *ISI 2004*, LNCS 3073, 241-255.

U. S. Department of the Interior, (2007). 'Canyon Ferry Dam'. Bureau of Reclamation, Montana Area Office, Billings, MT. Website: http://www.usbr.gov/dataweb/dams/mt00568.htm

USGS Manual on Hydrology (2000). 'ConnDOT Drainage Manual'. p. 6.10-1. Website: http://ct.gov/dot/lib/dot/documents/ddrainage/6.10.pdf

Watts, D. J., and Strogatz, S. H. (1998). 'Collective dynamics of small-world networks'. *Nature* 393(4), 440-442.

Wolak, F. A. (2003). 'Lessons from the California electricity crisis'. Center for the Study of Energy Markets, University of California Energy Institute.

Woo, C. K. (2001). 'What went wrong in California'a electricity market?'. *Energy,* 26, 747-758.

Yamaguchi, N., and Yamazaki, F. (2001). 'Estimation of strong motion distribution in the 1995 Kobe earthquake based on building damage data'. *Earthquake Engineering Structural Dynamics*, 30(6), 787-801.

Zuberek, W.M. (1980). 'Timed Petri Nets and preliminary performance evaluation'. *IEEE, CH1494-4/80/0000-0088.*

Zuberek, W. M. (1985). 'Performance evaluation of concurrent systems using timed Petri Nets'. *Proceedings of the 1985 ACM Computer Science Conference-Agenda for Computing Research: The Challenge for Creativity,* 1985 Mar. 12-14.

Zuberek, W.M. (1987). 'Modified M-timed Petri Nets in modeling and performance evaluation of systems'. *ACM,* 0-89791-218-7/87/0002-0261.

Zuberek, W.M. (1988). 'Timed Petri Net models of queuing systems'. *IEEE,* 0896-582X/87/0000/0324.

Zuberek, W.M. (1991). 'Timed Petri Nets: definitions, properties, and applications'. *Microelectronics and Reliability,* 31(4), 627-644.